VILNIUS UNIVERSITETY

Birutė
ZABLOCKIENĖ

Prevention of influenza viral pneumonia using zanamivir and antisense oligonucleotide against inducible nitric oxide synthase

DOCTORAL DISSERTATION

Biomedical Sciences,
Medicine 06B

VILNIUS 2019

This dissertation was written between 2013 and 2018 (Vilnius University).

Academic supervisor:
Prof. Habil. Dr. Arvydas Ambrozaitis (Vilnius University, Biomedical sciences, Medicine − 06 B).

Academic advisor:
Prof. MD, MPH Stefan Gravenstein (Brown University, U.S.A., Biomedical sciences, Medicine − 06 B).

VILNIAUS UNIVERSITETAS

Birutė
ZABLOCKIENĖ

Gripo virusinės pneumonijos prevencija naudojant zanamivirą ir priešprasminį oligonukleotidą prieš indukuojamą azoto oksido sintazę

DAKTARO DISERTACIJA

Biomedicinos mokslai,
medicina 06B

VILNIUS 2019

Disertacija rengta 2013– 2018 metais Vilniaus universitete.

Mokslinis vadovas:
prof. habil. dr. Arvydas Ambrozaitis (Vilniaus universitetas, biomedicinos mokslai, medicina − 06 B).

Mokslinis konsultantas:
prof. MD, MPH Stefan Gravenstein (Brown universitetas, JAV, biomedicinos mokslai, medicina − 06 B).

CONTENT

ABBREVIATIONS

A/PR/8/34	–	A/Puerto Rico/8/34 influenza virus
ANOVA	–	one-way analysis of variance
ARDS	–	acute respiratory distress syndrome
ASO	–	antisense oligonucleotides
BAL	–	bronchoalveolar lavage
β-actin	–	beta actin
bFGF	–	basic fibroblast growth factor
CCL2	–	C-C motif chemokine ligand 2
COX-2	–	cyclooxygenase-2
CXCL10	–	C-X-C motif chemokine ligand 10
DAD	–	diffuse alveolar damage
DANA	–	2,3-dehydro-2-deoxy-N-acetylneuraminic acid
DNA	–	deoxyribonucleic acid
dsRNA	–	double stranded ribonucleic acid
ESR	–	electron spin resonance
FAD	–	flavin adenine dinucleotide
FMN	–	flavin mononucleotide
H&E	–	hematoxylin and eosin
HA	–	hemagglutinin
HSV-1	–	herpes simplex virus type 1
H_2O_2	–	hydrogen peroxide
IAV	–	influenza A virus
IAV PA	–	influenza A virus polymerase acidic protein
IFN-α/β	–	interferon alpha/beta
IFN-γ	–	interferon-gamma
IL-1β	–	interleukin 1-beta
iNOS	–	inducible nitric oxide synthase
IRF-1	–	interferon regulatory factor 1
L-NMMA	–	N^G-monomethyl-L-arginine
LPS	–	lipopolysaccharide
LSD	–	least significant difference
M1	–	matrix protein 1
M2	–	matrix ion channel
MMP	–	matrix metalloproteinase
20-MOE	–	20-O-methoxyethyl
mRNA	–	messenger ribonucleic acid
NA	–	neuraminidase
NADPH	–	nicotinamide adenine dinucleotide phosphate

NEP	–	nuclear export protein
NF-κB	–	nuclear factor κB
NI	–	neuraminidase inhibitor
NO	–	nitric oxide
NO_2	–	nitrogen dioxide
NO_2^-	–	nitrite
NOS	–	nitric oxide synthase
NP	–	nucleoprotein
NS	–	nonsignificant
NS2	–	nonstructural protein 2
O_2^-	–	superoxide
OD	–	optical density
ODN	–	oligodeoxynucleotide
20-OME	–	20-O-methyl
$ONOO^-$	–	peroxynitrite
PA RNA	–	RNA encoding viral polymerase acidic protein
PB1	–	polymerase basic subunit 1
PB2	–	polymerase basic subunit 2
p	–	level of statistical significance
p.i.	–	post infection
PBS	–	phosphate buffered saline
PMO	–	phosphoroamide morpholino oligomer
Prop5	–	programmed cell death protein 5
PS	–	phosphorothioate
(qRT)-PCR	–	real-time quantitative polymerase chain reaction
Raf/MEK/ERK	–	Raf/Mitogen-activated protein kinase/ERK kinase (MEK) / extracellular-signal-regulated kinase (ERK)
RNA	–	ribonucleic acid
RNase H	–	ribonuclease H
RNP	–	ribonucleoprotein
RSV	–	respiratory syncytial virus
SARS	–	severe acute respiratory syndrome
SEM	–	standard error of the mean
SPSS	–	Statistical Package for Social Science
STAT	–	signal transducer and activator of transcription
STAT-6	–	signal transducer and activator of transcription 6
$TCID_{50}$	–	50% tissue culture infectious dose
TipDC	–	the TNF-α/iNOS-producing dendritic cell subset
TNF-α	–	tumor necrosis factor-alpha
TRAIL	–	tumor necrosis factor related apoptosis inducing ligand

INTRODUCTION

The research problem

Influenza remains a serious public health problem that causes severe illness and death in high risk populations. Worldwide, annual influenza epidemics result in about 3 to 5 million severe illnesses, and 290 000 to 650 000 deaths (1).

The various studies associate severe disease with the development of influenza viral pneumonia (2, 3) with or without secondary bacterial pneumonia (4-6). Some of the pulmonary abnormalities of fatal influenza viral pneumonia might be induced by the release of host inflammatory mediators, rather than by a direct viral cytopathic effect (7, 8).

Influenza infection induces a cascade of host immune responses that involves production of proinflammatory cytokines and recruitment of inflammatory cells in infected lungs (9-13). Cytokines such as interferon-gamma (IFN-γ) and tumor necrosis factor-alpha (TNF-α) stimulate the production of inducible nitric oxide synthase (iNOS) leading to high-output synthesis of nitric oxide (NO), predominantly in macrophages (13-16). In turn, the NO and excessive amounts of reactive nitrogen intermediates can lead to significant lung immunopathology (11, 13, 17). Reducing or preventing infection or NO production could prevent such immunopathology.

Neuraminidase inhibitors (NIs) currently offer the only treatment option for influenza in most clinical settings. NIs reduce influenza replication and can improve survival rate, but prove less helpful for some seriously ill, high-risk patients and in A(H5N1) disease (18, 19). An increasing number of recently discovered NI-resistant viruses present a continuing need for new, novel anti-influenza therapies and creative strategic approaches (20-23).

Animal experiments that affect iNOS function and NO production in host cells show therapeutic promise for the control of lung inflammation and damage from influenza (10, 14, 24). Suppression of virus spread within the respiratory tract by NIs could indirectly cause a reduction in iNOS expression and NO synthesis. NIs reduced NO generation in influenza virus-infected and IFN-γ-activated RAW 264.7 macrophage cell line *in vitro,* but the mechanism of this phenomenon is not fully clear (25). However, it is unknown whether NIs have the capacity to suppress net NO production during influenza virus infection and, in this way, reduce lung tissue damage under *in vivo* conditions.

A relatively new approach to inhibit iNOS activity involves antisense-mediated gene knock-down. In the present study, the hypothesis that influenza A virus (IAV) induced lung inflammation in mice can be reduced using antisense oligodeoxynucleotide targeting iNOS mRNA or its combination with NI zanamivir was investigated.

Aim of the study

To evaluate if zanamivir and/or antisense oligonucleotide against inducible nitric oxide synthase prevents influenza viral pneumonia.

Objectives of the study

1. To evaluate the effect of A/PR/8/34 influenza virus infection of BALB/c mice on IAV RNA, IFN-γ, TNF-α and iNOS mRNA relative levels in lungs, nitrite concentration in bronchoalveolar lavage (BAL) fluid, weight changes and lung histological damage.
2. To evaluate the zanamivir's treatment effects on IAV RNA, IFN-γ, TNF-α and iNOS mRNA relative levels in lungs, nitrite concentration in BAL fluid, weight changes and lung histological damage with A/PR/8/34 influenza virus infection.
3. To assess the antisense oligonucleotide against inducible nitric oxide synthase treatment effects on IAV RNA, IFN-γ, TNF-α and iNOS mRNR relative levels in lungs, nitrite concentration in BAL fluid, weight changes and lung histological damage during A/PR/8/34 influenza virus infection.
4. To evaluate the combination of zanamivir and antisense oligonucleotide against inducible nitric oxide synthase treatment effects on IAV RNA, IFN-γ, TNF-α and iNOS mRNA relative levels in lungs, nitrite concentration in BAL fluid, weight changes and lung histological damage during A/PR/8/34 influenza virus infection.

Scientific novelty of the study

Several scientific novelties are presented in the dissertation. First, the capacity of zanamivir to suppress net NO production during influenza virus infection and, in this way, to reduce lung tissue damage under *in vivo* conditions, was analysed for the first time. Second, the effect of antisense oligodeoxynucleotide to iNOS mRNA or its combination with zanamivir treatment of influenza infected mice has not been previously evaluated.

Practical value of the study

The neuraminidase inhibitors (NIs) are currently the only option in most clinical settings, however they may be insufficient for seriously ill, high-risk patients or in influenza A(H5N1) disease. An increasing number of drug resistant viruses have been discovered recently. Thus there is a continuing need for new influenza therapies using novel targets and creative strategies. As treatment with antisense oligodeoxynucleotide to iNOS mRNA can reduce lung inflammation caused by influenza virus infection in mice, this more targeted approach, in combination with antiviral strategies, could be a potential new option in the treatment of influenza virus infection.

Defended statements of the dissertation

1. Infection of BALB/c mice with A/PR/8/34 influenza virus induces lung histological damage, which is associated with weight loss, higher expression of cytokines, iNOS mRNA and nitrite concentration in lungs.
2. Zanamivir reduces lung damage by suppressing IAV replication, with a result of less NO production in influenza infected mice.
3. Antisense oligodeoxynucleotide to iNOS mRNA reduces lung inflammation caused by influenza virus infection in mice by inhibiting NO production.
4. Zanamivir and antisense oligodeoxynucleotide to iNOS mRNA combination treatment diminishes lung inflammation by suppressing IAV replication and inhibiting NO production in influenza infected mice.

1. LITERATURE REVIEW

1.1 The influenza viruses

Influenza is a contagious respiratory illness caused by influenza viruses. These viruses belong to the family *Orthomyxoviridae*, are enveloped and possess segmented, single-stranded, negative-sense RNA genomes (26). There are four types of influenza viruses: types A, B, C and D (1).

Influenza A virus infects people and many different mammalian and avian species, causes seasonal epidemics of disease and has the potential to cause a pandemic. Influenza A viruses are further classified into subtypes based on the combinations of the distinct virus surface proteins, hemagglutinin (HA) and neuraminidase (NA). For influenza A, there are 18 unique hemagglutinin subtypes and 11 unique neuraminidase subtypes. Currently, widely circulating in people are the influenza A subtypes A(H1N1) and A(H3N2) viruses (1). Depending on the named origin host, influenza A viruses can be classified as avian influenza, swine influenza, or other types of animal influenza viruses (27).

Influenza B virus circulates among humans and causes seasonal epidemics. Currently circulating influenza type B viruses belong to either B/Yamagata or B/Victoria lineage (1).

Influenza C virus can infect both humans and pigs but infections are generally mild and are rarely reported (1).

Influenza D virus was first isolated in 2011, it primarily affects cattle and is not known to infect or cause illness in people (1, 28).

1.2 The influenza virus structure

The viral particles are made of a viral envelope with a host cell-derived lipid membrane, wrapped around a central core. The glycoproteins HA and NA used to classify the virus project from the viral membrane (29). HA mediates binding of the virus to target cells and entry of the viral genome into the target cell, while NA is involved in the release of progeny virus from infected cells, by cleaving sugars that bind the mature viral particles (30). The matrix (M2) ion channels present in influenza A viruses traverse the lipid envelope. The envelope and its three integral membrane proteins HA, NA, and M2 overlay a matrix of M1 protein, which encloses the virion core. The nuclear export protein (NEP; also called nonstructural protein 2, NS2) and

the ribonucleoprotein (RNP) complex lie internal to the M1 matrix. RNP is responsible for transcription and replication of influenza. It consists of the viral RNA segments coated with nucleoprotein (NP) and the heterotrimeric RNA-dependent RNA polymerase, composed of two "polymerase basic" and one "polymerase acidic" subunits (PB1, PB2, and PA) (29).

1.3 Influenza epidemiology and pathogenesis

Influenza has been recognised since the 16th century and spreads rapidly through communities globally (31). It may occur in several forms: epidemic (seasonal or interpandemic) influenza and sporadic pandemics caused by influenza A viruses (IAV). Worldwide, annual epidemics are estimated to result in about 3 to 5 million cases of severe illness and 290–650 thousand deaths in high risk populations (1).

Four influenza pandemics have occurred in the past 100 years: A(H1N1) Spanish influenza in 1918, A(H2N2) Asian influenza in 1957, A(H3N2) Hong Kong influenza in 1968, and A(H1N1) swine influenza in 2009. The most severe pandemic occurred in 1918 and caused over 50 million deaths worldwide (32). The 2009 A(H1N1) pandemic caused 151 700–575 400 deaths in its first year of circulation (33). There is concern that newly emerging strains of IAV from animal reservoirs (eg, avian-origin A(H5N1) and A(H7N9) viruses) could gain efficient transmissibility in human beings and cause a severe pandemic (34, 35). An especially notorious strain is the highly pathogenic avian-origin influenza virus A(H5N1), which has a reported mortality rate of approximately 53% (36). In March 2013, in Eastern China, there was an outbreak of the novel H7N9 influenza virus, which although less pathogenic in avian species, resulted in 131 confirmed cases and 36 deaths in humans over a two-month span (37).

An important complication of influenza virus infection is viral pneumonia (3, 4, 13). Seasonal influenza infection is the most common cause of pneumonia-related death in the developed world (38). The overall incidence of acute respiratory distress syndrome (ARDS) attributable to seasonal IAV infection has been estimated at 2.7 cases per 100 000 person-years and can account for 4% of all hospitalisations for respiratory failure during the influenza season (39).

Influenza viral pneumonia often occurs with or is followed by bacterial pneumonia. Researchers who reassessed data from the influenza pandemics of 1918, 1957, and 1968 have suggested that most deaths during these

periods probably resulted from secondary bacterial pneumonia (4). This finding contrasts with avian H5N1-associated pneumonia, which seems to be a primarily viral infection (40). In patients with 2009 pandemic A(H1N1) infection, secondary bacterial infection developed in 4–24% of cases (41-43). Some of the pulmonary abnormalities of fatal influenza pneumonia might be induced by the release of host inflammatory mediators, rather than by a direct viral cytopathic effect (7, 8). In patients who succumb to IAV infection, post mortem examination of the lung almost always reveals diffuse alveolar disease, but viral RNA is present in only a subset of patients (41). These results and findings from published studies of IAV infection in animals suggest that mortality in IAV infection might result from an overly exuberant immune response or impaired viral clearance (44, 45).

Acute respiratory distress syndrome (ARDS) is a severe complication of influenza infection. ARDS involves damage to the epithelial–endothelial barrier, fluid leakage into the alveolar lumen, and respiratory insufficiency. The most important part of the epithelial–endothelial barrier is the alveolar epithelium, strengthened by tight junctions. Upon entering the alveolus, influenza virus infects its main target, epithelial cells, which undergo apoptosis or necrosis, opening the epithelial layer. Influenza virus infected epithelial cells also produce cytokines that recruit neutrophils and monocytes to the alveolus by direct chemotaxis. Activation of endothelial cells in influenza virus infection results in the upregulation of adhesion molecules for leucocyte extravasation and the production of cytokines such as CCL2, CXCL10, interferon-α, interleukin-6, TNF-α, and interferon-γ. Both processes further attract neutrophils and macrophages to the alveolus. Recruited neutrophils produce reactive oxygen species, which can cause tissue damage. Neutrophils also produce cytokines in response to influenza virus infection. In particular, the production of CXCL10 could damage the epithelial–endothelial barrier by triggering the production of superoxide or enhancing neutrophil chemotaxis. Recruited macrophages can damage the epithelial–endothelial barrier in several ways. They can express tumor necrosis factor related apoptosis inducing ligand (TRAIL), which interacts with death receptor 5 on the epithelial cell and induces epithelial cell apoptosis. Macrophages are important producers of proinflammatory cytokines, which further exacerbate the inflammatory response and could damage the epithelial–endothelial barrier. By the activation of inducible nitric oxide synthase (iNOS), recruited macrophages can increase concentrations of nitric oxide (NO) and peroxynitrite (ONOO$^-$), which cause tissue damage (13).

Results of mouse respiratory infection models clearly demonstrate the contribution of free radicals, including NO, to the development of acute lung inflammation and mouse mortality during the viral infection (46-50).

1.4 Biosynthesis of nitric oxide

NO have multiple biological functions, including involvement in the pathological process of influenza infection. In the respiratory tract, NO is produced by a wide variety of cell types, including epithelial cells, airway neurons, inflammatory cells (monocytes, macrophages, neutrophils, mast cells) and vascular endothelial cells (46, 51). NO is synthesized from L-arginine in a reaction catalyzed by a family of nitric oxide synthase (NOS) enzymes. Conversion of L-arginine to NO and L-citrulline requires also nicotinamide adenine dinucleotide phosphate (NADPH) and oxygen (O_2) as co-substrates and tetrahydrobiopterin (BH4), flavin adenine dinucleotide (FAD), flavin mononucleotide (FMN) and iron (heme) as cofactors (46, 52). The NOS is structurally divided into two major domains, the reductase and oxygenase domains (46, 53). Calmodulin couples these domains and transfers electrons between flavins and the heme moiety (46, 54). The NOS exists in three distinct isoforms. Constitutive neural NOS (nNOS or NOS I) is predominantly expressed within neurons in brain and peripheral nervous system. Constitutive endothelial NOS (eNOS or NOS III) is mainly expressed in endothelial cells (46, 55). Increase in free intracellular calcium concentration (Ca^{2+}) stabilizes the binding of calmodulin to eNOS and nNOS, and activates the enzyme to produce NO. NO production by constitutively expressed NOSs is transient and shortlived (46, 47, 55). The third isoform of NOS family is the inducible NOS (iNOS, NOS II). Exposure to microbial products such as lipopolysaccharide (LPS) and double stranded ribonucleic acid (dsRNA) or proinflammatory cytokines induces the expression of the iNOS gene in various inflammatory and tissue cells. Binding of calmodulin to iNOS is tight even at low Ca^{2+} concentrations and it can constantly produce high levels of NO for prolonged periods (46-50).

Thus, iNOS induction contributes to an increase in NO synthesis following influenza infection, however some differences in the clinical impact of mouse and human iNOS expression are described. There are differences in iNOS regulation and release, too.

1.5 Regulation of inducible nitric oxide synthase expression

Human iNOS shares 80% homology to murine iNOS at the amino acid levels, but translation of the results describing the mechanisms of mouse iNOS expression to that of human is not always straightforward (49, 56). The size of the iNOS promoter differs greatly between mouse (~1.5 kb) and man (up to 16 kb) (57). Many mouse cells readily express iNOS in response to LPS or to a single cytokine, whereas human cells usually require a combination of different cytokines for detectable iNOS expression and NO synthesis (47). Unlike rodent mononuclear phagocytes and granulocytes, both human macrophages and monocytes do not release significant amounts of NO *in vitro* when stimulated with the classical iNOS inducers – IFN-γ and LPS, although *in vivo* NO production during inflammatory processes seems evident (58). iNOS has been immunolocalized within the airway cells or human lung tissue that has been obtained from patients with ARDS, bacterial pneumonia, lung cancer, pulmonary sarcoidosis, idiopathic pulmonary fibrosis and asthma (59-64). Alveolar macrophages isolated from the lungs of patients with tuberculosis or ARDS following sepsis have been shown to express iNOS (65, 66). Uetani et al. (2000) in their study showed induction of iNOS gene expression in human airway epithelial cells by IAV or synthetic dsRNA (67). Despite the differences noted above, similarities exist between murine and human iNOS genes in terms of activating factors and conditions. The viral replication or viral components, bacterial LPS and cytokines, such as interleukin 1β (IL-1β), TNF-α, interferon α/β (IFN-α/β) and IFN-γ can stimulate expression of the iNOS gene in both mouse and human cells during infectious processes. These inducers mediate the activation of cellular transcription factors – nuclear factor κB (NF-κB), signal transducer and activator of transcription (STAT), interferon regulatory factor 1 (IRF-1), which, in turn, bind to their respective binding sites in the promoter region of iNOS gene and initiate transcription of the gene (57, 68-71). The expression of iNOS is regulated at transcriptional and posttranscriptional levels (72). LPS and IFN-γ induce mouse iNOS promoter activity 50–100-fold (57). Cytokine stimulation increases human iNOS promoter activity only approximately 7- to 10-fold, while mRNA expression increases more than 100-fold (73, 74). This demonstrates important differences in transcriptional and posttranscriptional regulation of iNOS expression between mouse and human cells (72). Recent evidence supports the idea that regulation of iNOS mRNA stability is an important means to regulate iNOS expression. In the unstimulated macrophages and monocytes, nuclear run-on

assays show continuous iNOS transcription, whereas human iNOS promoter constructs have basal activity (47). However, no iNOS mRNA or protein can be detected within the unstimulated macrophages and monocytes, indicating that iNOS mRNA is highly unstable in these cells (47).

The data about iNOS expression and exact mechanisms of action during infections in human are lacking and deserve further study. Currently it is better described in murine models.

1.6 Molecular mechanisms of nitric oxide action during infections in murine models

During microbial infections, excessive NO produced by iNOS has diverse functions ranging from antimicrobial and antiinflammatory host defense and cytoprotection to proinflamatory and cytotoxic activities (17). The host defense function of NO is best characterized by antimicrobial and cytoprotective activities that have been observed in bacterial, fungal, and parasitic infections in in $vitro$ and murine models (75-78). In contrast, NO-mediated inflammation and pathogenesis in in $vitro$ and murine models have been documented in viral infections like hepatitis C virus, human immunodeficiency virus, Dengue virus, herpes simplex virus, respiratory sincytial virus or influenza virus (14, 79, 80).

The chemical and biological reactivities of NO produced in inflamed tissues during infection or inflammation are greatly affected by concomitant production of oxygen radicals, particularly superoxide (O_2^-) and hydrogen peroxide (H_2O_2). The interaction of NO with reactive oxygen species causes formation of several reactive nitrogen oxides, such as $ONOO^-$ and nitrogen dioxide (NO_2). Excessive $ONOO^-$ formation leads to the formation of nitrated proteins, inhibition of mitochondrial respiration, depletion of cellular energy, nucleic acid damage, apoptosis and necrotic cell death, resulting in cellular/ tissue injury (17, 47, 81).

3-Nitrotyrosine has been used as a marker of peroxynitrite formation and tissue injury. Tyrosine nitration is also becoming increasingly recognized as a functionally signifcant protein modification. Nitration of proteins and enzymes modulates their catalytic activity, cell signaling and cytoskeletal organization (17, 47, 81). Another marker of nitrative stress during viral infections is 8-nitroguanosine, which is formed by nitration of guanosine by $ONOO^-$ or NO_2 (17). The first report of NO-dependent guanosine nitration during viral infection in murine model was provided in 2003 (24). In that

study, extensive 8-nitroguanosine formation in bronchial and bronchoalveolar epithelial cells during both influenza virus and Sendai virus infection was demonstrated. The 8-nitroguanosine formation correlated well with NO production and 3-nitrotyrosine generation. On the other hand, 8-nitroguanosine staining was absent in the airways of genetically modified mice that had a homozygous deficiency for iNOS (iNOS$^{-/-}$) and were infected with influenza virus, suggesting iNOS or NO may be necessary for the formation of 8-nitroguanosine. In subsequent studies in murine models, certain unique features of 8-nitroguanosine were identifed. This line of work established that 8-nitroguanosine has a potent redox-active property and mutagenic potential. Electron spin resonance (ESR) analysis determined that 8-nitroguanosine stimulated generation of O_2^- from cytochrome P450 reductase and iNOS (24, 82). This process is pathophysiologically significant because O_2^- causes increased oxidative damage and ONOO$^-$ formation (17). ONOO$^-$ not only damages host tissues and cells in a nonselective manner, it also affects biomolecules of a host in a relatively selective fashion. For example, ONOO$^-$ activates matrix metalloproteinases (MMPs) – the enzymes that participate in the destruction of the extracellular matrix, which leads to tissue damage and remodeling (83, 84). MMPs are also known to have a critical role in apoptosis induction (84). ONOO$^-$ readily inactivates both tissue inhibitor of MMP and α1-proteinase inhibitor, which is a major proteinase inhibitor in human plasma (85, 86). ONOO$^-$ also activates cyclooxygenase – the key enzyme for production of potent inflammatory prostaglandins (87). Thus, ONOO$^-$ produced during virus-induced inflammation may promote tissue injury in many ways. Other important functions of ONOO$^-$ include the induction of apoptosis and necrosis, possibly via mitochondrial damage, which leads to cytochrome c release (88). The main pathologic effects of NO are presented in **Figure 1.**

1.7 Role of nitric oxide on influenza virus infection in mice

During viral and other microbial infections, NO is produced by iNOS in macrophages and phagocytic cells as an innate host response to the infectious agent. Studies with murine models on the molecular mechanism of iNOS activation revealed that several cytokines, including IFN-γ, TNF-α, and IL-1, are responsible for this activation, with IFN-γ playing the pivotal role (89, 90). IFN-γ is a cytokine of major importance for inducing iNOS and NO overproduction during viral infections (17).
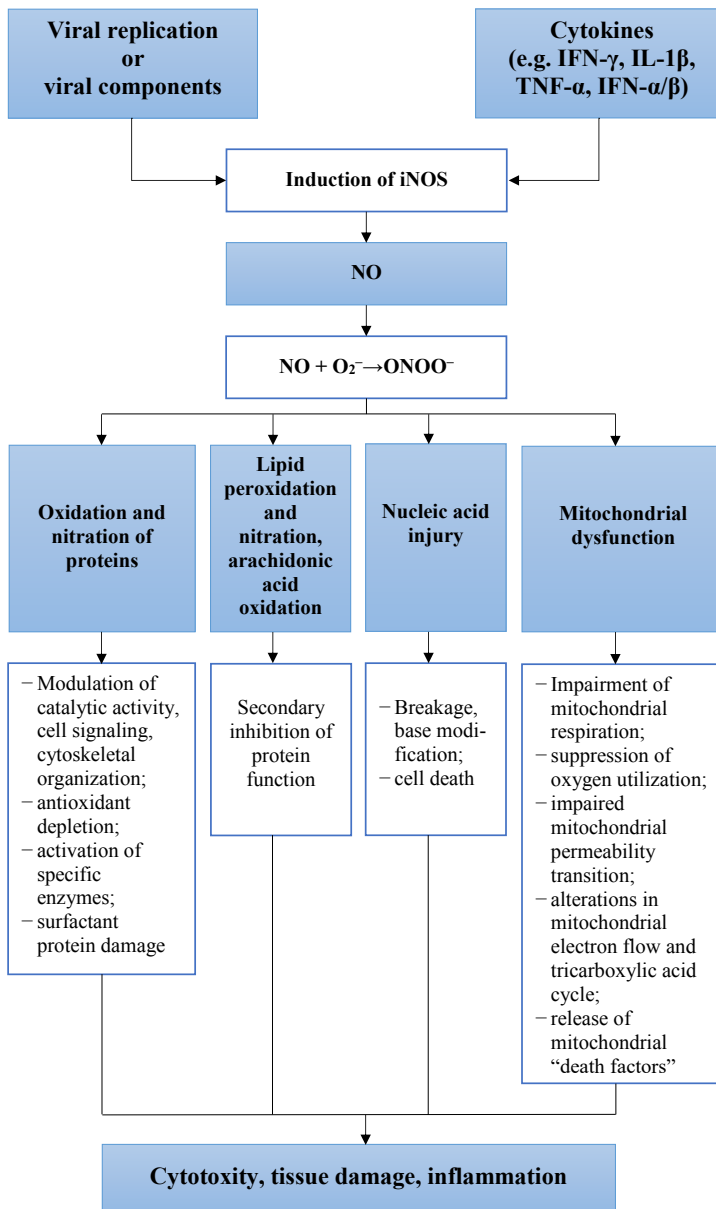
Figure 1. **NO production and its main pathologic effects during pathogenesis of viral infections.**

Inflammatory signals, such as viral products or proinflammatory cytokines, induce the expression of iNOS, that synthesizes NO. Reaction between NO and O_2^- results in a formation of peroxynitrite, which is a strong oxidant and nitrating agent which modifies proteins, lipids and nucleic acids with mitochondrial damage and produces pathologic effects during infectious process.

As an effector molecule produced by phagocytic cells, NO has antiviral activity that is associated with nonspecific damage of host cells and tissues worsening the clinical course of viral infections. Therefore, in spite of the antiviral activity, excessive production of NO could also amplify viral pathogenesis (17). This was demonstrated in a series of investigations on influenza virus infection in mice. In 1996, Akaike et al. (14) demonstrated that overproduction of NO in mouse lungs during influenza virus infection leads to the development of pneumonia. Both the enzymatic activity and mRNA expression of the iNOS were greatly increased in the mouse lungs, and it was mediated by IFN-γ. The chronology of iNOS induction in the lung correlated well with that of pulmonary consolidation rather than that of viral replication (iNOS expression began to increase on the 4th day after virus infection followed by rapid increment until 8 days after infection and diminished quickly thereafer). To establish the occurrence of NO overproduction directly in the mouse lung after infection with influenza virus, lung tissue was analyzed via ESR spectroscopy with a dithiocarbamate and iron complex as a spin trap for NO. Inhibition of NO by N^G-monomethyl-L-arginine (L-NMMA) treatment of the influenza virus-infected mice resulted in significant improvement of the survival rate. Immunohistochemistry with a specifc anti-3-nitrotyrosine antibody showed intense staining of alveolar phagocytic cells, such as macrophages and neutrophils, and intraalveolar exudate in the virus-infected lung. 3-Nitrotyrosine formation as a consequence of peroxynitrite caused protein nitration thus indicating generation of peroxynitrite in the pathological process of influenza virus-induced pneumonia (14). NO-mediated pathogenesis of viral pneumonia was further investigated using genetically deficient iNOS$^{-/-}$ mice. The results revealed that influenza virus infection of the wild-type (iNOS$^{+/+}$) mice increased NO levels in the bronchoalveolar lavage fluid and led to high mortality apparently because of the associated consolidating pneumonia with massive inflammatory foci and edema within the lungs. The mice lacking the iNOS gene survived with little histopathologic evidence of pneumonia (91). Protein nitration as indicated by formation of 3-nitrotyrosine is not the only marker of nitrative stress occurring during viral infections (17). In 2003, Akaike et al. reported NO-dependent nucleic acid damage during viral infection *in vivo* with guanosine nitration and 8-nitroguanosine formation. Wild-type mice and mice deficient in iNOS were infected with influenza or Sendai virus. Formation of 8-nitroguanosine in the virus-infected lungs was assessed immunohistochemically with an antibody

specific for 8-nitroguanosine. The most intense immunostaining for 8-nitro-guanosine was detected in bronchial and bronchiolar epithelial cells at 6–8 days post infection. The staining was lighter in alveolar macrophages. The time profile of 8-nitroguanosine production correlated well with that of NO production and 3-nitrotyrosine generation during influenza virus infection. Moreover, the 8-nitroguanosine staining colocalized with iNOS immuno-staining and was absent in the airways of iNOS$^{-/-}$ mice infected with influenza virus. A significant improvement of the survival as well as reduced pathological change in the lung was found in both iNOS$^{-/-}$ and iNOS$^{+/-}$ mice compared with iNOS$^{+/+}$ mice. iNOS$^{+/+}$ mice infected with influenza virus or Sendai virus had extensive inflammatory cell infiltration and alveolar exudates as well as destruction of pulmonary architecture, whereas in the iNOS$^{-/-}$ mice these changes were significantly less. It is noteworthy that 8-nitroguanosine markedly stimulates O_2^- generation from cytochrome P450 reductase and iNOS *in vitro* (7). The enhanced antiviral antibody secretion during influenza virus infection was also reported in the study with iNOS-deficient mice (10). The data of this investigation suggest that an increased virus-specific antibody response, rather than an enhanced cytotoxic T-cell response, may account for the reduced susceptibility of iNOS$^{-/-}$ mice to influenza A virus infection. Previous studies have demonstrated that influenza A virus replication is sensitive to CD8+ T cell-mediated cytolysis, NK cell effector activity and the presence of virus-specific antibody (92-94). Each of these components of the immune response during infection of iNOS$^{-/-}$ mice with a sublethal dose of virulent influenza A virus was examined in this study. Both influenza A virus specific CD8+ T cell and NK-cell cytolytic activities were similar in iNOS$^{-/-}$ and iNOS$^{+/+}$ mice. Thus, the T-cell and NK-cell cytotoxic responses do not contribute to the increased viral clearance in iNOS$^{-/-}$ mice. However, the virus-infected iNOS$^{-/-}$ mice produced higher levels of virus-specific IgG2a antibody. Furthermore, more viable B cells and plasmablasts, along with greater levels of IFN-γ, were found in iNOS$^{-/-}$ splenocyte cultures stimulated with B-cell mitogens. iNOS$^{-/-}$ mice demonstrated a delay in manifestation of clinical illness and developed a statistically lower clinical illness score from day 7 of infection compared with iNOS$^{+/+}$ mice. Also, there was a significant attenuation in the extent of lung lesions in iNOS$^{-/-}$ mice. Inflammatory cell migration and proinflammatory cytokine production were attenuated significantly in the lungs of influenza A virus-infected iNOS$^{-/-}$ mice. Importantly, this correlated directly with lower clinical illness and lung lesions

observed in iNOS$^{-/-}$ mice, suggesting that iNOS exacerbates viral pneumonia by contributing to the recruitment of inflammatory leucocytes and to the prolonged expression of proinflammatory cytokines (10). Aldridge et al. (95) analyzed the possibility for a new therapeutic intervention proposed for the case of a catastrophic pandemic. They showed that challenging mice with virulent influenza A viruses, including H5N1 strains, caused an increased selective accumulation of a particular dendritic cell subset, the TNF-α/iNOS-producing DCs (tipDC), in the pulmonary airways. However, although it might be expected that eliminating the tipDCs would ameliorate the disease process, the authors found the opposite phenomenon. The tipDCs also drive a local, protective CD8+ "killer" T cell response in the virus-infected respiratory tract. Most interestingly, this study established that partially compromising tipDC recruitment can be protective. Giving mice the peroxisome proliferator-activated receptor-γ agonist pioglitazone diminishes but does not prevent tipDC recruitment, while allowing for sufficient CD8+ T cell expansion to protect against an otherwise lethal or at least highly pathogenic influenza virus challenge (95). It is noteworthy that not only influenza virus infection causes pneumonia associated with iNOS. Other pneumotropic viral infections are also responsible for NO induced damage of lung tissues. A study with herpes simplex virus type 1 (HSV-1)- induced pneumonia in mice was performed (80). Immunohistochemical staining demonstrated iNOS induction and the nitrotyrosine antigen in the lungs of infected, but not of uninfected mice, suggesting that NO contributes to the development of pneumonia. Infected mice treated with the NOS inhibitor, L-NMMA, had less histological evidence of pneumonia, improved survival and pulmonary compliance of HSV-1 infected mice compared with those receiving placebo treatment, despite the presence of high pulmonary viral titers (80). Stark et al. (79) examined the effect of respiratory syncytial virus (RSV) infection on expression of iNOS and the role of NO in the host responses to RSV *in vivo*. NO production, iNOS mRNA and protein levels were significantly increased in RSV infected mice, and immunohistochemical analysis clearly identified iNOS in the respiratory epithelium. Suppression of NO synthesis using iNOS inhibitors increased RSV titers in the lungs, on the other hand, it reduced lung inflammation and RSV-induced airway hyper-responsiveness (79).

Taken together, these data demonstrate the importance of NO in pathogenesis of influenza- and some other viruses-induced pneumonia.

1.8 Role of nitric oxide on influenza virus infection in humans

Data about the implication of NO to the pathogenesis of influenza virus infection in humans are lacking. After the recent 2009 pandemics, more studies focused on human lung histopathology in the course of influenza A (H1N1) virus infection were performed with attention to nitrative stress. Increased NO and reactive oxygen species formation plays a critical role in lung dysfunction during acute lung injury and ARDS (59). Nin et al. (96) analysed light microscopy fndings as well as changes in the nitro-oxidative stress in lung tissue samples from pandemic 2009 influenza (A/H1N1) viral pneumonia and ARDS fatalities. Study specimens came from 6 intensive care unit patients with lethal A/H1N1 influenza viral pneumonia. The predominant pathological findings were diffuse alveolar damage accompanied by hemorrhage, and in some cases, necrotizing bronchiolitis. All cases showed increased tyrosine nitration in the immunofluorescence studies, which indicates formation of peroxynitrite and subsequent protein nitration. The iNOS protein levels were increased in all cases. In addition, oxidized dihydroethidium staining, indicating the formation of oxygen free radicals, was universally increased. The increased oxidized dihydroethidium and nitrotyrosine reactivity were observed even in cases with prolonged ARDS, suggesting a role for prolonged oxidative and nitrative stress in the pathogenesis of ARDS in A(H1N1) influenza virus infection despite antiviral treatment. Other data from this study demonstrated viral proteins within macrophages and type I pneumocytes indicating they may remain in lung tissues for prolonged periods of time and possibly participating in the prolongation of the inflammatory response (96). In another study, a detailed histopathological analysis of the open lung biopsy specimens from five patients with ARDS with confirmed A(H1N1) was performed (97). Lung specimens underwent microbiologic analysis and examination by optical and electron microscopy. Immunophenotyping was used to characterize macrophages, natural killer (NK), T and B cells as well as the expression of cytokines and iNOS. Ultrastructural analysis showed viral-like particles in bronchiolar and alveolar epithelial cells in all cases. The main pathological findings revealed necrotizing bronchiolitis and diffuse alveolar damage; the altered respiratory epithelial cells probably served as the primary target of the infection. In these cases, expression in the lung of IFN-γ by small mononucleated cells and TNF-α by macrophages and alveolar epithelial cells was low. Conversely, a very strong expression of IL-4, IL-10 and iNOS by macrophages was found. The results of this study indicate that in swine-origin

influenza virus infection, altered innate and adaptive immune responses may lead to incomplete virus eradication in the primary target of the infection and, consequently, an imbalance between inflammation and immune down-regulation resulting in bronchiolar obliteration and diffuse alveolar damage (97). The nitrative stress during influenza infection may be evaluated not only by histopathological findings in the lungs, but also serologically. In 2011 Al-Nimer et al. (98) evaluated the levels of NO and peroxynitrite in the serum of patients during seasonal and pandemic A(H1N1) infection. They found the greater levels of serum NO and peroxynitrite in patients infected with seasonal and pandemic A(H1N1) influenza as compared to the healthy control subjects. Although side-by-side comparisons may not be valid, it is interesting to note that the reported serum concentrations of reactive nitrogen species were higher in seasonal influenza patients than pandemic influenza patients.

Despite the differences between murine and human iNOS genes and their induction mechanisms, the evidence supports that infectious processes, including influenza, can trigger a nitrative stress in human lungs contributing to pulmonary inflammation and tissue injury. More investigations are needed to extend our understanding of the reactive nitrogen oxides' role in inflammation and on the iNOS expression regulatory mechanisms, especially in human cells. This may offer new insights for the development of novel treatment of diseases complicated by increased iNOS expression and NO overproduction.

1.9 The pathology of influenza virus infections in humans

The pathology caused by influenza viruses in humans depends on the virulence of the infecting agent and host response. Human influenza viruses in the respiratory tract predominantly attach to ciliated epithelial cells of upper respiratory tract, trachea, and bronchi (99, 100); however, high-virulence viruses [1918 A(H1N1), A(H5N1), and 2009 A(H1N1)] also tend to infect pneumocytes and intraalveolar macrophages. The localization and amount of the inflammatory reaction will depend on the infected cells. Thus, low-virulence viruses [seasonal A(H3N2) and A(H1N1)] cause primarily inflammation, congestion and epithelial necrosis of the larger airways (trachea, bronchi and bronchioles), whereas high-virulence viruses have equal inflammation in these localizations with additional, more extensive areas of inflammation in the alveoli. In susceptible individuals, inflammation of the alveolar walls will result in diffuse alveolar damage (101).

In addition, the pathological picture will change if bacterial superinfection is present. Bacterial pneumonia, either community acquired or nosocomial, with more extensive necrosis and more prominent infiltration of neutrophils, are common in severe influenza and complicate the histopathologic appearance (2, 102). In the 1918 A(H1N1) pandemic, an estimated 96% of the mortality was attributed to secondary bacterial pneumonia (4). In later pandemics, the percentage of mortality attributed to secondary bacterial pneumonia declined in favor of deaths from primary influenza viral pneumonia, likely because of the widespread use of antibiotics (103). Evidence of bacterial coinfection has been described in 29% of pandemic A(H1N1) influenza related deaths (104).

Different fatality and age distribution of deaths were observed with various influenza viruses. The case fatality rate in the 1918 pandemic was considerably higher than it was in other pandemics (102). In the 1957 and 1968 pandemics and especially in interpandemic seasonal influenza cases, fatal cases have mostly occured in people with underlying chronic illnesses or at the extremes of age (2). In comparison with seasonal influenza, deaths associated with novel A(H1N1) infection have disproportionately affected older children and young adults, many of whom lacked known risk factors for serious complications from influenza (102), a pattern similar to the 1918 influenza pandemic. The mortality rate of the highly pathogenic avian-origin influenza virus A(H5N1) has been reported to reach 60%; here, also, the majority of patients are young and without underlying medical conditions (37).

The variable spectrum of influenza histopathology is associated with both the clinical picture and length of the disease course before death. The spectrum of observed pathologic changes in severe influenza cases appears to vary little from pandemic to pandemic or in interpandemic years (2, 101, 102).

Uncomplicated influenza is a mild inflammation of the upper respiratory tract and diffuse superficial necrotizing tracheobronchitis (100). There is desquamation of epithelial cells, edema and hyperemia in the lamina propria, and infiltration with lymphocytes and histiocytes (102). The most common complication of influenza is extension of the virus infection to the lung, resulting in pneumonia.

Classic histopathologic studies of influenza autopsies have clarified the changes characteristic of severe influenza viral pneumonia, namely, capillary and small vessel thromboses, interstitial edema and inflammatory infiltrates, the formation of hyaline membranes in alveoli and alveolar ducts, varying degrees of acute intraalveolar edema and/or hemorrhage, and diffuse alveolar

damage in addition to necrotizing bronchitis and bronchiolitis (2). The pathologic result of influenza virus infection of the alveoli is diffuse alveolar damage. In the early stage, it is characterized by necrosis of alveolar epithelium and flooding of the alveolar lumina by edema fluid, mixed with variable proportions of fibrin, erythrocytes, alveolar macrophages, and neutrophils. Some alveoli are lined by hyaline membranes, which are composed of cellular and proteinaceous debris and appear as dense, glassy eosinophilic membranes lining the alveolar ducts and alveolar spaces (102, 105). The alveolar septa are widened because of hyperemia, edema, and infiltration by mainly neutrophils. Alveolar capillaries and small pulmonary blood vessels may contain fibrin thrombi. At the later stage of diffuse alveolar damage, there is type II pneumocyte hyperplasia, interstitial fibrosis of alveolar septa, and infiltration predominantly by lymphocytes and plasma cells (102). Hemophagocytosis was also a common histological finding in patients with 2009 A(H1N1) or A(H5N1) autopsies, and the possibility of hemophagocytic syndrome should be considered in patients with severe infection (2, 101, 106). In secondary or coincident bacterial pneumonias a massive infiltration of neutrophils into alveolar air spaces is observed, and alveolar hemorrhage and edema are less pronounced than in primary influenza virus pneumonia (2).

In a study, describing 2009 A(H1N1) influenza pathology and pathogenesis of 100 fatal cases in the United States, the most frequent histopathological findings in airways were inflammation and edema. The inflammation was usually mild and consisted predominantly of mononuclear cells. Necrosis of epithelium (26%) and hemorrhage (18%) were less frequently observed. Lung tissues in all case-patients showed a spectrum of histopathological changes of diffuse alveolar damage (DAD), including edema, hyaline membranes, inflammation, and fibrosis. The nature and extent of DAD generally corresponded to the duration of clinical illness of the patients. Bacterial pneumonia was present in 29% of case-patients in this series (107).

Mauad *et al*. in another study of lung pathology in fatal 2009 A(H1N1) infection also observed that the fatalities were related to extensive diffuse alveolar damage, with variable degrees of pulmonary hemorrhage and necrotizing bronchiolitis. Interestingly, they noticed, that patients with necrotizing bronchiolitis had a more severe neutrophil-predominant inflammatory exudate compared with the others and were more prone to developing bacterial coinfections. The severe alveolar hemorrhage was associated with comorbidities, such as chronic cardiovascular disease and

coagulopathies, conditions that predispose the patients to increased alveolar pressure and bleeding (108).

In limited autopsy studies of fatal H5N1 virus infection lungs presented with diffuse alveolar damage. In most cases, H5N1 antigens and RNA were detected in extrapulmonary organs, suggesting disseminated systemic H5N1 infection and viremia. An acute intra-alveolar edema, congestion and/or hemorrhage, desquamation of pneumocytes, interstitial and intra-alveolar inflammatory cell infiltration, fibrosis and type II pneumocyte hyperplasia were observed in a study of five fatal H5N1 cases (109).

It should be noted that the pathological descriptions in humans come mostly from autopsy material and only changes associated with lethal outcomes and predominantly late-stage disease have been well characterized. More complete data on the pathology of influenza virus infection are available from the murine model.

1.10 The pathology of influenza virus infections in a mouse model

Mice have many advantages as a model for influenza virus research, including their relatively low cost, ready availability, small size, and ease of handling and housing. Susceptibility of mice to influenza virus infection vary according to their genetic background, the influenza virus strain, and the virus inoculum. The main drawback to the mouse model is the need to use mouse-adapted viruses in order to achieve productive infection and clinically apparent signs of disease. Additionally, murine influenza is a primarily lower respiratory tract infection that is physiologically dissimilar from typical uncomplicated influenza in humans (110).

The clinical signs of influenza virus infection in mice have some differences from those of typical human influenza (110, 111). Upon infection with certain influenza virus strains, mice display marked anorexia and demonstrate behaviors consistent with physical discomfort or lethargy. Unlike humans, though, mice have been reported to become hypothermic upon influenza virus infection, rather than mounting a febrile response (111). Importantly, influenza in mice characteristically manifests as a primary viral pneumonia, which is demonstrated clinically by labored breathing and cyanosis and post-mortem by severe pulmonary histopathology (111, 112).

Experimental animal models and humans infected with influenza A viruses share many histologic features, including desquamation of the ciliated

epithelium of the tracheobronchial airways and peribronchial mononuclear cell inflammatory infiltrates, evidence of viral degeneration of alveolar lining, hyperemia and congestion, septal inflammatory infiltrates, the appearance of macrophages with necrotic cellular debris in air spaces, and intraalveolar edema and hemorrhage (2). Numerous studies have examined 1918 A(H1N1) influenza viruses in murine models (8, 113-115). Experimental infection with the 1918 A(H1N1) virus caused high mortality in mice, with lesions restricted to the respiratory tract. The most consistent histologic lesions included necrotizing bronchitis, bronchiolitis, and alveolitis with alveolar edema and alveolar hemorrhage, with viral antigen in ciliated bronchiolar epithelial cells, type II pneumocytes, and alveolar macrophages (102, 116). The alveolitis was peribronchiolar to diffuse in distribution and primarily neutrophilic in character, although histiocytes also were prominent. Lungs of mice infected with the 1918 A(H1N1) virus had about 3 times more inflammatory cells than those of mice infected with a seasonal A(H1N1) virus but similar numbers as those infected with H5N1 virus (102, 113).

Experimental pandemic A(H1N1) virus infection in mice resulted in prominent bronchiolitis and alveolitis with viral antigen in ciliated bronchiolar epithelial cells, type II pneumocytes, and alveolar macrophages. Compared to currently circulating seasonal human A(H1N1) viruses, pandemic A(H1N1) virus replicated more efficiently in the mouse lungs and caused more severe lesions (102, 117).

Experimental H5N1 virus infection in mice generally caused severe disease and high mortality. The main histologic lesions occurred in the respiratory tract. There was epithelial necrosis in the nasal cavity, trachea, bronchi, and bronchioles, with fibrin and neutrophils in the airway lumina. Alveolitis was characterized by the presence of serous fluid mixed with fibrin, erythrocytes, and neutrophils in alveolar lumina, as well as increased numbers of alveolar macrophages (102, 118, 119).

Most histopathologic studies of human influenza autopsies demonstrated DAD. However, DAD in mice has only recently been reported (120). After inoculation of mice with two adapted highly virulent influenza A subtypes, A(H1N1) and A(H5N1), the final common feature was DAD by day 7 or in dying mice, whichever came first; note that there were differences in pathologic signature and course of ARDS. Some of the changes in lung morphology were identical for both viruses. First, a clear topographic extension of the lesions was perceptible between the first and the last day of infection, with centrifugal spreading from the terminal bronchioles or the alveoli adjacent to the airways.

Qualitatively, all alterations characterizing the exudative phase of the DAD were identifiable, with intense congestion of the alveolar capillaries, marginated intracapillary neutrophils, necrosis of the alveolar epithelium, interstitial and alveolar edema, hyaline membranes, and invasion of the alveoli by (mostly) mononucleate cells. On the other hand, there was no cuboidalization of the alveoli (hyperplasia of type II pneumocytes) or hyperplasia or squamous metaplasia of the airway epithelia. These results indicate either or both extremely rapid disease progression and nearly complete elimination of type II pneumocytes. Despite these similarities, there were differences between subtypes of influenza viruses. The lung lesions attributable to the subtype A(H1N1) strain were characterized by the following: 1) earlier and much more extensive degeneration, necrosis, and desquamation of the airway epithelium; 2) a much higher cell density of the peribronchial, peribronchiolar, interstitial, and intra-alveolar infiltrates; 3) the presence of dense cuffs of mononuclear cells around the arterioles; 4) far less extensive alveolar edema; and 5) only rare alveolar hemorrhage. The lesions caused by the subtype H5N1 strain were distinguishable by the late and mild, regressive alterations of airway epithelium, the extent of alveolar edema, a low cell density of inflammatory infiltrates, a high number of alveolar hemorrhagic foci, and the unusual finding where the pulmonary arterioles appear to be dissected from the surrounding tissues due to the magnitude of the perivascular edema. Interestingly, no arteriolar cuff of infiltrated mononucleate cells was observed. Some blood-vessel walls also showed hemorrhage inside the muscle layer. These results suggest that the pathogenesis of fatal infections from different highly virulent influenza A viruses are not the same (120).

Fukushi et. al., (112) described the sequence of pathological changes from interstitial pneumonia to DAD in the lungs of mice infected with PR8 influenza virus. Interstitial pneumonia was observed early in the course of infection, but DAD was found later, when the mice were dying or dead. The histopathological characteristics of DAD of PR8-infected mice, with hyaline membrane formation, inflammatory cell accumulation and pulmonary edema, closely resembled the characteristics of DAD at the exudative stage in humans. Histopathological examination of mice sacrificed 2 to 6 days post-infection showed graddually expanding interstitial pneumonia from the pulmonary parenchyma around bronchioles to the entire lungs, but without DAD. DAD with severe alveolar collapse was found 8 days post-infection in mice where death was imminently expected within 24 hours; this was present in all of the dead mice, several of which were autopsied immediately after their deaths.

The results indicate that DAD is not a postmortem change and pulmonary expansion of DAD is implicated in contributing to lethal PR8 infection in the mouse model (112). This is consistent with the observation of DAD in autopsies of many patients who died with severe viral pneumonia and ARDS induced by influenza virus (2).

1.11 Principles of antiviral treatment of influenza

Influenza A virions have three surface proteins, the hemagglutinin (HA), neuraminidase (NA), and the matrix (M2) protein. The HA binds to terminal sialic acids on cellular receptors, preceding virus endocytosis. The low endosome pH activates the influenza A M2 membrane proton channel to acidify the virus interior before HA-mediated fusion. This acidification triggers the release of the virus ribonucleoprotein (RNP). After replication, the viral proteins appear on the host cell membrane. Here the membrane with viral surface proteins buds from the cell membrane as whole progeny virions, except still attached to the cell membrane sialic acid via the HA. The NA of progeny virions cleaves sialic acids from the cell receptors from the virion HA, releasing the virus from the cell. By cleaving sialic acid, the NA also prevents self aggregation and clumping, facilitating its spread to other cells.

Two major classes of antivirals have been in use for the treatment and prevention of influenza, the M2 inhibitors and the NA inhibitors (NIs). By blocking the M2 proton channel, the M2 inhibitors prevent endoviral acidification and release of the virus RNP for migration to the nucleus of the cell. The NA inhibitors (NIs) prevent release of newly formed virions from the cell surface. Since the M2 protein is only found in influenza A viruses, the M2 inhibitors, amantadine and rimantadine, only act on influenza A viruses; this limits their use to influenza A. Their use has been further limited because resistant viruses emerge rapidly in treated patients. (121).

There are several NIs licensed globally for the treatment and prevention of influenza. Zanamivir was the first in this class followed by oseltamivir (122, 123). Zanamivir was developed based on two key findings. Firstly, the transition-state analog 2,3-dehydro-2-deoxy-N-acetylneuraminic acid (DANA) was known to be a weak inhibitor of the NA. Secondly, the structure of the sialic acid substrate in complex with the enzyme active site revealed an empty negatively charged pocket in the region of the C4 on the sugar ring. This suggested that substitution of the C4-OH with a larger basic residue might lead to higher affinity binding (124). A single substitution of the C4-OH with

a 4-guanidino group enhanced binding more than 10 000- fold over DANA. Zanamivir is administered by oral inhalation as it is not readily absorbed. Oseltamivir was subsequently designed based on knowledge from zanamivir. While based on DANA, it has a cyclohexene ring with two substitutions compared with DANA. It has a C4 amino group and a bulky hydrophobic pentyl ether side chain in place of the glycerol side chain. It is administered as the prodrug oseltamivir phosphate and converted by hepatic esterases to the active compound oseltamivir carboxylate. The NIs prevent release and spread of progeny virions by blocking NA function (121, 125). In mouse influenza models the NIs were effective in reducing pulmonary virus titers, lung consolidation and mortality scores (125-127).

However, oseltamivir-resistant seasonal A(H1N1) viruses, and to a lesser degree pandemic 2009 A(H1N1) influenza viruses, have been reported worldwide. Emergence of drug resistance against antiviral compounds is a common problem, with some influenza virus strains developing resistance to oseltamivir over a remarkably short time frame (127-130).

On October, 2018 a new antiviral medication for treatment of influenza A and B, Baloxavir marboxil (trade name Xofluza), was approved by the U.S. Food and Drug Administration. It may be used for the treatment of acute uncomplicated influenza in people 12 years of age and older who have been symptomatic for no more than 48 hours and is given as a single dose by mouth (131). It acts unlike neuraminidase inhibitors which inhibit the liberation of viruses from the infected cell surface. Baloxavir marboxil inhibits the cap-dependent endonuclease activity of the influenza polymerase (132).

Treatment of influenza infection is indicated for patients hospitalized with suspected or confirmed influenza and individuals at high risk of developing influenza-related complications. Treatment can also be considered for uncomplicated influenza infections in low-risk individuals who present within 48 h of symptom onset (133). While some investigators have questioned the clinical benefit of oseltamivir for uncomplicated IAV and influenza B virus infection, most studies suggest improved clinical outcomes in severely ill patients, even when therapy is administered relatively late in the infection (134-137).

The limited effectiveness of antivirals in some clinical situations and emergence of drug resistance still present a need for new infuenza treatment strategic approaches.

1.12 Principles of antisense oligonucleotide therapy

A relatively new approach to inhibit iNOS activity involves antisense mediated gene knock-down. Antisense oligonucleotides (ASO) are short single-stranded synthetic nucleic acid polymers, consisting usually of 15–25 nucleotides that induce the inhibition of target gene expression by exploiting their ability to bind to the target messenger RNA (mRNA) by Watson Crick base-pairing. The antisense effects (sequence-specific effects) of ASO are mainly due to the hybridization with the target mRNA in a sequence-dependent complementary manner (binding is performed via hydrogen bonds) (138). In contrast to chemical inhibitors, the ASO technique does not primarily affect the protein and its enzymatic activity. ASO are designed to selectively block gene expression at the point of transcription prior to translation and thereby block production of the relevant protein.

There are some advantages for targeting RNA over protein molecules. As a single copy of RNA could be a template for the synthesis of multiple copies of a protein, it would be more efficient to regulate the mRNA level rather than the protein level to block the protein function (138). Another benefit of using oligonucleotide strategy comes from the complete decoding of the human genome, which greatly shortens the time between identification of gene targets and the design and validation of oligonucleotide products (139).

Since the first report, describing the use of ASO targeting Rous sarcoma virus 35S RNA as a potential oligonucleotide therapy, there have been some disappointments with some early drugs entering clinical trials (140). Early on, unmodified or minimally modified compounds were rushed to the clinic without conjugates or delivery vehicles. Massive dose requirements and limited clinical efficacy created a negative view of the technology, damaging the reputation of the field of oligonucleotide therapeutics for years. But advances in oligonucleotide chemistry and understanding of fundamental principles that define the *in vivo* behavior of oligonucleotides have enabled oligonucleotide therapeutics to achieve clinical utility in some tissues (141). Four ASO compounds have received marketing authorization (Fomivirsen for Cytomegalovirus retinitis in 1998, Mipomersen for Homozygous familial hypercholesterolemia in 2013; Eteplirsen for Duchenne muscular dystrophy and Nusinersen for Spinal muscular atrophy in 2016) and more than 100 clinical trials with antisense compounds are listed on ClinicalTrials.gov (142, 143). As naked ASO can be easily degraded by nucleases in the biological fluid, various chemical modifications have been developed to improve its

stability, potency, and safety in biological systems (139). Phosphorothioate (PS)-containing oligonucleotides were one of the earliest and remain one of the most widely used backbone modifications for antisense drugs (144, 145). PS-containing ASO differ from natural nucleic acids in that one of the nonbridging phosphate oxygen atoms is replaced with a sulfur atom. The PS linkage greatly increases resistance to nucleolytic degradation and PS oligodeoxynucleotides are able to efficiently elicit RNase H cleavage of the target RNA, which is critical in the mechanism of action of many antisense drugs. Additionally, the PS modification confers a substantial pharmacokinetic benefit by increasing the binding to plasma proteins, which prevents rapid renal excretion and facilitates binding to other acceptor sites that facilitate uptake to tissues (145). To further enhance stability *in vivo* and target mRNA binding affinity, second generation ASOs were designed with additional modifications such as 20-O-methyl (20-OME) or 20-O-methoxyethyl (20-MOE) coupled with PS backbone. However, 20-sugar modifications block the recruitment of RNase H (146). Therefore, a chimeric "gapmer" ASO structure was developed, which maintains a sequence of simple PS-modified backbone residues, referred to as the gap, to facilitate RNase H activity and sugar-modified residues on either side of the gap as protective wings (147). The third generation ASOs were developed with a variety of modifications including peptide nucleic acid, locked nucleic acid, and phosphoroamide morpholino oligomer (PMO) in the ASO furanose ring, ribose sugar, and backbone structure, which further enhance their nuclear resistance, target affinity, and pharmacokinetics (148).

Different types of ASO mechanisms can be broadly classified as cleavage-dependent mechanisms and occupancy-only mechanisms. Oligonucleotides that work through an RNase H–dependent cleavage mechanism are the best understood class of ASO, accounting for the majority of drugs in development (145). RNase H is a family of enzymes present in all mammalian cells that mediates the cleavage of the RNA in an RNA-DNA heteroduplex, leading to the degradation of the targeted mRNA, and thus preventing translation to a specific protein (138, 149). Some ASOs target the 5' end or AUG initiation codon region of the target mRNA to prevent translation by steric hindrance of ribosomal activity without degradation of the targeted mRNA (150). Other mechanisms of ASO-mediated gene silencing include interference with mRNA maturation such as inhibition of 5' cap formation, modulation of splicing, and blockade of polyadenylation of pre-mRNA in the nucleus (151).

1.13 Respirable antisense oligonucleotides

The lungs represent the site of entry and intracellular establishment of many airborne pathogens including viruses (e.g., influenza, SARS, RSV) and bacteria (e.g., *Streptococcus pneumonia*, *Mycoplasma pneumonia*, *Mycobacterium tuberculosis*) and is a frequent site of tumor development, genetic diseases (e.g., cystic fibrosis), and immunological disorders (e.g., bronchitis, asthma, lung fibrosis, chronic obstructive pulmonary disease) (152). Respiratory diseases are uniquely suitable for the inhalation route of drug administration, and this route offers dosing advantges because it eliminates first-pass metabolism by the liver. In the lungs, uptake of aerosolized oligonucleotides has been demonstrated in immune cells like alveolar macrophages, as well as in structural cells such as bronchial and alveolar epithelial cells (153, 154). Absorption of oligonucleotides by inhalation, occurring mainly within the respiratory tracts with minimum systemic absorption, is a proposed advantage over oral or systemic administration (139). ASO delivered as aerosols directly to the lungs, minimize the potential for non-antisense systemic side effects and toxicity (155). The majority of oligonucleotide therapies are given systemically; however, effective delivery of the ASO to their intracellular sites of action still remains a major challenge (139). Current approaches to facilitate oligonucleotide delivery include lipid and polymer-based nanoparticles and various ligand-oligonucleotide conjugates (156). The airways are uniquely lined with surfactants that are mostly zwitterionic lipids. These surfactant lipids possess cationic properties at the pH of the respiratory tract. When anionic oligonucleotides are inhaled, they tend to be adsorbed by the surfactants, resulting in reformulated particles that have been hypothesized to be efficiently taken up into the cells (155). To date, most inhaled oligonucleotide products that have demonstrated efficacy in humans through aerosolization of simple aqueous solutions and do not contain any carrier molecules to enhance delivery (157). Local delivery of ASO to the airways is effective at smaller doses compared with other routes of administration (138).

In the treatment of asthma, ASO can be used for silencing of gene expression, at post-transcriptional level, for many molecular targets: cell membrane receptors (G-protein coupled receptors, cytokine and chemokine receptors), membrane proteins, ion channels, cytokines and related factors, signaling non-receptor protein kinases (tyrosine kinases, such as Syk, and serine/theonine kinases, such as p38 MAP kinase) and regulators of transcription belonging to Cys4 zinc finger of nuclear receptor type

(GATA-3) or beta-scaffold factors with minor groove contacts (p65, STAT-6) classes/superclasses of transcription factors (158). A number of ASOs targeting different signaling pathways involved in pathogenesis of pulmonary fibrosis have also been investigated, like basic fibroblast growth factor (bFGF), TNF-α or NF-κB p65 subunit's ASOs (139).

1.14 Antisense oligonucleotides against influenza

Rapid increase in drug-resistant influenza virus isolates, and pandemic threat posed by highly pathogenic avian influenza A and swine flu viruses provide clear reasons for fast tracking development of novel antiviral drugs. Nucleic acid-based drugs represent a promising class of novel antiviral agents that can be designed to target various seasonal, pandemic and avian influenza viruses (159). Nucleic acids can be focused on various influenza virus gene targets or designed to elicit broad-spectrum antiviral responses in the host.

The experimental usage of ASOs against influenza viral targets has been reported in both *in vitro* tissue culture as well as *in vivo* animal infection model systems. ASOs targeting the polymerase (PA, PB1, PB2) and nucleoprotein (NP) genes were shown to be able to inhibit the replication of influenza A virus (H1N1 and H5N1) *in vitro* and *in vivo* (160-162). Antisense ODNs (15-mer) directed against a conserved region of the influenza A virus HA gene have also been shown to be effective in the post–exposure treatment of influenza A virus infection in mice. In this study, both un-encapsulated and liposome-encapsulated ASOs, administered intranasally, were completely effective in the treatment of mice against an otherwise lethal respiratory challenge (163). The modified ASOs, phosphorodiamidate morpholino oligonucleotides conjugated with arginine-rich peptides were evaluated for their ability to inhibit influenza A/PR/8/34 virus (H1N1) replication in cell culture (164). These ASOs were designed to base pair with influenza A virus RNA sequences that are highly conserved across viral subtypes and considered critical to the influenza virus biological-cycle, such as gene segment termini and mRNA translation start site regions. Several phosphorodiamidate morpholino oligonucleotides were highly efficacious and two of them, targeted to the PB1 AUG translation start site and to the 3'-terminal region of viral NP RNA, proved to be potent against several influenza A strains, suggesting that phosphorodiamidate morpholino oligonucleotides may represent a broadspectrum approach against influenza (164). *In vivo* studies in mice demonstrated that PMO administration improved survival from influenza infection from 0% to 30–95%, with the survival

rate dependent on the dose, timing of PMO administration, mRNA/vRNA sequence targeted by the PMO and the viral strain (165, 166). In addition, a phosphorodiamidate morpholino oligomer, radavirsen (AVI-7100), targeting expression of the M1 and M2 genes has been designed. Radavirsen is effective against influenza A (H1N1 and H3N2) in animal models and currently is in phase I clinical trials as a candidate agent for treatment of influenza infections (167, 168).

Host-directed therapy is an emerging approach in the field of anti-infectives. The strategy behind host-directed therapy is to interfere with host cell factors that are required by a pathogen for replication or persistence, to enhance protective immune responses against a pathogen, to reduce exacerbated inflammation and to balance immune reactivity at sites of pathology (169). A number of influenza antiviral drugs targeting host factors with different mechanisms of action are under development (170). One among them is the sialidase drug DAS181, which removes sialic acids on respiratory epithelial cells and prevents virus attachment to the receptor (171). Inhibitors of the Raf/MEK/ERK signaling pathway have also been demonstrated to be successful in inhibiting virus infection (172). Treatment with immunomodulatory drugs targeting the host immune system, such as COX-2 inhibitors and S1P agonists have been found to alleviate tissue damage caused by virus-induced cytokines and also suppress virus replication (173-175). ASOs targeting host factors in infuenza infection are also under investigation. Antisense peptide-conjugated morpholino oligomer targeting the hemagglutinin-activating cellular protease inhibited influenza virus infection in human airway cell cultures (176). Another ASO, Prop5, that targets programmed cell death protein 5, administered intranasally manifested anti-IAV activity at reducing death of infected mice, lessening weight loss, reducing viral load and titres, and preventing lung consolidation (177).

There is evidence that affecting iNOS function in host cells has therapeutic potential for control of lung inflammation and damage during influenza (10, 14, 24). Potential applications for *in vivo* gene therapy using NOS overexpression or inhibition may cover a broad range of vascular or inflammatory disorders (178). Direct inhibition of the iNOS expression with antisense ODNs against iNOS mRNA has been demonstrated in animal models for encephalomyelitis, sepsis, cerebral and renal ischaemia, inflammatory bowel diseases (179-183). However, to our knowledge the present study is the first to demonstrate the therapeutic effects of antisense oligonucleotide to iNOS mRNA in the mouse influenza model.

2. MATERIALS AND METHODS

2.1 Animals

Female BALB/c mice (6−12 weeks of age) weighing 18−20 g were obtained from the Charles River Laboratories, Inc., Wilmington, MA, USA. The mice were housed within microisolator cages in an isolation room, and all experimental procedures were performed in a biosafety cabinet using biosafety level 2 containment. Experimental groups and the number of mice are listed in **Table 1**. The animals were anesthetized by intraperitoneal injection a mixture of ketamine (50 mg/kg) and xylazine (50 mg/kg) before every procedure: virus inoculation, any treatment and euthanasia. The experimets with mice were performed in Eastern Virginia Medical School, Norfolk, VA, U.S.A. All protocols involving experiments with mice were approved by the Institutional Animal Care and Use Committee, Eastern Virginia Medical School, Norfolk, VA, U.S.A. (permit no. 07-003). The animal experiments were carried out within the provisions of the Animal Welfare Act (Public Law 99-198), the National Research Council, the Public Health Service Policy on Humane Care and Use of Laboratory Animals, the "Guide for the Care and Use of Laboratory Animals (1996)", the Health Research Extension Act of 1985 Public Law 99-158 (11/20/86), and United States Department of Agriculture regulations.

2.2 Influenza virus infectivity

The mouse-adapted influenza A/Puerto Rico/8/34 (A/PR/8/34) (H1N1) virus, a kind gift of Dr. Bradley S. Bender (College of Medicine, University of Florida, Gainesville, FL, USA), was propagated in the allantoic cavities of 10-day-old embryonated chicken eggs as previously described (184). For the determination of influenza A/PR/8/34 virus infectivity titer, confluent monolayers of Madin-Darby canine kidney cells (American Type Culture Collection No. CCL-34, Manassas, VA, USA) were inoculated with the virus stock of serial 10-fold dilutions. The 50% tissue culture infectious dose (TCID$_{50}$) was evaluated according to the extent of viral cytopathic effect in monolayers after 96 h. The virus infectivity titer was calculated using Kärber method, and it was determined as $10^{8.4}$ TCID$_{50}$/mL (184). Afterwards, different serial dilutions of the virus stock were tested on mice by challenging them with a single 20 µL dose of the virus suspension (10 µL/nostril) for

Table 1. The experimental groups and number of mice

Mouse group	Number of mice
Negative controls	29
• Uninfected, treated with PBS, euthanized on day 5	3
• Uninfected, treated with lactose, euthanized on day 3	3
• Uninfected, treated with lactose, euthanized on day 5	3
• Uninfected, treated with zanamivir, euthanized on day 3	3
• Uninfected, treated with zanamivir, euthanized on day 5	3
• Uninfected, treated with iNOS antisense ODN, euthanized on day 3	3
• Uninfected, treated with iNOS antisense ODN, euthanized on day 5	3
• Uninfected, treated with zanamivir + iNOS antisense ODN, euthanized on day 3	4
• Uninfected, treated with zanamivir + iNOS antisense ODN, euthanized on day 5	4
Positive controls	17
• Influenza infected, euthanized on day 3	3
• Influenza infected, euthanized on day 5	3
• Influenza infected, treated with PBS, euthanized on day 5	3
• Influenza infected, treated with lactose, euthanized on day 3*	4
• Influenza infected, treated with lactose, euthanized on day 5**	4
Zanamivir treatment group	10
• Influenza infected, treated with zanamivir, euthanized on day 3	5
• Influenza infected, treated with zanamivir, euthanized on day 5	5
iNOS antisense ODN treatment group	12
• Influenza infected, treated with iNOS antisense ODN, euthanized on day 3	6
• Influenza infected, treated with iNOS antisense ODN, euthanized on day 5***	6
Zanamivir + iNOS antisense ODN treatment group	12
• Influenza infected, treated with zanamivir + iNOS antisense ODN, euthanized on day 3	6
• Influenza infected, treated with zanamivir + iNOS antisense ODN, euthanized on day 5****	6

*1 mouse found dead on day 1, harvested; **2 mice found dead on day 4, harvested;
***2 mice found dead on day 4, harvested; ****1 mouse euthanized on day 4.

iNOS antisense ODN – inducible nitric oxide synthase antisense oligodeoxynucleotide

five days in order to determine the virus infectivity titer that produces a significant infection without causing death. According to the body weight loss and survival rate of mice, the virus infectivity titer of $10^{7.6}$ TCID$_{50}$/mL was determined and selected for further experiments.

2.3 Compounds and dosage

Zanamivir (5-(acetylamino)-4-((aminoiminomethyl)-amino)-2,6-anhydro-3,4,5-trideoxy-D-glycero-D-galacto-non-2-enonic acid) was obtained from GlaxoSmithKline, Research Triangle Park, NC, USA as drug Relenza™ consisting of a powder mixture of 5 mg of zanamivir and 20 mg of lactose per blister.

The antisense oligonucleotide to iNOS was synthesized as an unmodified oligodeoxyribonucleotide (ODN) with phosphodiester internucleotide linkages at Sigma-Aldrich, St. Louis, MO, USA. The antisense ODN sequence comprised of 21 nucleotides: 5′-CAAGCCATGTCTGAGACTTTG-3′, corresponding to bases 1 through 21 of the translation initiation site of mouse iNOS mRNA, as reported by Ding et al (179).

Lactose was obtained from Sigma-Aldrich, St. Louis, MO, USA.

The compounds were prepared in sterile phosphate-buffered saline (PBS), pH 7.4, for intranasal administration of 20 µL (10 µL/nostril) to the mice. The dosage of zanamivir (2 mg/kg) and antisense ODN (5 mg/kg) for the mice was based on therapeutic dose ranges of these compounds provided in the literature (125, 127, 177, 179, 185). In this regard, the doses of zanamivir and antisense ODN for the local delivery to target tissues are in the ranges of 0.3–12.5 mg/kg and 5–20 mg/kg, respectively. The dose of lactose (placebo) was 8 mg/kg. The compounds were administered in a single-dose regimen to minimize the animal stress caused by the treatment procedures.

2.4 Experimental design

The anesthetized mice were inoculated intranasally with 20 µL of influenza A/PR/8/34 virus suspension containing infectivity titer of $10^{7.6}$ TCID$_{50}$/mL. At 3 h post-infection, mice were treated daily with 2 mg/kg dose of zanamivir, 5 mg/kg dose of antisense ODN or a combination of zanamivir (2 mg/kg) plus antisense ODN (5 mg/kg) for 3 or 5 days. These doses of zanamivir and antisense ODN were administered to the anesthetized mice in 20 µL of PBS using a single-dose regimen at the concentrations of 2 µg/µL and 5 µg/µL,

respectively. The negative controls were uninfected mice treated with either 20 µL of PBS, lactose, zanamivir, antisense ODN or combination of zanamivir and antisense ODN in the same dosages. The positive control groups consisted of infuenza infected only, infected and 20 µL of PBS or lactose treated mice in the same dosages (**Table 1**). Mice were monitored daily for morbidity, as measured by weight loss. After 3 or 5 days, mice were euthanized by axillary bleeding (terminal exsanguination), and then the lungs of mice were excised and subjected to bronchoalveolar lavage (BAL). For the BAL procedure, the trachea was cannulated and the lavage of lungs was performed twice with 1 mL of PBS. The collected BAL fluids were centrifuged at 735 × *g* for 5 min, and the supernatants were frozen at −80 °C until determination of nitrite levels. Immediately after the BAL procedure, the left lung was placed in 4% paraformaldehyde (Thermo Fisher Scientific, Waltham, MA, USA) until processing for histological examination. The right lung was immersed in the TRIzol™ reagent (Thermo Fisher Scientific, Waltham, MA, USA) and homogenized on dry ice by using a Tissue Tearor (Dremel, Racine, WI, USA). The lung tissue homogenates were centrifuged at 12 000 × *g* for 5 min at 4 °C, and the supernatants were frozen at −80 °C. Afterwards, they were used for isolation of RNA followed by determination of the levels of viral RNA, iNOS and cytokine (*i.e.*, IFN-γ, TNF-α) mRNA applying a multiplex real-time quantitative reverse transcription (qRT)-PCR.

The basic statements of the experiment and analysed parameters are presented in the **Figure 2.**

2.5 RNA isolation and multiplex real-time quantitative reverse transcription (qRT)-PCR

Total RNA was isolated from lung homogenates using TRIzol™ reagent according to the instructions provided by Thermo Fisher Scientific, Waltham, MA, USA. The levels of viral RNA (encoding influenza A virus (IAV) polymerase acidic (PA) protein, which is highly conserved and essential for efficient viral replication), iNOS, IFN-γ, TNF-α and beta (β)-actin mRNA were determined by the multiplex real-time qRT-PCR using SensiFAST™ Probe No-ROX One-Step Kit (Bioline Reagents Ltd, London, UK). Primers and hydrolysis probes, comprising of the nucleotide sequences shown in **Table 2**, were synthesized by Biolegio B.V., Nijmegen, Netherlands. The primer and probe sequences were designed using Vector NTI Advance™
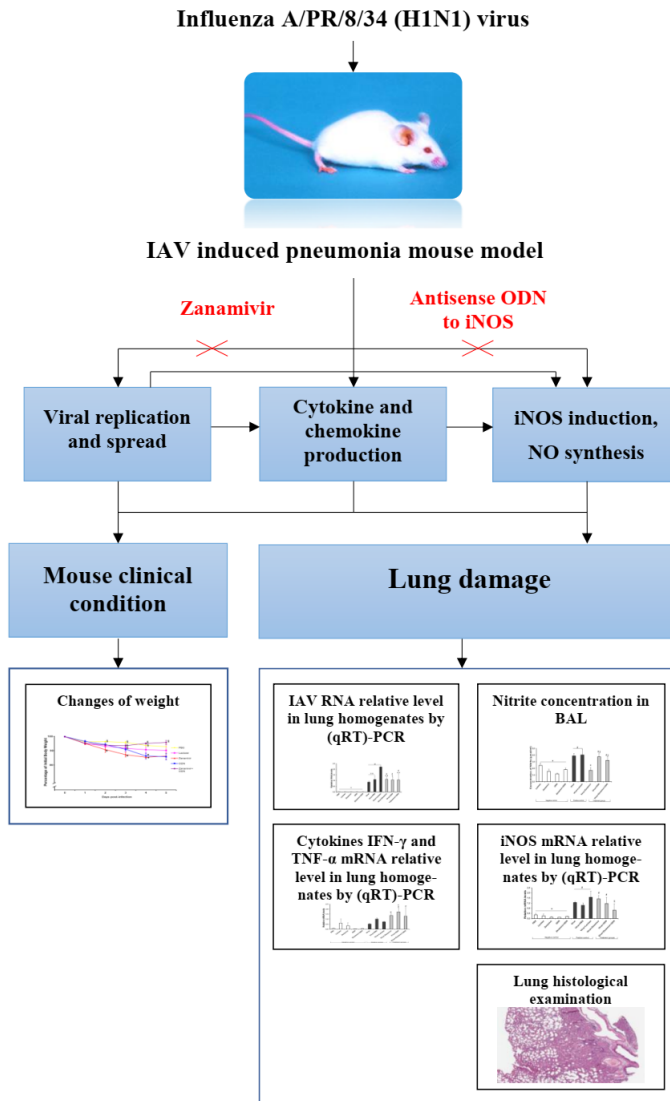
Figure 2. **The evaluated parameters of the IAV induced pneumonia mouse model experiment.**

Influenza A/PR/8/34 virus infected mice were treated with either zanamivir or antisense ODN to iNOS, or both combined. Changes of mouse weight, IAV RNA, cytokines IFN-γ, TNF-α mRNA relative levels in lung homogenates, nitrite concentration in BAL, iNOS mRNA relative level in lung homogenates and lung histology were evaluated.

Table 2. Primer and probe sequences used in the multiplex real-time quantitative reverse transcription (qRT)-PCR

Primer/probe	Sequence	Amplicon size
IAV PA forward primer	5′-TCTCAGCGGTCCAAATTCCTGC-3′	
IAV PA reverse primer	5′-GGTTTAACAACATTGGGTTCCTTCCAT-3′	146 bp
IAV PA probe	5′-HEX-TGAGGACCCAAGTCATGAAGGAGAGGGA-BHQ1-3′	
iNOS forward primer	5′-CTTGTGCTGTTCTCAGCCCAACAATA-3′	
iNOS reverse primer	5′-TGGAACATTCTGTGCTGTCCCAG-3′	95 bp
iNOS probe	5′-FAM-TGGCTCCCCGCAGCTCCTC-BHQ1-3′	
IFN-γ forward primer	5′-GCCAAGTTTGAGGTCAACAACCC-3′	
IFN-γ reverse primer	5′-CGCTTCCTGAGGCTGGATTCCGG-3′	101 bp
IFN-γ probe	5′-FAM-TCATCCGAGTGGTCCACCAGCTGT-BHQ1-3′	
TNF-α forward primer	5′-CCAGACCCTCACACTCAGATCATC-3′	
TNF-α reverse primer	5′-CTCCTCCACTTGGTGGTTTGCTAC-3′	85 bp
TNF-α probe	5′-HEX-TCGAGTGACAAGCCTGTAGCCCACGT-BHQ1-3′	
β-actin forward primer	5′-GCACMATGAAGATCAAGATCATTGCTCC-3′	
β-actin reverse primer	5′-TCRTACTCCTGCTTGCTGATCCAC-3′	118 bp
β-actin probe	5′-ROX-TCCTGGCCTCRCTGTCCACCTTCC-BHQ2-3′	

program (Thermo Fisher Scientific, Waltham, MA, USA) for sequence alignment and FastPCR online (http://primerdigital.com/tools/pcr.html) java applet for primers test. All multiplex one-step reactions were carried out in a total volume of 15 μL using 1 μL of the isolated RNA sample and primers at a concentration of 200 nM each, and probes at a concentration of 100 nM each. The multiplex one-step qRT-PCR assays were performed employing a real-time thermocycler Rotor-Gene Q 5plex model with software version 1.7 (Qiagen GmbH, Hilden, Germany) under the following conditions: first strand cDNA was synthesized at 48 °C for 10 min and then denatured at 95 °C for 2 min; followed by 50 cycles of denaturation at 95 °C for 10 s and annealing/extension at 60 °C for 1 min. The multiplex one-step reactions were carried out in two separate rounds, i.e. the IFN-γ, TNF-α plus β-actin mRNA levels were quantified in the first round, and the iNOS, viral PA RNA plus β-actin mRNA levels were measured in the second round. The expression of β-actin mRNA was used as an internal standard for normalization of the viral PA RNA and target mRNA levels between different samples. The $2^{-\Delta\Delta C_T}$ algorithm was applied for calculation of the relative quantities of PCR amplification product reflecting the relative levels of viral PA RNA and target mRNA (186).

2.6 Nitrite determination

The levels of nitrite (NO_2^-), an indicator of NO synthesis in biological systems, were determined in BAL fluids using a modified Griess reagent (Sigma-Aldrich, St. Louis, MO, USA) as directed by the manufacturer: 100 μL of BAL fluid was mixed with 100 μL of modified Griess reagent in 96-well plates, and incubated at room temperature for 15 min. A microplate-reader spectrophotometer PowerWave X 340 (BioTek Instruments, Inc., Winooski, VT, USA) was employed to measure the optical density (OD) of BAL fluid samples at a wavelength of 540 nm. This method for the determination of nitrite produced in biological systems is based on the Griess reaction, which involves formation of a chromophore during the reaction of nitrite with sulfanilamide and heterocyclic amines such as N-(1-naphthyl)-ethylenediamine (the Griess reagents) under conditions of low pH. During this reaction acidified nitrite undergoes diazotization with sulfanilamide to form a diazonium salt. The diazonium salt then couples to N-(1-naphthyl)-ethylenediamine to form a deep purple azo compound with a characteristic absorption spectrum.
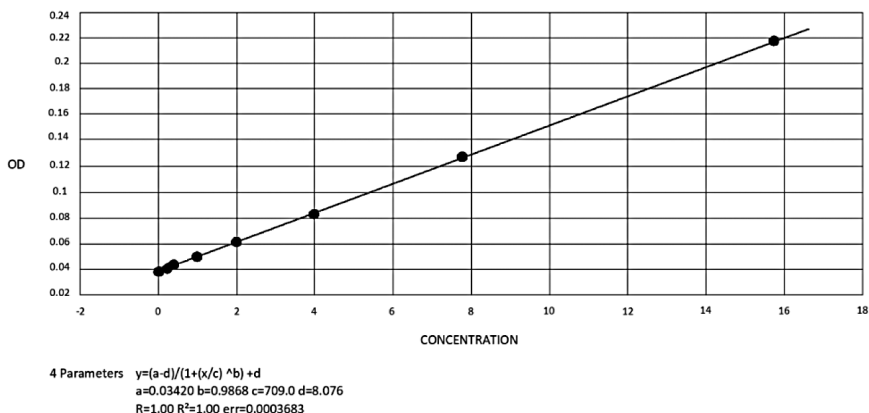
Figure 3. A standard curve with 0.12 μmol/mL to 15.63 μmol/mL of NaNO$_2$ generated applying a four-parameter logistic fit.

Y axis – optical density (OD); X axis – concentration of NaNO$_2$.

Nitrite concentrations were calculated using the KC4 software, version 2.5 (BioTek Instruments, Inc., Winooski, VT, USA), by comparison OD of the samples containing formed NO$_2^-$ to a standard curve of sodium nitrite (NaNO$_2$). The lower limit of NO$_2^-$ detection was 0.12 μmol/mL, and the upper limit of NO$_2^-$ detection was 15.63 μmol/mL. A four parameter logistic fit was the selected type of the standard curve fitting technique. An example of NaNO$_2$ standard curve is presented in **Figure 3**.

The equation characterizing a four parameter logistic fit is as follows:

$$y = \frac{a-d}{(1+(x/c)^b)} + d,$$

where **a** represents the (theoretical) response at concentration = 0, **b** represents the measure of slope of curve at its inflection point, **c** is the value of **x** at inflection point, **d** represents the (theoretical) response at infinite concentration, **x** is the concentration, and **y** is the response (OD). Other statistical measures (used for characterization of the standard curve) included the R and R^2 values. The R is a measure of linear association between two variables. Values of R range between −1 and +1. A value of 0 indicates no linear relationship. The R^2 is a goodness-of-fit measure of a linear model, so-called the coefficient of determination. It ranges in value from 0 to 1. Small values indicate that the model does not fit the data well. In the experiments, the values of R and R^2 were no less than 0.9996.

2.7 Histological examination

The histological examination was performed in the National Center of Pathology, Vilnius, Lithuania. The harvested lung tissues were embedded in paraffin, cut into 5 µm sections and stained with hematoxylin and eosin (H&E). Coded lung samples were examined using light microscopy by a pathologist in the blinded approach. The following indicative parameters of pulmonary histopathology were evaluated: perivascular lymphocytic, peribronchial lymphocytic, focal and diffuse leucocytic infiltrations; praesense of alveolar macrophages; damage of alveolar/bronchial epithelium; hyperemia; capillary thromboses; bronchiolitis; pleuritis; alveolar hemorrhage, collapse, fibrosis, edema and hyaline membranes. Each of these parameters was graded subjectively by scoring on a scale from 0 (absence of pathological changes) to 3 (maximum extent of pathological changes), and the sum of scores comprised the histological score for each mouse.

2.8 Statistical analysis

Data were analyzed using the Statistical Package for Social Science (SPSS) software version 21.0 for Windows (IBM Corp., Armonk, NY, USA). Differences between the experimental groups were evaluated applying one-way analysis of variance (ANOVA) followed by a *post hoc* least significant difference (LSD) test for multiple comparisons. Data are presented as means ± standard error of the mean (SEM). Spearman's correlation analysis was used for evaluation of correlation between the variables. A *p* value less than 0.05 was considered to indicate a statistically significant difference.

3. RESULTS

3.1 Relative influenza A viral RNA levels in mouse lungs

IAV PA RNA was not detected in negative control mice whilst increased viral loads were present in the lungs of all groups of IAV-infected mice as quantified by multiplex one-step RT-qPCR assay on day 3 *p.i.* (**Figure 4**). Between the two infected (positive) control groups, the infected group treated with lactose had significantly (*p*=0.013) higher IAV PA RNA level compared with the group that was infected without any treatment. All non-control treatment groups showed significantly less relative IAV PA RNA level vs. IAV infected lactose treated mouse group (*p*=0.016, *p*<0.001, *p*=0.017 respectively). IAV infected and zanamivir or zanamivir + ODN treated mouse viral loads were similar, however IAV infected and ODN treated mice relative IAV PA RNA levels were significantly smaller vs. Virus + Zanamivir treatment group (*p*=0.039).
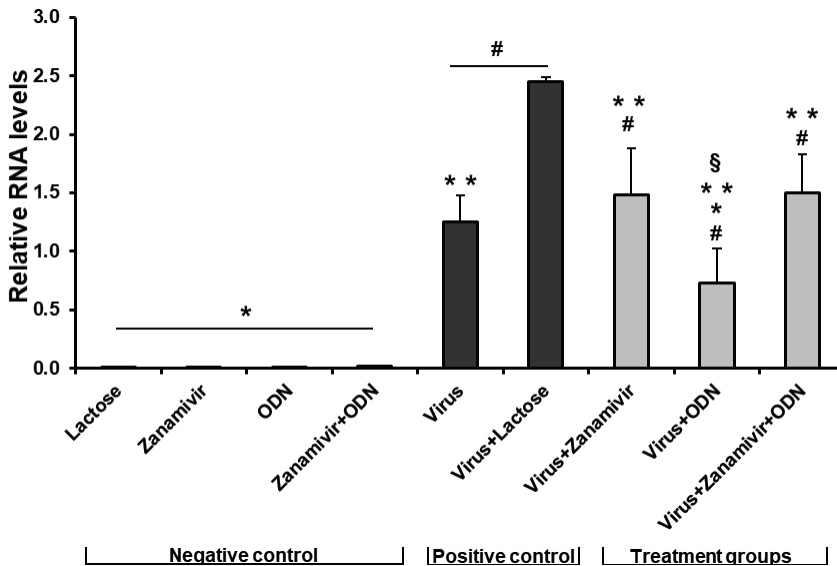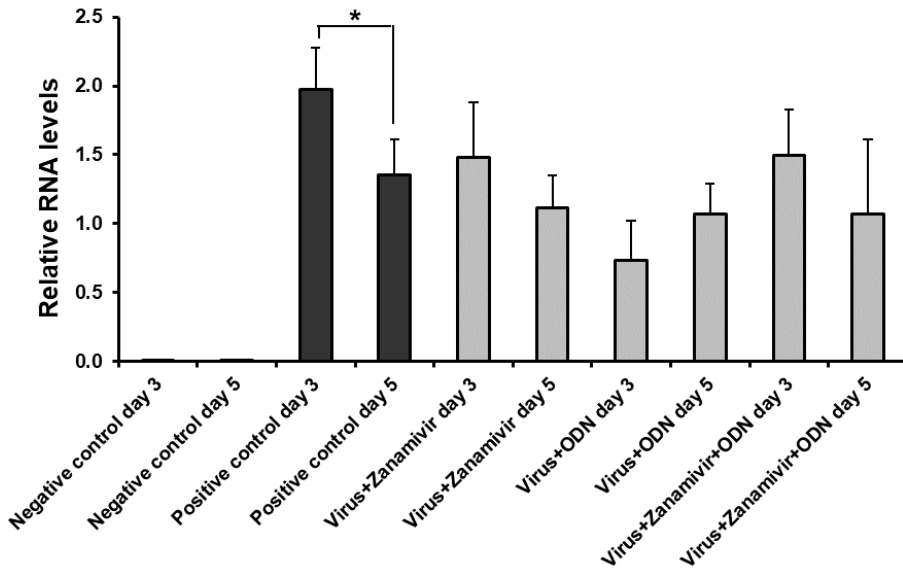

Figure 4. **Relative viral PA RNA levels in lungs of control and treatment groups of mice on day 3 after IAV infection.**

Data are shown as mean ± SEM. Significantly different at p<0.05 [#]vs. negative mouse control group, n=11, *vs. positive mouse control group, n=5, **vs. IAV infected and Lactose treated mice, n=3 and [§]vs. infected Zanamivir treated mice, n=4.
Infected ODN treated, n=4; infected Zanamivir and ODN treated, n=4.
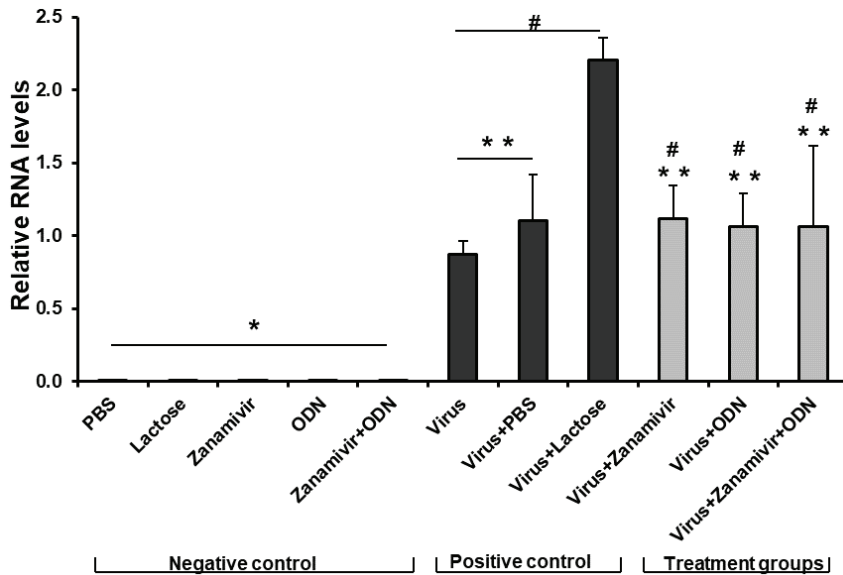
Figure 5. Relative viral PA RNA levels in lungs of control and treatment groups of mice on day 5 after IAV infection.

Data are shown as mean ± SEM. Significantly different at p<0.05 #vs. negative mouse control group, n=15, *vs. positive mouse control group, n=7, **vs. IAV infected and Lactose treated mice, n=2.

Infected Zanamivir treated, n=4; infected ODN treated, n=4; infected Zanamivir and ODN treated, n=4.

On day 5, viral PA RNA was not detected in negative mouse control group and increased viral loads were present in the lungs of all groups of virus-infected mice (**Figure 5**). Of the positive control group, the infected group treated with lactose had significantly higher IAV PA RNA level compared with infected-only (p=0.012) or infected and PBS treated (p=0.021) mouse groups. All treatment groups showed similar IAV PA RNA levels and were significantly less vs. the IAV infected and lactose treated mouse group (p=0.017, p=0.013, p=0.013 respectively).

The relative viral PA RNA levels between 3 and 5 days in experimental groups mouse lungs were compared (**Figure 6**). There were no significant differences in negative uninfected control nor treatment groups relative viral PA RNA levels between days 3 and 5. However, IAV expression diminished significantly on day 5 vs. day 3 in positive infected control groups (31.5%, p=0.045) mouse lungs.

Figure 6. **Comparison of relative viral PA RNA levels in mouse lungs of control and treatment groups on days 3 and 5 after IAV infection.**

Data are shown as mean ± SEM. Significantly different at $p<0.05$ 5th *vs. 3rd day viral PA RNA level.

Negative control, n=11 on day 3 (Lactose, Zanamivir, ODN and Zanamivir+ODN), n=15 on day 5 (PBS, Lactose, Zanamivir, ODN and Zanamivir+ODN); positive control, n=5 on day 3 (Virus and Virus+Lactose), n=7 on day 5 (Virus, Virus+PBS and Virus+Lactose); Virus+Zanamivir, n=4 on day 3, n=4 on day 5; Virus + ODN, n=4 on day 3, n=4 on day 5; Virus+Zanamivir+ODN, n=4 on day 3, n=4 on day 5.

3.2 Relative IFN-γ mRNA levels in mouse lungs

The relative IFN-γ mRNA level was 55.1% higher in positive (infected) versus negative (uninfected) control groups on day 3, however this difference did not reach significance (**Figure 7**). In infected and zanamivir treated mouse lungs IFN-γ mRNA level did not differ significantly from control groups. However, Virus + ODN treatment group had the significantly more IFN-γ mRNA expression vs. both control groups ($p=0.001$ vs. negative control and $p=0.034$ vs. positive control), and Virus + Zanamivir + ODN treatment group - vs. negative control group ($p=0.005$).
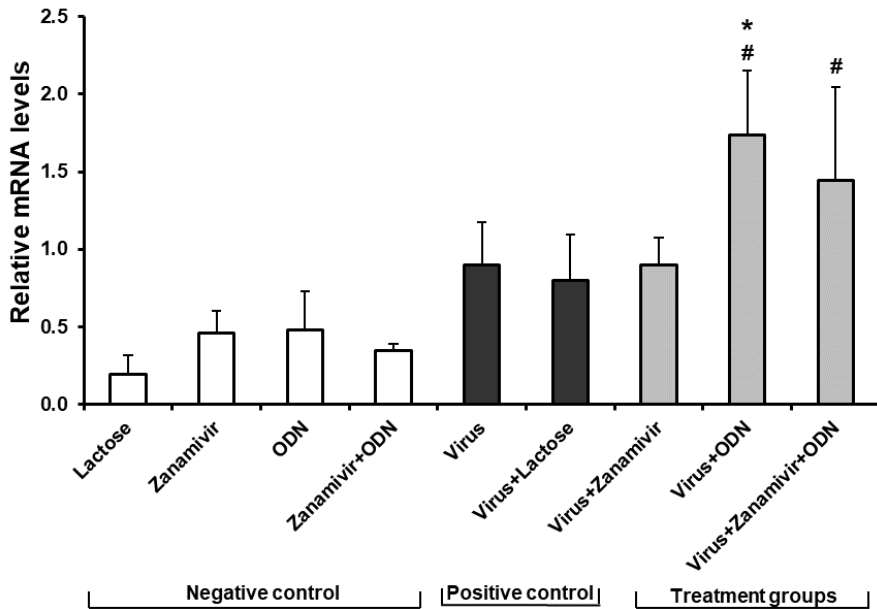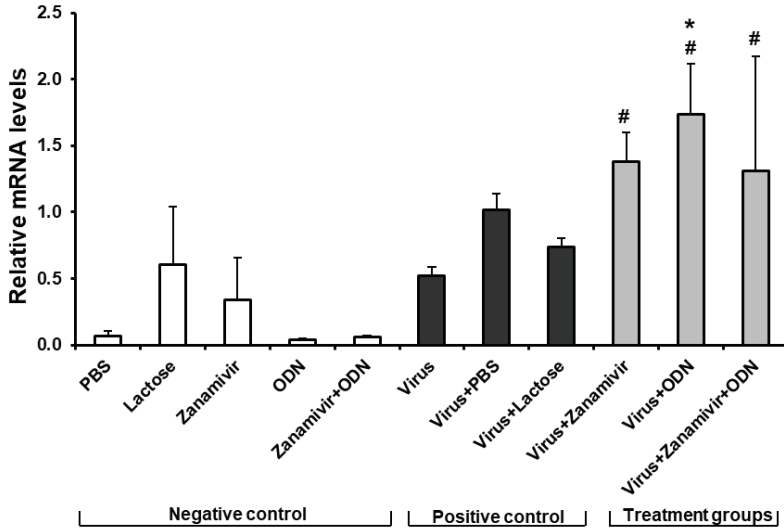
Figure 7. Relative levels of IFN-γ mRNA in mouse lung tissues on day 3 after IAV infection.

Data are shown as mean ± SEM. Significantly different at p<0.05 [#]vs. negative mouse control group, n=11, *vs. positive mouse control group, n=5.
Infected Zanamivir treated mice, n=4; infected ODN treated, n=4; infected Zanamivir and ODN treated, n=4.

Like on the 3rd day, the relative IFN-γ mRNA level was 72.0% higher in positive versus negative control groups on day 5, but this difference did not reach the significance (**Figure 8**). In all treatment groups significantly higher IFN-γ mRNA expressions vs. negative control were found (p=0.006 in infected and zanamivir treated, p=0.001 in infected and ODN treated and p=0.01 in infected and zanamivir + ODN treated mouse lungs). The highest relative level of IFN-γ mRNA was found in Virus + ODN treated mouse lungs, it was 20.7% higher than in Virus + Zanamivir treatment group and significantly higher vs. positive control group (p=0.04) mouse lungs.

We found no significant difference in relative IFN-γ mRNA levels on 5th versus 3rd day either in control or in IAV-infected treatment groups (**Figure 9**).
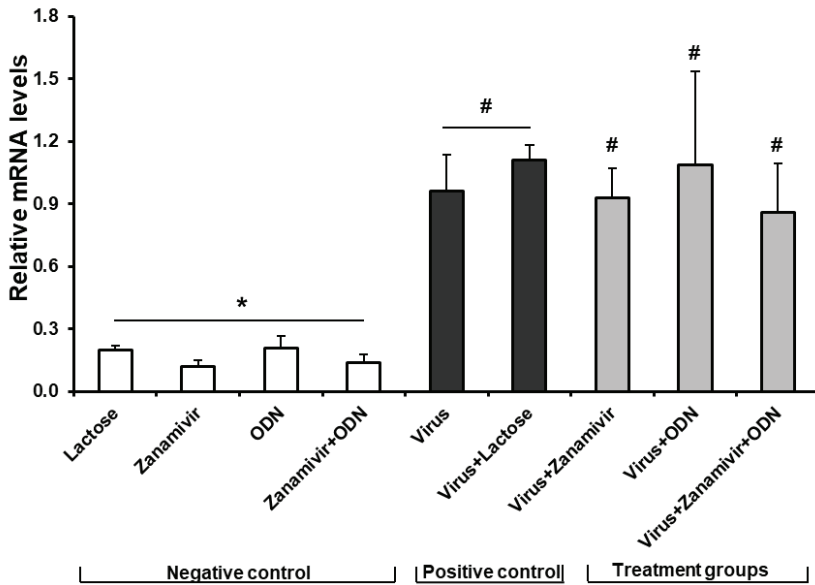
Figure 8. Relative levels of IFN-γ mRNA in mouse lung tissues on day 5 after IAV infection.

Data are shown as mean ± SEM. Significantly different at $p < 0.05$ [#]vs. negative mouse control group, n=15, [*]vs. positive mouse control group, n=7.
Infected Zanamivir treated mice, n=4; infected ODN treated, n=4; infected Zanamivir and ODN treated, n=4.
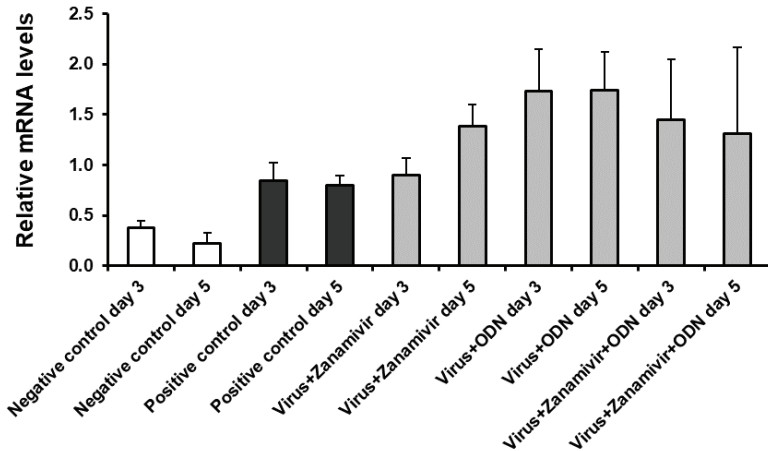
Figure 9. **Comparison of relative IFN-γ mRNA levels in mouse lungs of control and treatment groups on days 3 and 5 after IAV infection.**

Data are shown as mean ± SEM. Significance set at $p < 0.05$ 5th [*]vs. 3rd day.
Negative control, n=11 on day 3 (Lactose, Zanamivir, ODN and Zanamivir+ODN), n=15 on day 5 (PBS, Lactose, Zanamivir, ODN and Zanamivir+ODN); positive control, n=5 on day 3 (Virus and Virus+Lactose), n=7 on day 5 (Virus, Virus+PBS and Virus+Lactose); Virus+Zanamivir, n=4 on day 3, n=4 on day 5; Virus + ODN, n=4 on day 3, n=4 on day 5; Virus+Zanamivir+ODN, n=4 on day 3, n=4 on day 5.

50

3.3 Relative TNF-α mRNA level in mouse lungs

The relative levels of TNF-α mRNA in mouse lung tissue on day 3 after IAV infection are shown in **Figure 10**. The relative level of TNF-α mRNA was 84.2% greater in positive than in negative control groups ($p<0.001$). Mouse lung TNF-α mRNA level was similar in all IAV infected treatment groups and the infected control group (p=NS), but significantly higher than in the negative non-infected control groups (p=0.003, p<0.001, p=0.006 for infected treatment of zanamivir, ODN and zanamivir + ODN combination, respectively).
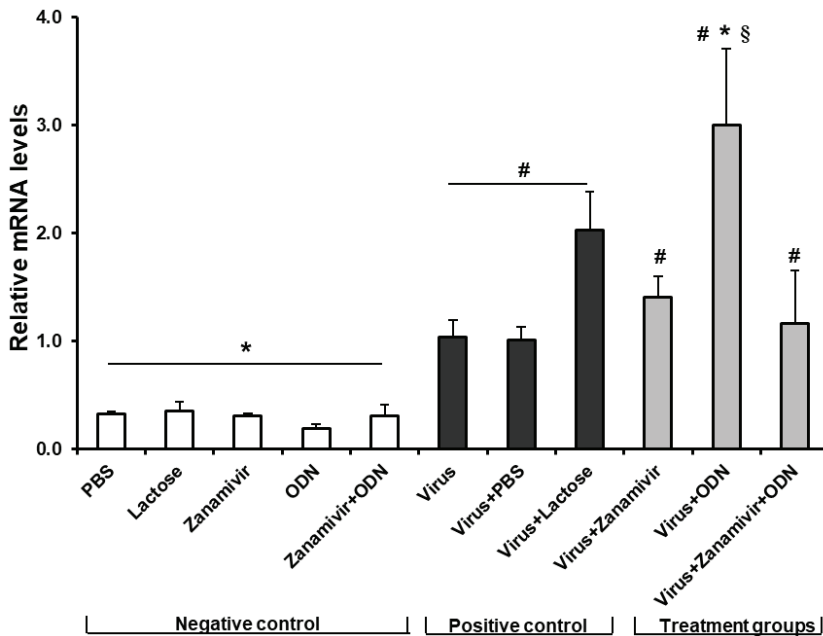

Figure 10. Relative levels of TNF-α mRNA in mouse lung tissues on day 3 after IAV infection.

Data are shown as mean ± SEM. Significantly different at p<0.05 vs. #vs. negative mouse control group, n=11, *vs. positive mouse control group, n=5.
Infected Zanamivir treated mice, n=4; infected ODN treated, n=4; infected Zanamivir and ODN treated, n=4.

On the 5th day of the experiment, the relative TNF-α mRNA level was 76.9% higher in positive than in negative control groups ($p=0.001$). TNF-α mRNA level was higher in all IAV infected treatment groups vs. negative control, ($p=0.004$ in infected and zanamivir treated, $p<0.000$ in infected and ODN treated, and $p=0.019$ in infected and zanamivir + ODN treated mouse lungs). However, the highest relative level of TNF-α mRNA was found in Virus + ODN treatment group mouse lungs: it was 53.0% higher than in Virus + Zanamivir treatment group ($p=0.001$) and higher vs. positive control group ($p<0.001$) mouse lungs. The level of TNF-α mRNA in combination treatment group was significantly smaller ($p<0.001$) than in Virus+ODN and had a tendency to lessen (17.0% decrease) compared to Virus+Zanamivir treatment groups (**Figure 11**).

Figure 11. Relative levels of TNF-α mRNA in mouse lung tissues on day 5 after IAV infection.

Data are shown as mean ± SEM. Significantly different at p<0.05 [#]vs. negative mouse control group, n=15, *vs. positive mouse control group, n=7 and [§]vs. infected Zanamivir treated mice, n=4.

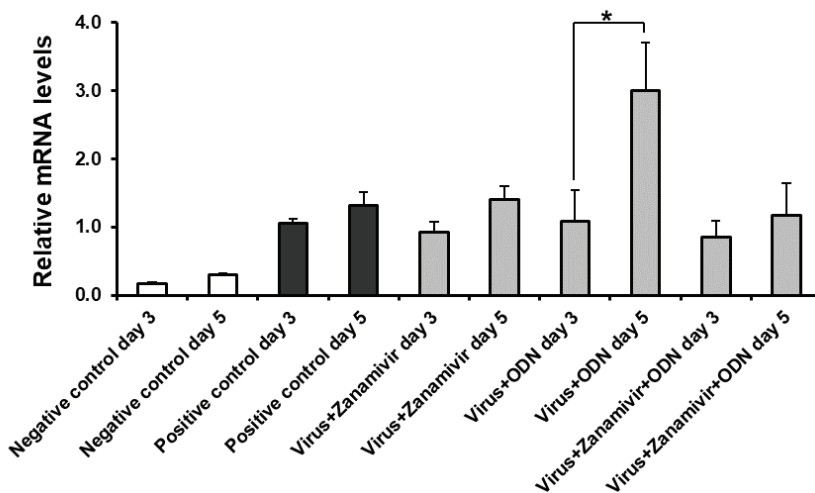Infected ODN treated, n=4, infected Zanamivir and ODN treated, n=4.

Figure 12. **Comparison of relative TNF-α mRNA levels in mouse lungs of control and treatment groups on days 3 and 5 after IAV infection.**

Data are shown as mean ± SEM. Significantly different at p<0.05 5th *vs. 3rd day. Negative control, n=11 on day 3 (Lactose, Zanamivir, ODN and Zanamivir+ODN), n=15 on day 5 (PBS, Lactose, Zanamivir, ODN and Zanamivir+ODN); positive control, n=5 on day 3 (Virus and Virus+Lactose), n=7 on day 5 (Virus, Virus+PBS and Virus+Lactose); Virus+Zanamivir, n=4 on day 3, n=4 on day 5; Virus + ODN, n=4 on day 3, n=4 on day 5; Virus+Zanamivir+ODN, n=4 on day 3, n=4 on day 5.

There were no significant difference in relative TNF-α mRNA levels between 5th versus 3rd day in negative or positive control group mouse lungs. However in IAV-infected and ODN treated mouse lungs the TNF-α mRNA expression was significantly bigger on 5th day than on 3rd day (p<0.001). The TNF-α mRNA relative level was similar between 5th and 3rd day in IAV-infected and zanamivir or zanamivir plus ODN combination treated mouse lungs (**Figure 12**).

3.4 Relative iNOS mRNA level in mouse lungs

As presented in **Figure 13**, IAV infection caused significant up-regulation of the iNOS gene by day 3, resulting in 54.0% higher mRNA levels in mice from the positive control group vs. the negative control group (*p*=0.001). The greatest effect in reducing iNOS mRNA level between the treatment groups was observed in the Virus+Zanamivir treatment group (31.3% smaller vs. positive control group) and was similar to that found in the negative control group. In the Virus+ODN treatment group, iNOS mRNA level was 22.2% lower as

compared to the positive control group and also was similar to the negative control group. The iNOS mRNA expression in Virus+Zanamivir+ODN group was similar to the positive control group and significantly higher than that found in the negative control group mouse lungs (p=0.005).

Significantly higher relative levels of iNOS mRNA were detected in the positive vs. the negative control group on the 5th day of the experiment (87.8%, p<0.001) (**Figure 14**). IAV-infected and zanamivir or ODN treated mice showed significantly higher iNOS mRNA expression vs. negative control group (p<0.001 and p=0.002 respectively). Although the relative levels of iNOS RNA were less in the Virus+ODN mouse group on the 5th day (8.5% decrease) compared to the positive control group, it did not reach significance. Between the treatment groups, the highest relative iNOS mRNA level was found in the zanamivir treatment group. The level was 23.7% less in the Virus+ODN treatment group, and 57.2% (p=0.027) in the Virus+Zanamivir+ODN treatment group vs. the Virus+Zanamivir treatment group.
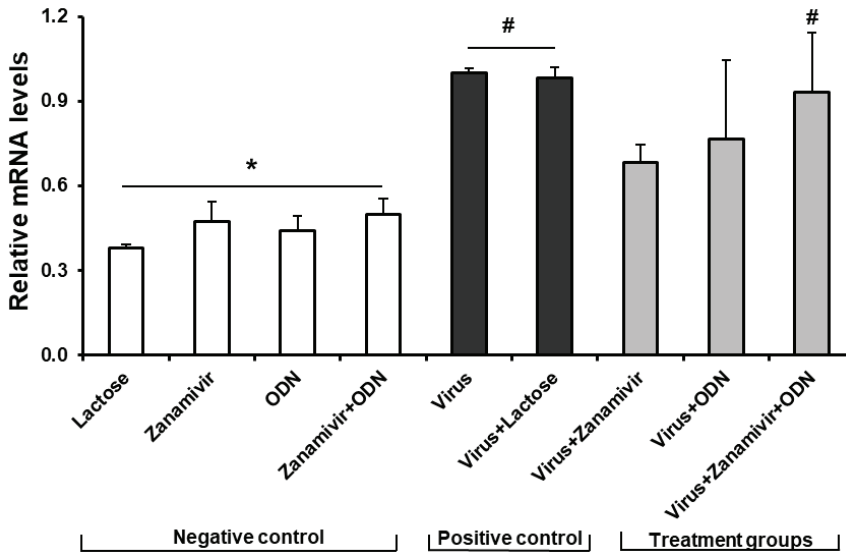

Figure 13. Relative levels of iNOS mRNA in mouse lung tissues on day 3 after IAV infection.

Data are shown as mean ± SEM. Significantly different at p<0.05 [#]vs. negative mouse control group, n=11, *vs. positive mouse control group, n=5.
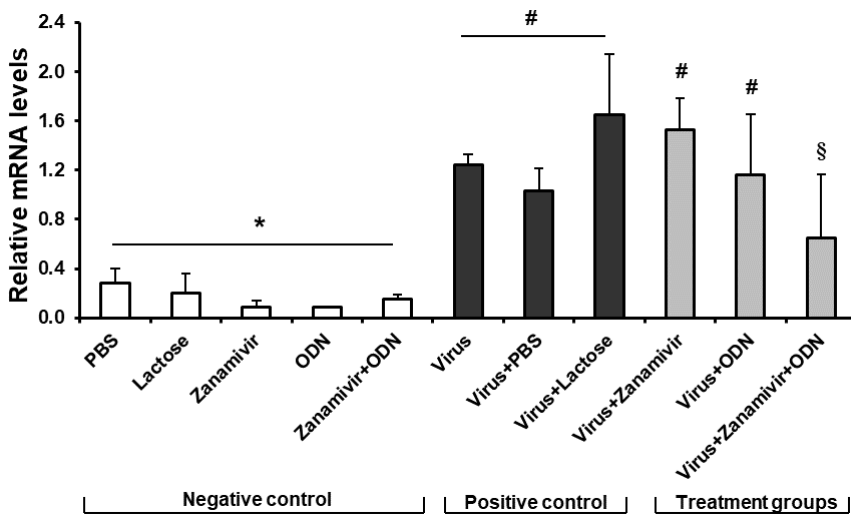Infected Zanamivir treated mice, n=4; infected ODN treated, n=4; infected Zanamivir and ODN treated, n=4.

Figure 14. Relative levels of iNOS mRNA in mouse lung tissues on day 5 after IAV infection.

Data are shown as mean ± SEM. Significantly different at $p<0.05$ [#]vs. negative mouse control group, n=15, [*]vs. positive mouse control group, n=7, and [§]vs. infected Zanamivir treated mice, n=4.

Infected ODN treated, n=4; infected Zanamivir and ODN treated, n=4.

Comparison of the relative iNOS mRNA levels in the lungs of mouse control and treatment groups on days 3 and 5 after IAV infection are shown in **Figure 15**. Significantly higher iNOS mRNA expression is noted on the 5th day vs. the 3rd day in IAV-infected and zanamivir treated mice (*p*=0.008), however it was not significantly different in ODN or Zanamivir plus ODN treatment groups.
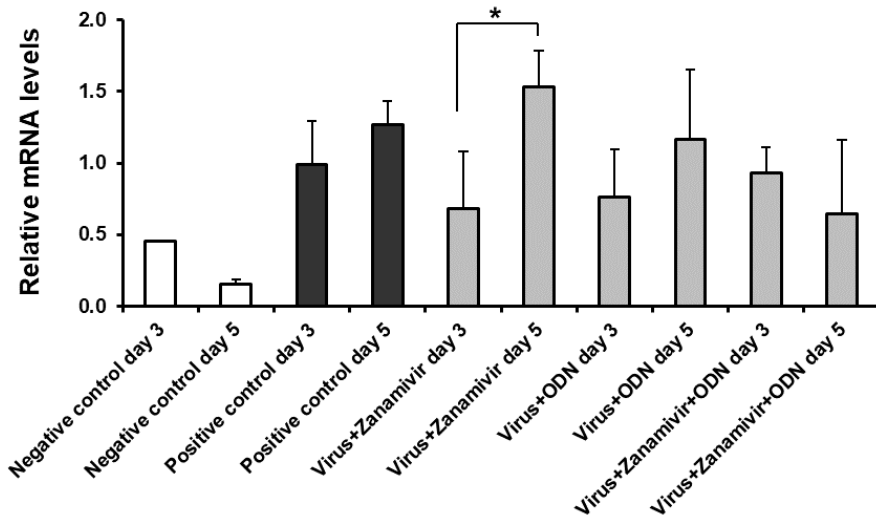
Figure 15. **Comparison of relative iNOS mRNA levels in mouse lungs of control and treatment groups on days 3 and 5 after IAV infection.**

Data are shown as mean ± SEM. Significantly different at p<0.05 5th *vs. 3rd day iNOS mRNA level.

Negative control, n=11 on day 3 (Lactose, Zanamivir, ODN and Zanamivir+ODN), n=15 on day 5 (PBS, Lactose, Zanamivir, ODN and Zanamivir+ODN); positive control, n=5 on day 3 (Virus and Virus+Lactose), n=7 on day 5 (Virus, Virus+PBS and Virus+Lactose); Virus+Zanamivir, n=4 on day 3, n=4 on day 5; Virus + ODN, n=4 on day 3, n=4 on day 5; Virus+Zanamivir+ODN, n=4 on day 3, n=4 on day 5.

3.5 Nitrite concentration in BAL fluid

The enhanced NO synthesis in the lungs was observed in influenza infected (positive control) mice vs. uninfected (negative control) on day 3 ($p<0.001$). NO concentration was significantly higher in influenza infected and ODN ($p=0.001$) or Zanamivir+ODN ($p=0.007$) treatment groups compared to negative control group. In the group of influenza infected and zanamivir treated mice the concentration of NO was significantly smaller vs. positive control group (57.5%, $p=0.001$), and vs. treatment groups with ODN (54.1%, $p=0.005$) or Zanamivir+ODN (46.9%, $p=0.026$) (**Figure 16**).
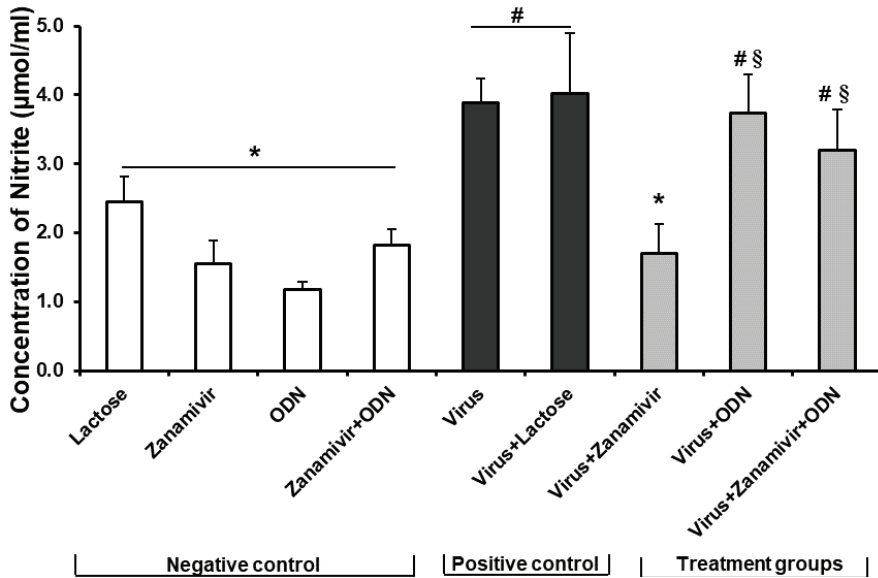
Figure 16. **Nitrite (NO_2^-) concentration in mouse bronchoalveolar lavage fluids on day 3 post infection.**

Data are shown as mean±SEM. Significantly different at $p<0.05$ [#]vs. negative mouse control group, n=13, *vs. positive mouse control group, n=6, and [§]vs. infected Zanamivir treated mice, n=4.

Infected ODN treated, n=4; infected Zanamivir and ODN treated, n=5.

The concentrations of nitrite in experimental mouse groups' BAL fluids on day 5 are shown in **Figure 17**. Similarly to day 3, on day 5 the enhanced NO synthesis was observed in influenza infected (positive control) mice vs. uninfected (negative control) (*p*=0.003). In influenza infected and Zanamivir+ODN treatment group mouse lungs had significantly lower nitrite concentrations as compared to those in the positive control group (39.3%, *p*=0.005).
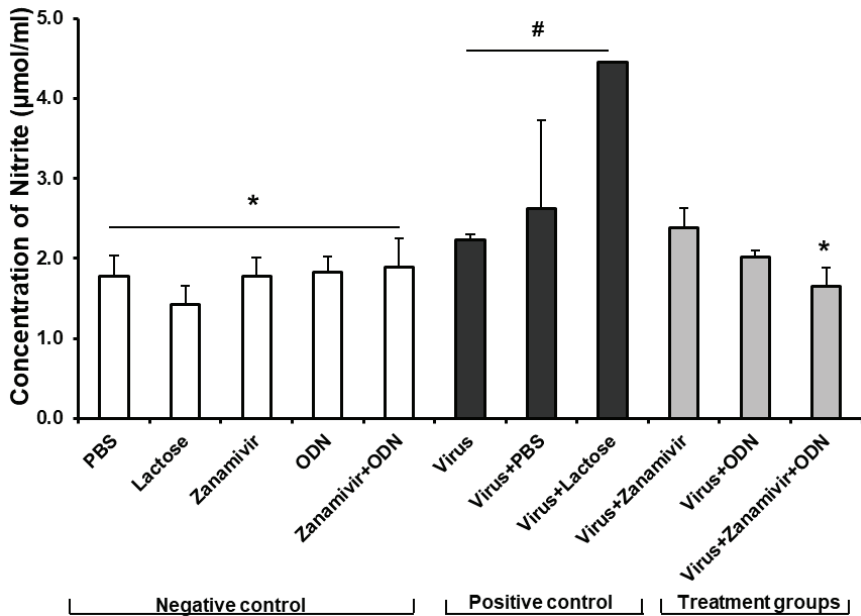
Figure 17. **Nitrite (NO$_2^-$) concentration in mouse bronchoalveolar lavage fluids on day 5 post infection.**

Data are shown as mean±SEM. Significantly different at p<0.05 [#]vs. negative mouse control group, n=11 and *vs. positive mouse control group, n=5.

Infected Zanamivir treated mice, n=4; infected ODN treated, n=3; infected Zanamivir and ODN treated, n=5.

The concentrations of nitrite (NO$_2^-$) between 3 and 5 days in experimental mouse bronchoalveolar lavage fluids were compared (**Figure 18**). There were no significant differences in negative control and virus + Zanamivir treatment groups' nitrites between days 3 and 5. However, concentration of nitrites dropped significantly on day 5 from that of day 3 in the positive control group (30.0%, *p*=0.025), influenza infected and ODN (46.0%, *p*=0.007) or combination of zanamivir and ODN treated (46.9%, *p*=0.004) mouse lungs.
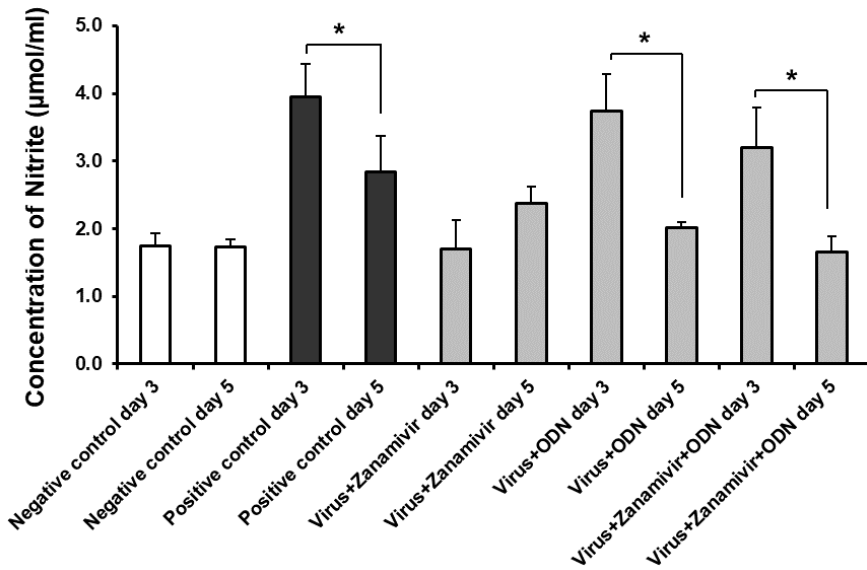
Figure 18. **Comparison of nitrite (NO_2^-) concentration in mouse bronchoalveolar lavage fluids between 3 and 5 days post infection.**

Significantly different at p<0.05 5th *vs. 3rd day nitrite concentration.
Negative control, n=13 on day 3 (Lactose, Zanamivir, ODN and Zanamivir+ODN), n=11 on day 5 (PBS, Lactose, Zanamivir, ODN and Zanamivir+ODN); positive control, n=6 on day 3 (Virus and Virus+Lactose), n=5 on day 5 (Virus, Virus+PBS and Virus+Lactose); Virus+Zanamivir, n=4 on day 3, n=4 on day 5; Virus + ODN, n=4 on day 3, n=3 on day 5; Virus+Zanamivir+ODN, n=5 on day 3, n=5 on day 5.

3.6 Body weight changes

The daily body weights (expressed as percentage of initial body weight) of *negative mouse control group* for the 5-day experiment are shown in **Figure 19**. All mice lost weight. Compared to day 0, the PBS treated mice had lost 4.3% of their weight by day 3 and 7.5% by day 5. The Zanamivir mouse treatment group weight loss reached significance on day 3 (13.5%, *p*=0.003) and weighed even less, but not significantly so, on day 5 (14.6%, *p*=0.099) vs. the PBS treatment group. The ODN mouse treatment group lost weight similar to both the PBS and Zanamivir treatment groups (8.5% on day 3 and 15.1% on day 5). On the contrary, body weight loss of zanamivir and ODN combination treated mice was significantly less as compared to the zanamivir only treated mice on days 3 and 5 (6.8%, *p*=0.004 on day 3 and 4.3%, *p*=0.018 on day 5) and started recovering from weight loss starting by day 4.
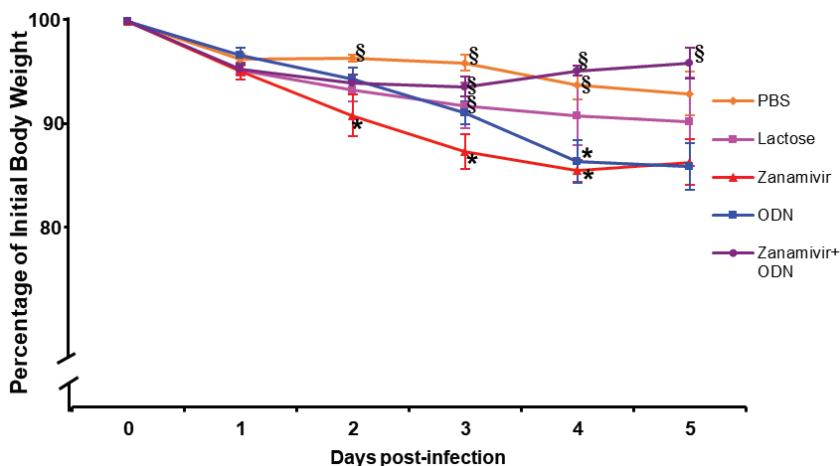
Figure 19. **Body weights over 5 days across negative control group mice.**

The body weights are expressed as a percentage of their initial weight at day 0. Data are shown as mean ±SEM. $p<0.05$ compared with *PBS, n=3 on day 3, n=3 on day 5; §Zanamivir, n=6 on day 3, n=3 on day 5.

Lactose, n=6 on day 3, n=3 on day 5; ODN, n=6 on day 3, n=3 on day 5; Zanamivir+ODN, n=8 on day 3, n=4 on day 5.

The daily body weights of the *positive mouse control group* for the 5-day experiment are shown in **Figure 20**. All influenza infected mouse groups lost weight similarly during the first few days. By day 5, weight loss of influenza only infected mice was 19.0%, and influenza infected and lactose treated mice was 20.6% of their initial weight. Influenza infected and PBS treated mice lost less weight than influenza only infected mice (14.6%, $p=0.02$).

The daily body weights of *treatment* group mice for the 5-day experiment are shown in **Figure 21**. The positive mouse control group (influenza infected) lost significantly more weight vs. negative mouse control group (uninfected) starting from day 2. The infected and zanamivir treated mouse weight loss (9.4%) was smaller than for the positive control group (15.0%, $p=0.002$) and the influenza+ODN treatment group (14.3%, p=0.009) on day 3; there was no significant difference by day 5 (14.2%, $p=0.22$). The infected and ODN treated mice lost weight similarly to the positive mouse control group, and differed significantly from the negative mouse control group on days 3 (14.3% and 8.9%, $p<0.001$) and 5 (16.9% and 10%, $p=0.02$). The infected and zanamivir + ODN combination treated mouse group on day 3 lost 12.0% of their weight, more than the negative mouse control group, which lost only 8.9%, ($p=0.037$).
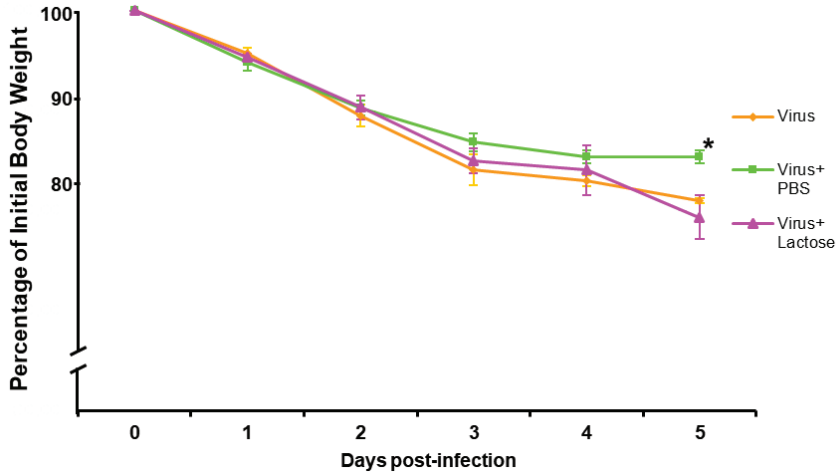
Figure 20. **Body weights of positive mouse control group during 5 days.**

The body weights are expressed as a percentage of their initial weight at day 0. Data are shown as mean ±SEM. $P<0.05$ compared with *Virus, n=6 on day 3, n=3 on day 5. Virus+PBS n=3 on day 3, n=3 on day 5; Virus+Lactose n=7 on day 3, n=2 on day 5.
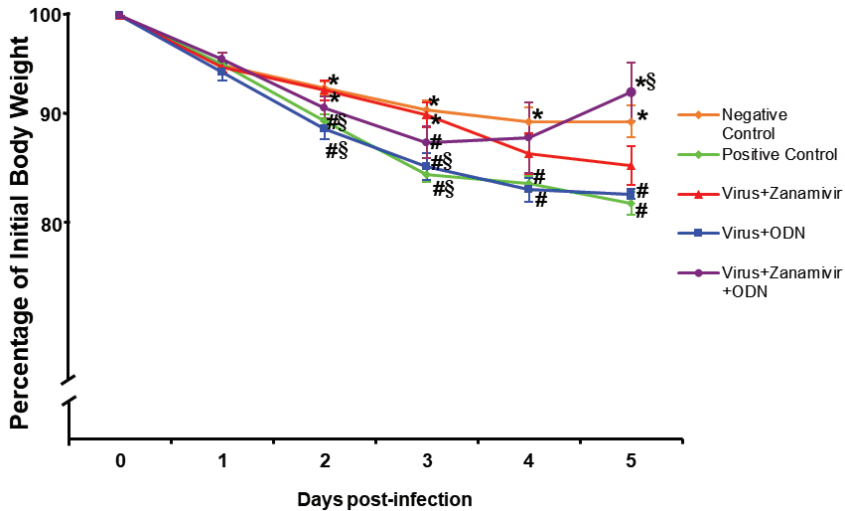

Figure 21. **Mouse body weights by treatment groups over 5 days.**

The body weights are expressed as a percentage of their initial weight at day 0. Data are shown as mean ±SEM. $P<0.05$ compared with [#]negative control, n=29 on day 3, n=16 on day 5; *positive control, n=16 on day 3, n=8 on day 5; [§]Virus+Zanamivir. Virus+Zanamivir, n=10 on day 3, n=5 on day 5; Virus+ODN, n=12 on day 3, n=4 on day 5; Virus+Zanamivir+ODN, n=12 on day 3, n=5 on day 5.

61

Interestingly, mice in the combination treatment group started to gain weight, and by day 5 their weight loss was only 7.2%, significantly more than the positive mouse control group (7.7%, $p=0.001$) and the Zanamivir treatment group mice (14.2%, $p=0.036$).

3.7 Mouse lung histopathology

As shown in **Table 3**, the IAV challenge in mice induced acute pulmonary inflammation marked by alveolar hemorrhage, focal and diffuse leukocytic infiltration, perivascular and peribronchial lymphocytic infiltration and bronchiolitis on day 3 *p.i.*, whereas these histopathological changes were absent in the uninfected mice (negative control). The mean cumulative histological score was significantly higher in positive vs. negative mouse control groups ($p<0.001$).

Treatment of the IAV-infected mice with zanamivir resulted in significantly less intense diffuse leukocytic infiltration ($p=0.019$) and peribronchial lymphocytic infiltration ($p=0.008$) compared with positive control mouse group. The mean cumulative histological score in the zanamivir-treated group was significantly less than that for the IAV-infected (positive control) mouse group ($p=0.018$).

The IAV-infected and treated with ODN mouse lungs had significantly less diffuse leukocytic infiltration ($p=0.014$) but more extensive perivascular lymphocytic infiltration ($p=0.039$) compared with the positive mouse control group. There was a greater degree of alveolar hemorrhage ($p=0.017$) and peribronchial lymphocytic infiltration ($p<0.001$) than in IAV infected and zanamivir treated mouse group lungs. The mean cumulative histological score in the ODN-treated group was significantly higher than for the negative control ($p<0.001$) and the IAV-infected zanamivir treated ($p=0.001$) mouse groups.

The IAV-infected and zanamivir plus ODN combination treated mouse lungs had significantly less diffuse leukocytic infiltration ($p=0.014$) than the lungs of the positive mouse control group. However, there was more focal leukocytic infiltration ($p=0.022$) and peribronchial lymphocytic infiltration ($p<0.001$) vs. IAV-infected and zanamivir only treated mouse lungs. The mean cumulative histological score in the IAV-infected and Zanamivir plus ODN-treated group was significantly greater than for the negative control ($p<0.001$) and the IAV-infected zanamivir treated ($p=0.01$) mouse groups.

Table 3. **The lung histopathology in experimental mouse groups on day 3 after influenza A virus infection**

Parameter	Negative control, n=13	Positive control, n=6	Virus+ Zanamivir, n=5	Virus+ ODN, n=6	Virus+ Zanamivir+ ODN, n=6
			Mouse group		
Alveolar hemorrhage	0.23±0.12	0.33±0.21	0.00±0.00	0.67±0.33§	0.33±0.21
Hyperemia	0.15±0.10	0.00±0.00	0.00±0.00	0.00±0.00	0.00±0.00
Focal leukocytic infiltration	0.00±0.00*	0.67±0.33#	0.00±0.00	0.50±0.34	0.83±0.31#§
Diffuse leukocytic infiltration	0.00±0.00*	0.33±0.33#§	0.00±0.00*	0.00±0.00*	0.00±0.00*
Perivascular lymphocytic infiltration	0.00±0.00*§	0.50±0.22#	0.60±0.25#	1.00±0.26#*	0.67±0.21#
Peribronchial lymphocytic infiltration	0.00±0.00*§	0.83±0.17#§	0.40±0.25#*	1.00±0.00#§	1.00±0.00#§
Bronchiolitis	0.00±0.00*	0.50±0.22#	0.40±0.25	0.83±0.31#	0.33±0.21
Alveolar macrophages	0.00±0.00	0.00±0.00	0.00±0.00	0.00±0.00	0.17±0.41#
Histological score[a]	0.38±0.18*	3.17±0.65#§	1.40±0.60*	4.00±0.73#§	3.33±0.61#§

[a]Mean cumulative histological score. Significantly different at $p<0.05$ vs. #negative control, *positive control, and §Virus+Zanamivir. Negative control: Lactose, Zanamivir, ODN and Zanamivir+ODN; positive control: Virus and Virus+Lactose.

The experimental mouse group lung histopathology after IAV infection on day 5 is shown in **Table 4.** The focal leukocytic infiltration ($p<0.001$), perivascular ($p<0.001$) or peribronchial ($p<0.001$) lymphocytic infiltration and bronchiolitis ($p<0.001$) were more expressed in positive control (IAV-infected) vs. negative control (uninfected) mouse lungs, with a mean cumulative histological score significantly that is bigger in the positive control group ($p<0.001$).

Treatment of the IAV-infected mice with zanamivir resulted in significantly less intense focal leukocytic infiltration ($p=0.028$) and perivascular lymphocytic infiltration ($p=0.037$) compared with the positive control mouse group. The mean cumulative histological score in the Zanamivir-treated group was significantly smaller than that for the IAV-infected (positive control) mouse group ($p=0.006$).

Table 4. The lung histopathology in experimental mouse groups on day 5 after influenza A virus infection

Parameter	Negative control, n=16	Positive control, n=8	Virus+ Zanamivir, n=5	Virus+ ODN, n=4	Virus+ Zanamivir+ ODN, n=5
Alveolar hemorrhage	0.13±0.09	0.50±0.19	0.20±0.20	0.00±0.00	0.00±0.00
Hyperemia	0.06±0.06	0.00±0.00	0.00±0.00	0.00±0.00	0.00±0.00
Focal leukocytic infiltration	0.00±0.00*§	1.75±0.25#§	1.00±0.00#*	1.00±0.41#*	0.80±0.58#*
Diffuse leukocytic infiltration	0.00±0.00	0.00±0.00	0.00±0.00	0.00±0.00	0.00±0.00
Perivascular lymphocytic infiltration	0.00±0.00*§	1.50±0.19#§	1.00±0.00#*	1.00±0.00#	1.20±0.37#
Peribronchial lymphocytic infiltration	0.00±0.00*§	0.75±0.16#	1.00±0.00#	1.00±0.00#	0.80±0.20#
Bronchiolitis	0.06±0.06*§	1.13±0.30#	0.60±0.25#	0.50±0.29*	0.60±0.25#
Alveolar macrophages	0.00±0.00	0.13±0.35	0.00±0.00	0.00±0.00	0.00±0.00
Histological score[a]	0.25±0.11*§	5.75±0.36#§	3.8±0.20#*	3.50±0.50#*	3.40±1.12#*

[a]Mean cumulative histological score. Significantly different at $p<0.05$ vs. #negative control, *positive control, and §Virus+Zanamivir. Negative control: PBS, Lactose, Zanamivir, ODN and Zanamivir+ODN; positive control: Virus, Virus+PBS and Virus+Lactose.

The lungs of IAV-infected mice treated with ODN had significantly less focal leukocytic infiltration ($p=0.041$) and bronchiolitis ($p=0.046$) than the positive mouse control group. The mean cumulative histological score in the ODN-treated group was significantly smaller vs. positive control group ($p=0.003$) mouse group.

The IAV-infected mice treated with zanamivir plus ODN significantly had less focal leukocytic infiltration ($p=0.006$) than the positive mouse control group. The mean cumulative histological score in the IAV-infected and Zanamivir plus ODN-treated group was significantly smaller than the positive control mouse group ($p=0.001$).

We did not observe damage to alveolar/bronchial epithelium, capillary thromboses, pleuritis, collapse, fibrosis, edema or hyaline membranes in lungs on either 3rd or 5th day in experimental mice.

The differences between mean cumulative histological scores in control and treatment mouse groups' lungs on day 3 post IAV-infection are presented in **Figure 22**. The histological score was significantly greater in the positive control vs. the negative control mouse group lungs $(p<0.001)$. The histological score was essentially unaffected in the negative control group, however inside the positive control group, the IAV-infected and the untreated mouse group had histological lung damage scores larger than that of the IAV-infected and lactose treated mice $(p=0.007)$. The score in IAV-infected and zanamivir treated mice was significantly smaller $(p=0.018)$, but there were no differences in the IAV-infected and ODN or zanamivir plus ODN treated mice vs. the positive control mouse group.
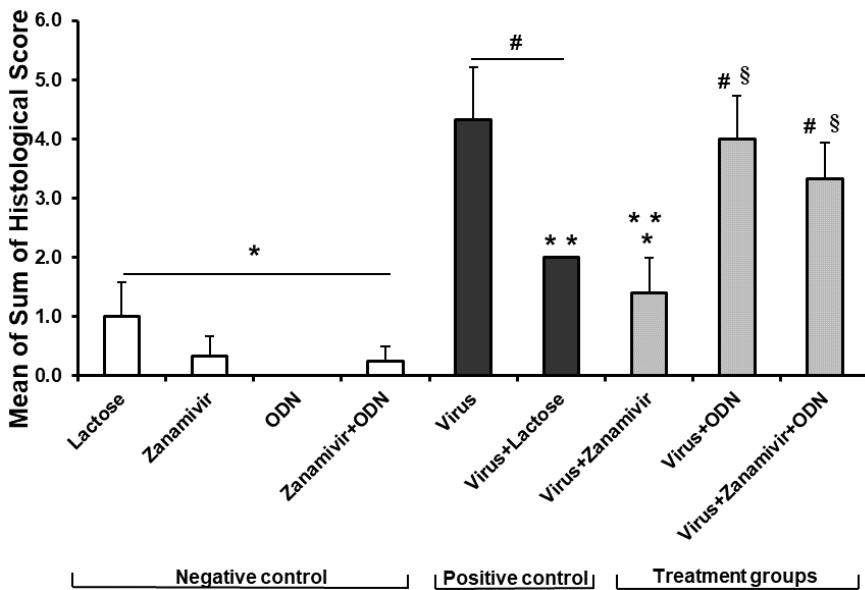

Figure 22. Mean cumulative histological score in mouse lungs on day 3 post in-fection.

Data are shown as mean±SEM. Significantly different at $p<0.05$ [#]vs. negative mouse control group, n=13, *vs. positive mouse control group, n=6, **vs. IAV infected and untreated mice, n=3 and [§]vs. infected Zanamivir treated mice, n=5.

Infected ODN treated, n=6; infected Zanamivir and ODN treated, n=6.

On the 5th day, the histological score was significantly higher in the positive control vs. the negative control mouse group lungs ($p<0.001$). All treatment groups' (IAV-infected and zanamivir treated, $p=0.006$; IAV-infected and ODN treated, $p=0.003$, and IAV-infected and zanamivir plus ODN treated, $p=0.001$) mean cumulative histological scores were significantly smaller than that of the positive control mouse group (**Figure 23**).
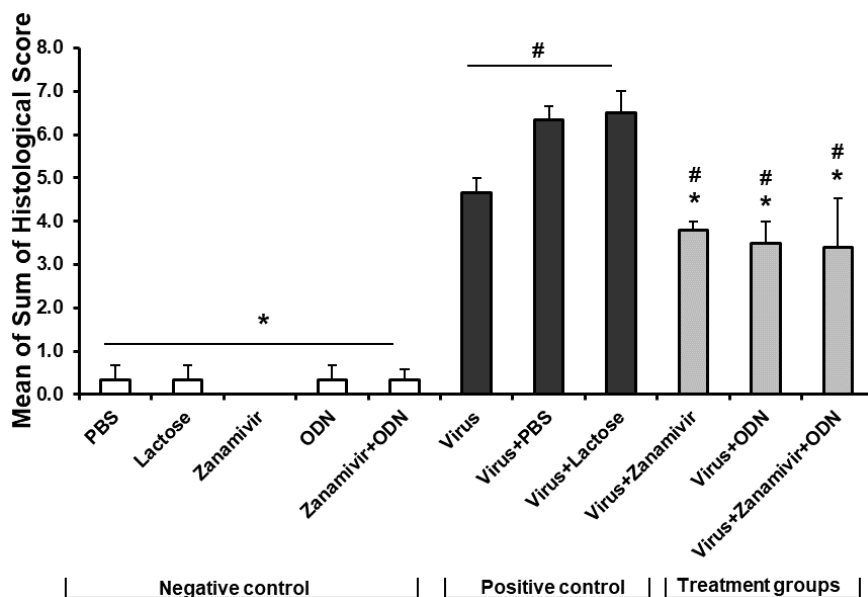

Figure 23. **Mean cumulative histological score in mouse lungs on day 5 post infection.**

Data are shown as mean±SEM. Significantly different at $p<0.05$ [#]vs. negative mouse control group, n=16, [*]vs. positive mouse control group, n=8, and [§]vs. infected Zanamivir treated mice, n=5.

Infected ODN treated, n=4; infected Zanamivir and ODN treated, n=5.

The compared mean cumulative histological score of experimental groups between 3rd and 5th days is presented in **Figure 24**. There were no differences in the negative control group on day 3 and day 5 post IAV-infection in the mouse lung histological scores. In the positive control group, the 5th day's mean cumulative histological score was signifficantly higher than the 3rd

day's score ($p<0.001$). The histological lung damage was more evident on day 5 vs. day 3 in the IAV-infected and zanamivir treated mouse lungs ($p=0.002$). There were no differences in histological lung damage between the 3rd and 5th days in IAV-infected and ODN or IAV-infected and Zanamivir plus ODN treated mouse groups.
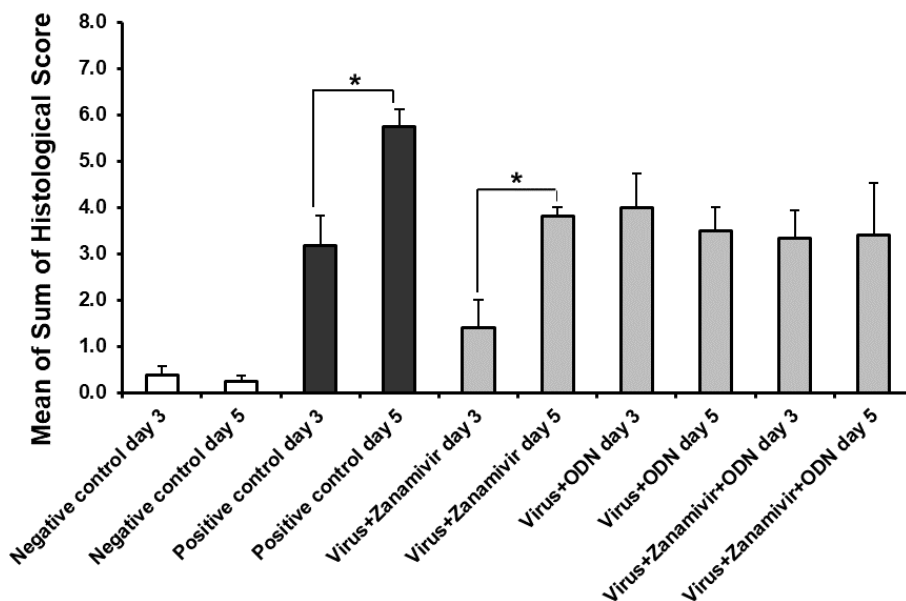

Figure 24. **Comparison of mean cumulative histological score in mouse lungs post influenza infection between 3 and 5 days.**

Significantly different at $p<0.05$ 5th *vs. 3rd day mean cumulative histological score. Negative control, n=13 on day 3 (Lactose, Zanamivir, ODN and Zanamivir+ODN), n=16 on day 5 (PBS, Lactose, Zanamivir, ODN and Zanamivir+ODN); positive control, n=6 on day 3 (Virus and Virus+Lactose), n=8 on day 5 (Virus, Virus+PBS and Virus+Lactose); Virus+Zanamivir, n=5 on day 3, n=5 on day 5; Virus + ODN, n=6 on day 3, n=4 on day 5; Virus+Zanamivir+ODN, n=6 on day 3, n=5 on day 5.

The photographs of 3rd day experimental group mouse lungs are shown in **Figure 25** and of the 5th day in **Figure 26**.
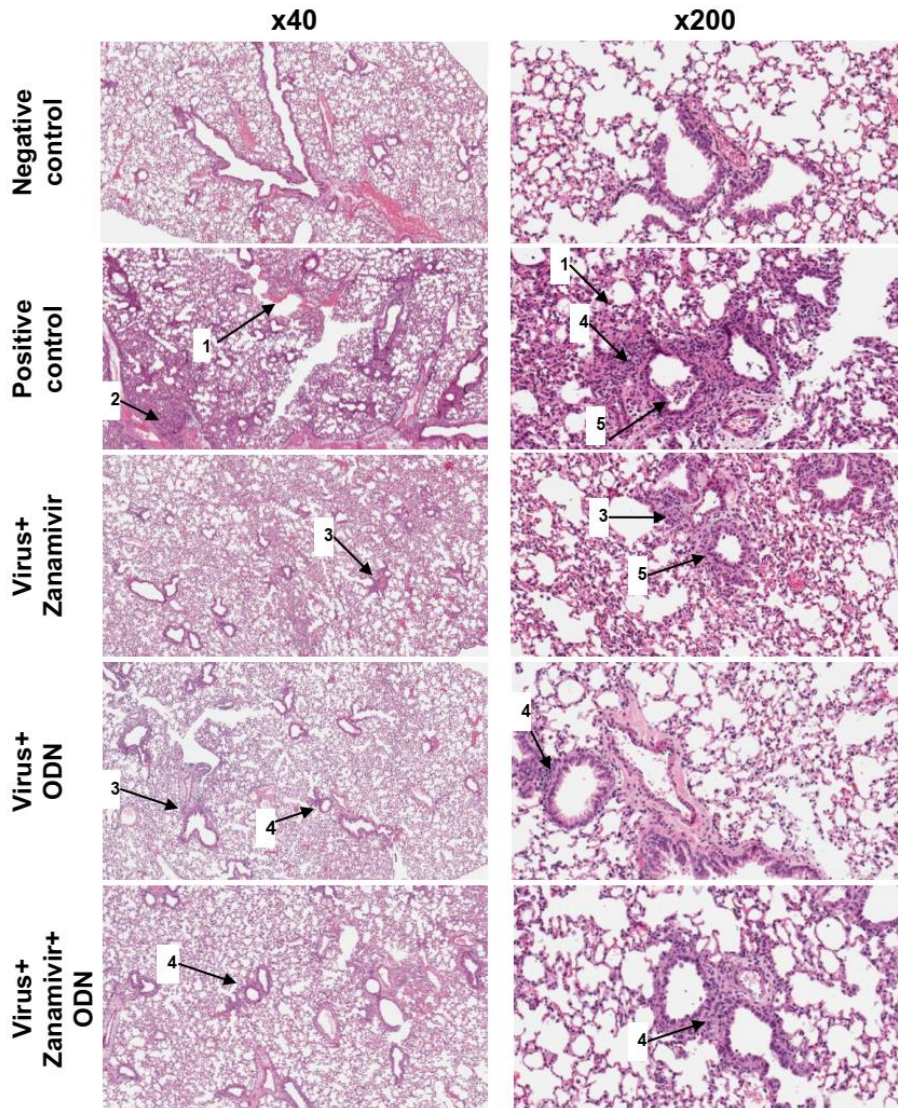
Figure 25. **Histological lung sections of BALB/c mice on day 3 stained with H&E.**

Arrows indicate: (1) alveolar hemorrhage, (2) focal leukocytic infiltration, (3) perivascular lymphocytic infiltration, (4) peribronchial lymphocytic infiltration, (5) bronchiolitis.

Figure 26. **Histological lung sections of BALB/c mice on day 5 stained with H&E.**

Arrows indicate: (1) alveolar hemorrhage (no alveolar hemorrhage noted on the day 5 photographs), (2) focal leukocytic infiltration, (3) perivascular lymphocytic infiltration, (4) peribronchial lymphocytic infiltration, (5) bronchiolitis.
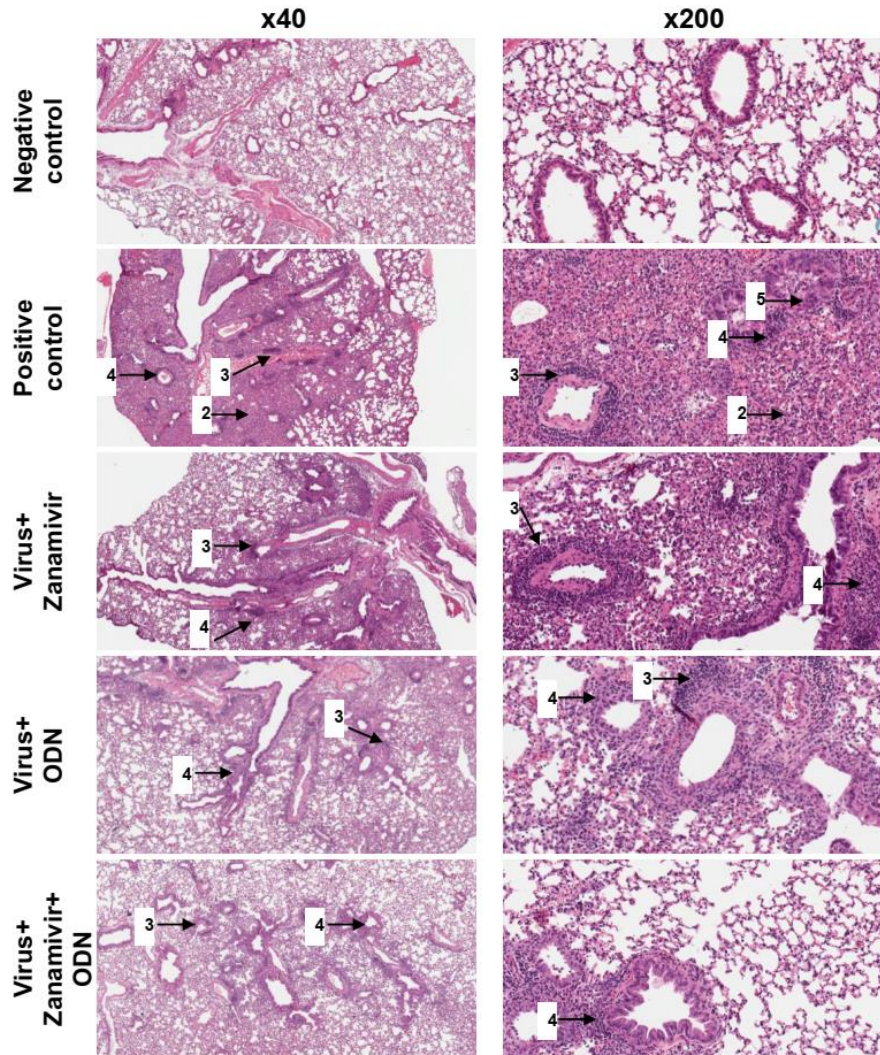
3.8 The correlation between lung damage and analysed parameters

The correlation coefficients between between lung damage mean cumulative histological score and analysed parameters in experimental mouse groups on day 3 after influenza A virus infection are shown in **Table 5**. A strongly positive correlation was found between lung damage score and TNF-α mRNA relative levels in mouse lungs. In addition, the mean cumulative histological score was found to be moderately positively correlated with relative nitrite concentration in BAL fluid, IAV PA RNA, iNOS mRNA and IFN-γ mRNA levels in mouse lungs and negatively correlated with mouse weight on day 3.

Table 5. **Correlation between lung damage mean cumulative histological score and mouse weight, nitrite concentration in BAL fluid, IAV PA RNA, iNOS mRNA, IFN-γ and TNF-α mRNA in experimental mouse groups lungs on day 3 after influenza A virus infection**

Parameter	Mean cumulative histological score	
	r	p value
Weight on day 3	-0.428[*]	0.009
Nitrites	0.546[*]	0.001
IAV PA RNA	0.595[*]	0.001
iNOS mRNA	0.428[*]	0.023
IFN-γ mRNA	0.476[*]	0.010
TNF-α mRNA	0.746[*]	<0.001

Spearman's correlation analysis was used. r: Spearman's correlation coefficient. A p value of <0.05 was considered significant (*)

The correlation coefficients between lung damage mean cumulative histological score and analysed parameters on day 5 after influenza A virus infection are shown in **Table 6**. Strongly positive correlations were found between the lung damage score and the relative IAV PA RNA and TNF-α mRNA levels in mouse lungs. The mean cumulative histological score was found to be moderately positively correlated with iNOS mRNA and IFN-γ mRNA relative levels in mouse lungs and moderately negatively correlated with mouse weight on day 5.

Table 6. Correlation between lung damage mean cumulative histological score and mouse weight, nitrite concentration in BAL fluid, IAV PA RNA, iNOS mRNA, IFN-γ and TNF-α mRNA in experimental mouse group lungs on day 5 after influenza A virus infection

Parameter	Mean cumulative histological score	
	r	*p* value
Weight on day 5	-0.495*	0.002
Nitrites	0.355	0.05
IAV PA RNA	0.822*	<0.001
iNOS mRNA	0.594*	<0.001
IFN-γ mRNA	0.571*	<0.001
TNF-α mRNA	0.690*	<0.001

Spearman's correlation analysis was used. *r*: Spearman's correlation coefficient. A *p* value of <0.05 was considered significant (*).

4. DISCUSSION

The role of iNOS and NO in inflammation and infection is complicated and ambiguous. The role depends on the organism and organ involved, the cell type, NO concentration and the stage of the inflammatory response, ultimately enhancing inflammation or abrogating it (187, 188). The NO antimicrobial and cytoprotective activities have been observed in bacterial, fungal, and parasitic infections in *in vitro* and murine models (75-78). Acute lung injury and sepsis are associated with increased iNOS-derived NO, but it was found recently, that iNOS plays a pivotal role in late response mediating resolution of lung injury (187). The iNOS expression post influenza infection differs in various organisms. For example, the iNOS expression in infected chickens occurs earlier and is greater at the organ level as compared with that in ducks; this may help explain the more severe disease associated with H5N1 infection in this species (189).

However, a deleterious role of NO-mediated inflammation and pathogenesis in influenza virus infection was demonstrated in a series of investigations in murine models or human authopsies (10, 14, 24, 96, 97). Similarly, we found the greater relative level of iNOS together with nitrite concentration in mouse lungs post influenza infection, compared to uninfected mice. The main findings of our experiment were that treatment of influenza infected mice with zanamivir was associated with less NO synthesis on 3rd day, and treatment with the combination of zanamivir and ASO to iNOS was associated with inhibition of NO synthesis in lungs, together with diminished lung damage and mice that appeared healthier on the 5th day post-infection. A detailed discussion of the results is given below.

4.1 Effect of influenza virus infection to analysed parameters

Mice are widely used as an animal model for influenza virus research. The susceptibility of mice to influenza viruses depends both on the mouse strain and on the influenza virus strain. The majority of influenza virus research in mice employs either BALB/c or C57BL/6 mouse strains. Researchers mostly use influenza virus specifically adapted through serial passage in the particular mouse strain they plan to use for their studies. In particular, the early human isolates, PR8 and WSN, have become the prototype lab strains used in the mouse model (111). In our study, we infected BALB/c mice with A/Puerto Rico/8/34 (A/PR/8/34) (H1N1) virus.

Murine models of influenza virus infection illustrate that females develop higher inflammatory immune responses and slower repair of damaged tissue following IAV infection. There are differences between the sexes in the outcome of infection also (190). Only female mice were used in our study to avoid the influence of sex to the results of the experiment.

The parameters commonly used to evaluate influenza viral pathogenicity in mice are body weight loss and mortality. In addition, viral titers and pathology scores may be monitored. Amelioration of these virological, clinical or histopathological parameters in the presence of an investigational drug suggests its efficacy in an animal model (111).

We detected no IAV PA RNA in negative control mice on either the 3rd or 5th day of the experiment. Increased viral loads were present in the lungs of all groups of IAV-infected mice at days 3 and 5 post infection. However, the IAV PA RNA level was higher in infected and lactose treated mice compared with untreated influenza-infected mice in our study, which could be interpreted to mean that the intranasal treatments themselves may facilitate viral replication (191).

Influenza infection induces a cascade of host immune responses that involve production of proinflammatory cytokines and recruitment of inflammatory cells in infected lungs (9-13). Cytokines such as IFN-γ and TNF-α stimulate the production of iNOS leading to high-output synthesis of NO, predominantly in macrophages (13-16). In turn, the NO and excessive amounts of reactive nitrogen intermediates can lead to significant lung immunopathology (11, 13, 17).

We found significantly higher TNF-α mRNA relative levels in the positive control group than in the negative control group on both analysed days. A similar relationship was observed in relative IFN-γ mRNA levels; they were higher in the positive as compared with the negative control group on both days. We detected significantly higher relative iNOS mRNA levels in mouse lungs in the positive control group as compared with the negative control group on both days. Interestingly, although IAV PA RNA expression is less on day 5 compared to day 3, the relative iNOS mRNA levels in mouse lungs of positive control groups on day 5 were not diminished, nor was the histological lung damage. On that basis we suggest that iNOS contributes to development of lung damage even if viral expression diminishes.

Akaike linked excessive NO production in influenza infected mouse lungs to iNOS activation (14). We observed a similar relationship on both day 3 and 5 post-infection, i.e., significantly increased NO synthesis in the lungs in

influenza infected (positive control) as compared with uninfected (negative control) mice. Concentration of nitrites diminished significantly on day 5 vs. day 3 in the positive control group. These results were similar to that described by Perone (113), where levels of NO in mice infected with 1918 and H5N1 viruses declined a little on day 5, but were the highest on day 7 after the inoculation, a time point that correlated with high numbers of total lung macrophages and neutrophils.

Clinical signs of influenza in the mouse usually develop 2–3 days after infection and vary considerably, depending on both mouse and virus strains, as well as the challenge dose. Symptoms include lethargy, anorexia and loss of body weight, huddling, ruffled fur, and death (192). We observed the mouse body weight changes over a 5-day period. The positive mouse control group (influenza infected) lost significantly more weight than the negative mouse control group (uninfected) from day 2 through day 5. Uninfected mice also lost some weight, perhaps a reflection of handling and procedure-related stress. Interestingly, inside the negative control group, body weight loss of zanamivir and ODN combination treated mice were significantly less than the zanamivir only treated mice on both days and the combination treatment group mice even gained weight starting day 4. There is no available explanation of this phenomenon in the literature; certainly one explanation could be that this was a direct or indirect pharmacological effect of the combination of zanamivir and antisense oligodeoxynucleotide to iNOS.

Experimental animal models and humans infected with influenza A viruses share many histologic features, including desquamation of the ciliated epithelium of the tracheobronchial airways and peribronchial mononuclear cell inflammatory infiltrates, evidence of viral degeneration of alveolar lining, hyperemia and congestion, septal inflammatory infiltrates, the appearance of macrophages with necrotic cellular debris in air spaces, and intraalveolar edema and hemorrhage (2). Murine influenza, however, has some physiological distinctions from typical uncomplicated influenza in humans (110). Most histopathologic studies from human influenza autopsies demonstrated DAD. However, DAD in mice has only recently been reported (120). Fukushi in his study (112) revealed the serial process of pathological changes from interstitial pneumonia to DAD in the lung of mice infected with influenza virus. Interstitial pneumonia was observed in the lung of live mice infected with PR8 virus when they were sacrificed. In contrast, DAD was found in dying and dead mice. Histopathological examination of live infected-mice sacrificed from 2 to 6 days postinfection revealed that interstitial pneumonia

gradually expanded from pulmonary parenchyma around bronchioles to the entire lungs, while DAD was not observed anywhere. DAD with severe collapse was found in mice at 8 days postinfection that were expected to die within 24 hours or had just died from influenza and autopsied immediately after their deaths.

In our study, the lung damage, expressed by mean cumulative histological score, was significantly higher in IAV infected (positive control) compared to uninfected (negative control) group mice. In IAV-infected mouse lungs the scope of the histological damage progressed over time, as the positive control's group mean cumulative histological score was signiffcantly greater on the 5th day than on the 3rd day. After IAV infection, the inflammation appeared to first affect the bronchi and caused peribronchial lymphocytic infiltration, as it was more evident on day 3 than on day 5. With the release of the cytokines and chemokines, endothelial permeability was increased, leukocyte migration was triggered and inflammation expanded from pulmonary parenchyma around bronchi to the entire lungs over time. As the bronchiolitis became more pronounced, focal leukocytic and perivascular lymphocytic infiltrations occurred progression from day 3 to day 5 in our study. We observed no hyaline membrane nor DAD in our mouse lungs, likely because we euthanized them well before they were actively dying as compared to that described by Fukushi (112).

The lung injury in influenza may be due to either a direct viral cytopathic effect and/or host factors. We found a positive correlation between mean cumulative histological score and IAV PA RNA relative level on both days, thus we infer a direct IAV-induced effect on mouse lungs. In our study, the lung mean cumulative histological score correlated positively with IFN-γ and TNF-α mRNA, iNOS mRNA relative levels in mouse lungs on both analysed days, as well as with nitrite concentration in BAL fluid on day 3. This may demonstrate the importance of host factors to lung injury during influenza. The histological score correlated negatively with mouse body weights on both days, however, weight loss might be induced by hightened levels of TNF-α in positive control group mouse lungs.

In summary, we observed infection with IAV induced lung damage associated with increased cytokine, iNOS and NO expression in lungs and mice weight loss on both 3 and 5 days after infection. This corresponds to the changes described in the literature after influenza infection in the mouse model (13-16).

4.2 Prevention of influenza viral pneumonia using zanamivir

Zanamivir (Relenza™) is an inhaled viral neuraminidase inhibitor with demonstrated effectiveness in mice following IAV for reducing pulmonary influenza virus titers, and scores for lung consolidation, morbidity and mortality, and, in people, for alleviating clinical symptoms of influenza infection (125, 127, 193). It is also reported to suppress production of NO in IAV-infected and IFN-γ-activated RAW 264.7 macrophages *in vitro* (25). In our study, for the first time, we tested the capacity of zanamivir to reduce pulmonary inflammation through the inhibition of NO synthesis under *in vivo* conditions, *i.e.* in IAV-infected mice.

We confirmed the antiviral effect of zanamivir treatment of the IAV infected mice in our study, with significantly reduced relative IAV PA RNA levels in IAV-infected and zanamivir treated mouse lungs compared to IAV-infected and lactose treated mice on both days. This positive control group with lactose was used as zanamivir (Relenza™) consists of a powder mixture of zanamivir and lactose per blister.

We did not observe reduced cytokines levels in our study in treatment with zanamivir of the IAV infected mouse group compared with the positive control on either day 3 or 5 post-infection. Zheng in the mouse influenza experiment also found that even if the viral replication had been suppressed in mice treated with antivirals, levels of cytokines and chemokines were still similar to that of untreated mice (194). We may suggest that once the viral infection has triggered the cytokine production, although viral replication may be suppressed by antiviral therapy, the proinflammatory cytokines and chemokines can continue to drive the immunopathologic progression.

We noted 31% less iNOS mRNA in the Virus+Zanamivir treatment group mouse lungs than in the lungs of the positive control group on day 3. But, on day 5, the level of iNOS mRNA in IAV-infected and zanamivir treated mouse lungs was not reduced compared to positive control. The iNOS mRNA expression in IAV infected-zanamivir treated mice increased singnificantly from day 3 to day 5.

We found similar trends in nitrite concentration and iNOS mRNA expression. In the group of influenza infected-zanamivir treated mice the concentration of nitrites was significantly less than in the positive control group on day 3. It is reasonable to relate these effects to the reduced IAV replication with zanamivir causing the decrease of viral load and inflammation. Yet it is possible that there is a direct inhibitory effect of zanamivir on NO production

in cytokines-activated macrophages, as was previously suggested by *in vitro* experiments (25). Kačergius et al. demonstrated a synergistic effect between influenza virus and IFN-γ in NO production within RAW 264.7 macrophages reduced by neuraminidase inhibitors. Unexpectedly, they observed that oseltamivir and zanamivir suppressed NO generation in macrophages stimulated with IFN-γ alone, even without influenza infection (25). We may also suppose that the effects of zanamivir on viral entry and cell lysis reduce net inflammation simply by limiting tissue necrosis and the effect of necrosis on generating non-specific inflammation that includes NO and macrophage activation. However, we found no later effect of zanamivir treatment of IAV-infected mice in reducing NO concentration, as on day 5 the concentration of nitrites was already similar to that found in positive control lungs and during that time it increased by 29% from the 3rd to the 5th day.

Moreover, the clinical condition of the mice was consistent with the weight changes. The infected and zanamivir treated mouse weight loss was significantly smaller than for the positive control group on day 3, but there were no significant differences on day 5.

The results of our study indicate that treatment with zanamivir suppressed lung damage in IAV-infected mice; in the Virus+Zanamivir treatment group the mean cumulative histological score was significantly lower than for the positive control group on both days. On day 3, we also found significantly less peribronchial lymphocytic infiltration, which may be present in the earlier stage of lung inflammation, than for the positive control group mouse lungs. The spread of lung inflammation was also less on day 5 in zanamivir treated, IAV-infected mice with significantly less intense focal leukocytic and perivascular lymphocytic infiltration as compared to mice in the positive control group. However, the histological lung damage was significantly greater on the 5th day than the 3rd day in the IAV-infected and zanamivir treated mouse lungs.

In summary, although IAV PA RNA relative level was less in infected-zanamivir treated mouse lungs on both days 3 and 5, the other analyzed parameters had different dynamics. We found lower levels of cytokines, iNOS mRNA expression, nitrite concentration, weight loss and histological damage on day 3 compared to day 5. One of the aims of experiment was to evaluate the combination of zanamivir and antisense oligodeoxynucleotide to iNOS effect in influenza infection. It is known, that in order to determine whether combination drug treatment is beneficial in mice, it is necessary to use sub-optimal antiviral doses. Otherwise, an overwhelmingly potent effect of the antiviral alone can mask any added benefit of the second compound (195). We

chose the 2 mg/kg dose of zanamivir after a pilot dose ranging study with this medication was completed and guided by clinical symptoms of IAV infected mice. It is known that intranasal liquid treatments facilitate virus production (probably through enhanced virus spread) and promote lung pathology (191). In order to produce uniform experimental conditions and not facilitate virus spread by repeated intranasal interventions, zanamivir, like the ODN antisense, was administered once per day in our study. Thus, the absence of zanamivir's inhibitory activity on iNOS mRNA expression and nitrite concentration on day 5 may be related to insufficient drug concentration. Nevertheless, the data of the 3rd day demonstrated the decrease in nitrite production in mouse lungs. This would mean that zanamivir contributes to two early outcomes – reduced virus replication (antiviral activity) and reduced NO production (secondary anti-inflammatory activity). However, additional studies with different doses and schemes of administration of zanamivir are needed to understand the mechanism by which this drug suppresses synthesis of NO.

4.3 Prevention of influenza viral pneumonia using antisense oligodeoxynucleotide to iNOS

To our knowledge, the present study is the first to demonstrate the therapeutic effects of ASO to iNOS mRNA in a mouse influenza model. We used an unmodified oligodeoxynucleotide with phosphodiester internucleotide linkages.

In our experiment, treatment with ODN to iNOS of influenza infected mice resulted in significantly lower pulmonary IAV PA RNA levels as compared to those in the Virus+Lactose mouse group. This suppressing effect was observed on both day 3 and 5. Surprisingly, the literature reports on any antiviral effect of iNOS suppression in mouse influenza infection model is contradictory. There are several experiments in the mouse influenza infection model that indicate an antiviral effect of suppressed iNOS gene expression (10, 91). However, other authors revealed no effect of iNOS in influenza virus clearance, even with the high pathogenic 1918 and H5N1 virus infections (14, 15, 113).

The observed antiviral mechanism of ODN to iNOS in our experiment is not fully understood and deserves further evaluation. We suggest that one of possible explanations could be the significantly higher IFN-γ mRNA expression in IAV-infected ODN treated mouse lungs compared to those from the positive mouse control group, which we detected on both day 3 and 5. Karupiah and coauthors also found the heightened IFN-γ release in influenza

infected iNOS deficient mice, and associated this as a requirment for influenza A virus clearance. This effect was unaccompanied by changes in antiviral cytotoxic T lymphocyte activity (91).

We did not find the expected significant reduction in either the relative levels of iNOS RNA or in the concentration of nitrites in Virus+ODN mouse group lungs on day 3 or 5 compared to that found in the positive control group's lungs. However, on day 5, we observed the tendency of reduced iNOS RNA expression and reduced nitrite concentration compared to the Virus+Zanamivir mouse group's lungs. Interestingly, the concentration of nitrites became significantly smaller on day 5 versus day 3 in Virus+ODN mice. Thus we may suppose that the action of iNOS ODN may be time dependent, or that the insufficient dose or administration scheme were used. We selected an antisense dose on the basis of other mouse experiments described in the literature, where antisense was applied via the respiratory rout (196, 197) and delivered once daily. Further experiments with different doses of ODN and longer observation time, and the measurement of not only iNOS mRNA level, but the iNOS protein concentration in mouse lungs should be worthwhile.

Despite absent significant reductions in iNOS mRNA level and nitrite concentrations in Virus+ODN group compared with those in the positive control, we found the obviously diminished mouse lung histological damage on day 5. The significantly less focal leukocytic infiltration and bronchiolitis were observed compared with the positive mouse control group on the 5th day. The mean cumulative lung damage histological score in the IAV-infected ODN-treated group was significantly smaller than in the positive control mouse group on day 5, however, the scores between these groups were similar on day 3. These results correspond to data in studies where mouse lung inflammation and damage were suppressed and the number of inflammatory cells in the airways was reduced in an influenza strain-independent manner when treated with other iNOS inhibiting compounds or when deficient in iNOS gene expression (10, 14, 24). We may suppose that reduced lung cellularity could be determined by the reduction of levels of the chemotactic factors. However, exact mechanisms of antisense ODN to iNOS-dependent effects on inflammatory cell accumulation in mouse lungs after influenza infection are unknown.

Surprisingly, in IAV-infected and ODN to iNOS treated mouse lungs the highest TNF-α mRNA level was found. An over-exuberant release of cytokine TNF-α can contribute to weight loss during influenza infection (198). Our results confirmed this association, as IAV-infected and ODN treated mice

steadily lost weight with significant difference to negative mouse control group on days 3 and 5, and this correlated with increased TNF-α mRNA in mouse lungs.

Despite the elevated level of TNF-α mRNA in ODN treated mice post-influenza infection, the inflammatory cell infiltration in that group's lungs was significantly less in our study. Although TNF-α levels were described to correlate directly with the severity of gross and histologic lung lesions in influenza infected mice (199), more recent studies reveal that, different from the traditional belief, this cytokine is critically required for negatively regulating the extent of lung immunopathology during acute influenza infection (200). Indeed, in a model of acute A(H1N1) influenza infection in TNF-α-deficient mice, TNF-α deficiency led not only to a greater extent of illness but also to heightened lung pathology and tissue remodeling with increased inflammatory cell infiltration and anti-influenza adaptive immune responses (200).

In summary, the iNOS RNA relative level and nitrite concentration in the Virus+ODN mouse group were similar to that in positive control mice. However, concentration of nitrites declined significantly from day 3 to day 5 in the Virus+ODN group; this suggests the action of antisense oligonucleotide to iNOS may be time dependent and needs to be evaluated over a longer duration in future studies. Even though iNOS mRNA and nitrite concentrations in Virus+ODN group compared with positive control were not signficantly less, we found substantially less mouse lung histological damage on day 5. The exact mechanisms of antisense to iNOS-dependent potential to reduce inflammatory cell accumulation in mouse lungs post-influenza infection are unknown and deserve to be evaluated in future studies.

4.4 Prevention of influenza viral pneumonia using zanamivir and antisense oligodeoxynucleotide to iNOS

An obvious strategy to optimize anti-influenza therapy is to combine drugs with different modes of action. Because host responses to infection also contribute to illness pathogenesis, improved outcomes might be gained from the combination of antiviral therapy with drugs that modulate the immune response in an infected individual (201). We analyzed how zanamivir and antisense oligodeoxynucleotide to iNOS combination treatment affect influenza infection in a mouse model.

Similar to the other treatment groups in our study, zanamivir and ODN to iNOS combination treatment of IAV-infected mice had an early antiviral

effect, as indicated by significantly less IAV PA RNA levels than in IAV-infected and lactose treated mice on both day 3 and 5 after infection. However, cytokines, iNOS mRNA, nitrite levels, histological lung damage and mouse clinical condition differed between treatment groups and in progression over time.

On day 3, we found that treatment of IAV-infected mice treated only with zanamivir had less NO synthesis, lung damage and weight loss. Different from the zanamivir and similarly to the ODN to iNOS treatment groups, on the 3rd day the combination treatment group did not have reduced iNOS RNA expression, nitrite concentration, lung damage or weight loss compared to the positive control group. Thus there was no early protective effect of combination treatment in IAV-infected mice.

Instead, there was obvious improvement by day 5 with combination treatment in our study. On the 5th day, the relative iNOS mRNA level in combination treatment mouse lungs was significantly less than in IAV-infected zanamivir-only treated mice. Respectively, we found the lowest nitrite concentration in the combination treatment group compared to the other treatment groups; it was significantly diminished as compared with the positive control. This could suggest, that combination treatment of zanamivir + ODN to iNOS suppressed nitrite production more than that of zanamivir alone.

The level of TNF-α mRNA in combination treatment group was significantly less than in the Virus+ODN and had a tendency to be even lower (17.0% less) compared to that in the Virus+Zanamivir treatment groups by day 5. This reduced expression of TNF-α mRNA may be associated with less weight loss. Indeed, by the 4th day, mice in the combination treatment group started to gain weight; by day 5, their weight loss was significantly less than in the positive control, even Zanamivir, and ODN to iNOS treatment groups. This could be interpreted that mice in Zanamivir+ODN treatment group were in better clinical condition.

We found the later (on day 5) protective lung damage effect in combination treatment of IAV-infected mouse group also, as the mean cumulative histological score was significantly smaller vs. positive control group mouse group, with significantly less focal leukocytic infiltration.

In summary, treatment of influenza infected mice with combination of zanamivir and antisense oligodeoxynucleotide to iNOS caused the early suppression of viral replication, similar like in other two treatment groups. However, the other evaluated parameters differed from zanamivir-only or ODN to iNOS-only treatment groups and in dynamics. The later (on 5th day)

effect was observed in diminishing lung damage, and it was associated with suppressed iNOS mRNA expression and NO synthesis in mouse lungs, lower expression of TNF-α mRNA and better mice cinical condition in combination treatment group.

CONCLUSIONS

1. Infection of mice with A/Puerto Rico/8/34 influenza virus induced lung inflammation, which was associated with significantly greater TNF-α mRNA, iNOS mRNA expression in lungs, higher NO concentration in BAL fluid, and more mouse weight loss.

2. Treatment of influenza infected mice with zanamivir caused the early suppression of viral replication and NO synthesis, and it was associated with less lung damage and weight loss.

3. The suppression of viral replication was early, but the protective lung damage effect was late and not associated with inhibition of NO synthesis in lungs in the treatment of influenza infected mice with antisense oligodeoxynucleotide to iNOS group. The increased expression of TNF-α mRNA was associated with significant mouse weight loss.

4. Treatment of influenza infected mice with the combination of zanamivir and antisense oligodeoxynucleotide to iNOS resulted in early suppression of viral replication, but the protective lung damage effect was late and associated with inhibition of NO synthesis in lungs. The lower expression of TNF-α mRNA could explain reduced weight loss.

PRACTICAL RECOMMENDATIONS

The study demonstrated several new findings. First, that treatment with zanamivir posesses the early capacity to suppress NO synthesis in mouse lungs after influenza infection. Second, that treatment with antisense oligodeoxynucleotide to iNOS mRNA can reduce lung inflammation caused by influenza virus infection in mice, and its combination with zanamivir has clinical benefit; thus, this treatment approach could be a potential new option in the treatment of influenza virus infection. However, there are several unresolved questions to fully understand the mechanisms of action of medications and additional studies should be worthwhile.

1. As the later effect (on day 5) of zanamivir's capacity to suppress NO synthesis was not observed, further experiments with different doses and schemes of administration of zanamivir are needed.

2. The observed antiviral mechanism of antisense ODN to iNOS in our experiment is not fully clear and should be evaluated in further studies.

3. We found no significant effect of antisense ODN to iNOS in suppressing NO synthesis, but different doses of medication and treatment and testing for additional days should be studied. Detection of not only iNOS mRNA level, but the iNOS protein concentration in mouse lungs should also help our understanding.

4. The exact mechanisms of the antisense ODN to iNOS-dependent potential to reduce inflammatory cells accumulation in mouse lungs post-influenza infection are unknown and should be evaluated in further studies.

THE AUTHOR'S CONTRIBUTION

Prof. Dr. Stefan Gravenstein, MD, MPH, formulated the idea and theme of the work.

The initial part of the experiment (inoculation of mice with virus, treatment with compounds, euthanazia, preparation of the study material) was performed in Eastern Virginia Medical School, Norfolk, VA, USA by Assoc. Prof. Dr. Tomas Kačergius.

The frozen material was transported and analysed further in Lithuania during the author's doctoral dissertation period. The author planned, searched for the required reagents and organised the performance of the multiplex real-time qRT-PCR analyses for determination of influenza viral PA RNA, iNOS, IFN-γ, TNF-α and beta (β)-actin mRNA relative levels. The author assisted in the histological examination of mouse lungs under the leadership of Assoc. Prof. Dr. Edvardas Žurauskas. The author processed and interpreted the results, performed the statistical analyses, presented the findings of the experiment at scientific conferences and produced publications.

ACKNOWLEDGEMENTS

REFERENCES

1. World Health Organization. Influenza (seasonal) fact sheet 2018 (Available from: http://www.who.int/mediacentre/factsheets/fs211/en/).

2. Taubenberger JK, Morens DM. The pathology of influenza virus infections. Annu Rev Pathol. 2008;3:499-522.

3. Kuiken T, Taubenberger JK. Pathology of human influenza revisited. Vaccine. 2008;26 Suppl 4:D59-66.

4. Morens DM, Taubenberger JK, Fauci AS. Predominant role of bacterial pneumonia as a cause of death in pandemic influenza: implications for pandemic influenza preparedness. J Infect Dis. 2008;198(7):962-70.

5. Klugman KP, Chien YW, Madhi SA. Pneumococcal pneumonia and influenza: a deadly combination. Vaccine. 2009;27 Suppl 3:C9-C14.

6. Ruuskanen O, Lahti E, Jennings LC, Murdoch DR. Viral pneumonia. Lancet. 2011;377(9773):1264-75.

7. de Jong MD, Simmons CP, Thanh TT, Hien VM, Smith GJ, Chau TN, et al. Fatal outcome of human influenza A (H5N1) is associated with high viral load and hypercytokinemia. Nat Med. 2006;12(10):1203-7.

8. Kash JC, Tumpey TM, Proll SC, Carter V, Perwitasari O, Thomas MJ, et al. Genomic analysis of increased host immune and cell death responses induced by 1918 influenza virus. Nature. 2006;443(7111):578-81.

9. Van Reeth K. Cytokines in the pathogenesis of influenza. Vet Microbiol. 2000;74(1-2):109-16.

10. Jayasekera JP, Vinuesa CG, Karupiah G, King NJ. Enhanced antiviral antibody secretion and attenuated immunopathology during influenza virus infection in nitric oxide synthase-2-deficient mice. J Gen Virol. 2006;87(Pt 11):3361-71.

11. La Gruta NL, Kedzierska K, Stambas J, Doherty PC. A question of self-preservation: immunopathology in influenza virus infection. Immunol Cell Biol. 2007;85(2):85-92.

12. Kumar Y, Liang C, Limmon GV, Liang L, Engelward BP, Ooi EE, et al. Molecular analysis of serum and bronchoalveolar lavage in a mouse model of influenza reveals markers of disease severity that can be clinically useful in humans. PLoS One. 2014;9(2):e86912.

13. Short KR, Kroeze E, Fouchier RAM, Kuiken T. Pathogenesis of influenza-induced acute respiratory distress syndrome. Lancet Infect Dis. 2014;14(1):57-69.

14. Akaike T, Noguchi Y, Ijiri S, Setoguchi K, Suga M, Zheng YM, et al. Pathogenesis of influenza virus-induced pneumonia: involvement of both nitric oxide and oxygen radicals. Proc Natl Acad Sci U S A. 1996;93(6):2448-53.

15. Suliman HB, Ryan LK, Bishop L, Folz RJ. Prevention of influenza-induced lung injury in mice overexpressing extracellular superoxide dismutase. Am J Physiol Lung Cell Mol Physiol. 2001;280(1):L69-78.

16. Bosca L, Zeini M, Traves PG, Hortelano S. Nitric oxide and cell viability in inflammatory cells: a role for NO in macrophage function and fate. Toxicology. 2005;208(2):249-58.

17. Zaki MH, Akuta T, Akaike T. Nitric oxide-induced nitrative stress involved in microbial pathogenesis. J Pharmacol Sci. 2005;98(2):117-29.

18. Hayden F. Developing new antiviral agents for influenza treatment: what does the future hold? Clin Infect Dis. 2009;48 Suppl 1:S3-13.

19. Hayden FG. Newer influenza antivirals, biotherapeutics and combinations. Influenza Other Respir Viruses. 2013;7 Suppl 1:63-75.

20. Moscona A. Medical management of influenza infection. Annu Rev Med. 2008;59:397-413.

21. Barik S. New treatments for influenza. BMC Med. 2012;10:104.

22. Han D, Wei T, Zhang S, Wang M, Tian H, Cheng J, et al. The therapeutic effects of sodium cromoglycate against influenza A virus H5N1 in mice. Influenza Other Respir Viruses. 2016;10(1):57-66.

23. Hussain M, Galvin HD, Haw TY, Nutsford AN, Husain M. Drug resistance in influenza A virus: the epidemiology and management. Infect Drug Resist. 2017;10:121-34.

24. Akaike T, Okamoto S, Sawa T, Yoshitake J, Tamura F, Ichimori K, et al. 8-nitroguanosine formation in viral pneumonia and its implication for pathogenesis. Proc Natl Acad Sci U S A. 2003;100(2):685-90.

25. Kacergius T, Ambrozaitis A, Deng Y, Gravenstein S. Neuraminidase inhibitors reduce nitric oxide production in influenza virus-infected and gamma interferon-activated RAW 264.7 macrophages. Pharmacol Rep. 2006;58(6):924-30.

26. Fields BN, Knipe DM, Howley PM. Fields virology. 5th ed. Philadelphia: Wolters Kluwer Health/Lippincott Williams & Wilkins; 2007.

27. World Health Organization. Influenza (Avian and other zoonotic). 2018.

28. Su S, Fu X, Li G, Kerlin F, Veit M. Novel Influenza D virus: Epidemiology, pathology, evolution and biological characteristics. Virulence. 2017;8(8):1580-91.

29. Bouvier NM, Palese P. The biology of influenza viruses. Vaccine. 2008;26 Suppl 4:D49-53.

30. Suzuki Y. Sialobiology of influenza: molecular mechanism of host range variation of influenza viruses. Biol Pharm Bull. 2005;28(3):399-408.

31. Bennett JE, Dolin R, Blaser MJ. Mandell, Douglas, and Bennett's principles and practices of infectious diseases. 8, editor. Philadelphia, PA: Elsevier; 2015. 3904 p.

32. Paules C, Subbarao K. Influenza. Lancet. 2017;390(10095):697-708.

33. Dawood FS, Iuliano AD, Reed C, Meltzer MI, Shay DK, Cheng PY, et al. Estimated global mortality associated with the first 12 months of 2009 pandemic influenza A H1N1 virus circulation: a modelling study. Lancet Infect Dis. 2012;12(9):687-95.

34. Webster RG, Peiris M, Chen H, Guan Y. H5N1 outbreaks and enzootic influenza. Emerg Infect Dis. 2006;12(1):3-8.

35. Horby P. H7N9 is a virus worth worrying about. Nature. 2013;496(7446):399.

36. Update: WHO-confirmed human cases of avian influenza A (H5N1) infection, November 2003-May 2008. Wkly Epidemiol Rec. 2008;83(46):415-20.

37. Poovorawan Y, Pyungporn S, Prachayangprecha S, Makkoch J. Global alert to avian influenza virus infection: from H5N1 to H7N9. Pathog Glob Health. 2013;107(5):217-23.

38. Herold S, Becker C, Ridge KM, Budinger GR. Influenza virus-induced lung injury: pathogenesis and implications for treatment. Eur Respir J. 2015;45(5):1463-78.

39. Ortiz JR, Neuzil KM, Rue TC, Zhou H, Shay DK, Cheng PY, et al. Population-based incidence estimates of influenza-associated respiratory failure hospitalizations, 2003 to 2009. Am J Respir Crit Care Med. 2013;188(6):710-5.

40. Beigel JH, Farrar J, Han AM, Hayden FG, Hyer R, de Jong MD, et al. Avian influenza A (H5N1) infection in humans. N Engl J Med. 2005;353(13):1374-85.

41. Writing Committee of the WHOCoCAoPI, Bautista E, Chotpitayasunondh T, Gao Z, Harper SA, Shaw M, et al. Clinical aspects of pandemic 2009 influenza A (H1N1) virus infection. N Engl J Med. 2010;362(18):1708-19.

42. Louie JK, Acosta M, Winter K, Jean C, Gavali S, Schechter R, et al. Factors associated with death or hospitalization due to pandemic 2009 influenza A(H1N1) infection in California. JAMA. 2009;302(17):1896-902.

43. Kumar A, Zarychanski R, Pinto R, Cook DJ, Marshall J, Lacroix J, et al. Critically ill patients with 2009 influenza A(H1N1) infection in Canada. JAMA. 2009;302(17):1872-9.

44. Iwasaki A, Pillai PS. Innate immunity to influenza virus infection. Nat Rev Immunol. 2014;14(5):315-28.

45. Brandes M, Klauschen F, Kuchen S, Germain RN. A systems analysis identifies a feedforward inflammatory circuit leading to lethal influenza infection. Cell. 2013;154(1):197-212.

46. Ricciardolo FL. Multiple roles of nitric oxide in the airways. Thorax. 2003;58(2):175-82.

47. Korhonen R, Lahti A, Kankaanranta H, Moilanen E. Nitric oxide production and signaling in inflammation. Curr Drug Targets Inflamm Allergy. 2005;4(4):471-9.

48. Morris SM, Jr., Billiar TR. New insights into the regulation of inducible nitric oxide synthesis. Am J Physiol. 1994;266(6 Pt 1):E829-39.

49. Chartrain NA, Geller DA, Koty PP, Sitrin NF, Nussler AK, Hoffman EP, et al. Molecular cloning, structure, and chromosomal localization of the human inducible nitric oxide synthase gene. J Biol Chem. 1994;269(9):6765-72.

50. Bogdan C. Nitric oxide and the immune response. Nat Immunol. 2001;2(10):907-16.

51. Barnes PJ, Belvisi MG. Nitric oxide and lung disease. Thorax. 1993;48(10):1034-43.

52. Hobbs AJ, Ignarro LJ. Nitric oxide-cyclic GMP signal transduction system. Methods Enzymol. 1996;269:134-48.

53. Marletta MA. Nitric oxide synthase structure and mechanism. J Biol Chem. 1993;268(17):12231-4.

54. Abu-Soud HM, Stuehr DJ. Nitric oxide synthases reveal a role for calmodulin in controlling electron transfer. Proc Natl Acad Sci U S A. 1993;90(22):10769-72.

55. Forstermann U, Schmidt HH, Pollock JS, Sheng H, Mitchell JA, Warner TD, et al. Isoforms of nitric oxide synthase. Characterization and purification from different cell types. Biochem Pharmacol. 1991;42(10):1849-57.

56. Guo Z, Shao L, Du Q, Park KS, Geller DA. Identification of a classic cytokine-induced enhancer upstream in the human iNOS promoter. FASEB J. 2007;21(2):535-42.

57. Lowenstein CJ, Alley EW, Raval P, Snowman AM, Snyder SH, Russell SW, et al. Macrophage nitric oxide synthase gene: two upstream regions mediate induction by interferon gamma and lipopolysaccharide. Proc Natl Acad Sci U S A. 1993;90(20):9730-4.

58. Muijsers RB, ten Hacken NH, Van Ark I, Folkerts G, Nijkamp FP, Postma DS. L-Arginine is not the limiting factor for nitric oxide synthesis by human alveolar macrophages in vitro. Eur Respir J. 2001;18(4):667-71.

59. Sittipunt C, Steinberg KP, Ruzinski JT, Myles C, Zhu S, Goodman RB, et al. Nitric oxide and nitrotyrosine in the lungs of patients with acute respiratory distress syndrome. Am J Respir Crit Care Med. 2001;163(2):503-10.

60. Tracey WR, Xue C, Klinghofer V, Barlow J, Pollock JS, Forstermann U, et al. Immunochemical detection of inducible NO synthase in human lung. Am J Physiol. 1994;266(6 Pt 1):L722-7.

61. Liu CY, Wang CH, Chen TC, Lin HC, Yu CT, Kuo HP. Increased level of exhaled nitric oxide and up-regulation of inducible nitric oxide synthase in patients with primary lung cancer. Br J Cancer. 1998;78(4):534-41.

62. Moodley YP, Chetty R, Lalloo UG. Nitric oxide levels in exhaled air and inducible nitric oxide synthase immunolocalization in pulmonary sarcoidosis. Eur Respir J. 1999;14(4):822-7.

63. Saleh D, Barnes PJ, Giaid A. Increased production of the potent oxidant peroxynitrite in the lungs of patients with idiopathic pulmonary fibrosis. Am J Respir Crit Care Med. 1997;155(5):1763-9.

64. Shiloh MU, MacMicking JD, Nicholson S, Brause JE, Potter S, Marino M, et al. Phenotype of mice and macrophages deficient in both phagocyte oxidase and inducible nitric oxide synthase. Immunity. 1999;10(1):29-38.

65. Nicholson S, Bonecini-Almeida Mda G, Lapa e Silva JR, Nathan C, Xie QW, Mumford R, et al. Inducible nitric oxide synthase in pulmonary alveolar macrophages from patients with tuberculosis. J Exp Med. 1996;183(5):2293-302.

66. Kobayashi A, Hashimoto S, Kooguchi K, Kitamura Y, Onodera H, Urata Y, et al. Expression of inducible nitric oxide synthase and inflammatory cytokines in alveolar macrophages of ARDS following sepsis. Chest. 1998;113(6):1632-9.

67. Uetani K, Der SD, Zamanian-Daryoush M, de La Motte C, Lieberman BY, Williams BR, et al. Central role of double-stranded RNA-activated protein kinase in microbial induction of nitric oxide synthase. J Immunol. 2000;165(2):988-96.

68. Taylor BS, Geller DA. Molecular regulation of the human inducible nitric oxide synthase (iNOS) gene. Shock. 2000;13(6):413-24.

69. Akaike T, Maeda H. Nitric oxide and virus infection. Immunology. 2000;101(3):300-8.

70. Jacobs AT, Ignarro LJ. Lipopolysaccharide-induced expression of interferon-beta mediates the timing of inducible nitric-oxide synthase induction in RAW 264.7 macrophages. J Biol Chem. 2001;276(51):47950-7.

71. Kačergius T, Ambrozaitis A. Contribution of nitric oxide to the pathogenesis of pulmonary infections (a review). Acta medica Lituanica, . 2003;10:169-73.

72. Turpeinen T, Nieminen R, Taimi V, Heittola T, Sareila O, Clark AR, et al. Dual specificity phosphatase 1 regulates human inducible nitric oxide synthase expression by p38 MAP kinase. Mediators Inflamm. 2011;2011:127587.

73. Rodriguez-Pascual F, Hausding M, Ihrig-Biedert I, Furneaux H, Levy AP, Forstermann U, et al. Complex contribution of the 3'-untranslated region to the expressional regulation of the human inducible nitric-oxide synthase gene. Involvement of the RNA-binding protein HuR. J Biol Chem. 2000;275(34):26040-9.

74. de Vera ME, Shapiro RA, Nussler AK, Mudgett JS, Simmons RL, Morris SM, Jr., et al. Transcriptional regulation of human inducible nitric oxide synthase (NOS2) gene by cytokines: initial analysis of the human NOS2 promoter. Proc Natl Acad Sci U S A. 1996;93(3):1054-9.

75. Nathan CF, Hibbs JB, Jr. Role of nitric oxide synthesis in macrophage antimicrobial activity. Curr Opin Immunol. 1991;3(1):65-70.

76. Doi T, Ando M, Akaike T, Suga M, Sato K, Maeda H. Resistance to nitric oxide in Mycobacterium avium complex and its implication in pathogenesis. Infect Immun. 1993;61(5):1980-9.

77. Umezawa K, Akaike T, Fujii S, Suga M, Setoguchi K, Ozawa A, et al. Induction of nitric oxide synthesis and xanthine oxidase and their roles in the antimicrobial mechanism against Salmonella typhimurium infection in mice. Infect Immun. 1997;65(7):2932-40.

78. James SL. Role of nitric oxide in parasitic infections. Microbiol Rev. 1995;59(4):533-47.

79. Stark JM, Khan AM, Chiappetta CL, Xue H, Alcorn JL, Colasurdo GN. Immune and functional role of nitric oxide in a mouse model of respiratory syncytial virus infection. J Infect Dis. 2005;191(3):387-95.

80. Adler H, Beland JL, Del-Pan NC, Kobzik L, Brewer JP, Martin TR, et al. Suppression of herpes simplex virus type 1 (HSV-1)-induced pneumonia in mice by inhibition of inducible nitric oxide synthase (iNOS, NOS2). J Exp Med. 1997;185(9):1533-40.

81. Szabo C, Ischiropoulos H, Radi R. Peroxynitrite: biochemistry, patho-physiology and development of therapeutics. Nat Rev Drug Discov. 2007;6(8):662-80.

82. Sawa T, Akaike T, Ichimori K, Akuta T, Kaneko K, Nakayama H, et al. Superoxide generation mediated by 8-nitroguanosine, a highly redox-active nucleic acid derivative. Biochem Biophys Res Commun. 2003;311(2):300-6.

83. Okamoto T, Akaike T, Sawa T, Miyamoto Y, van der Vliet A, Maeda H. Activation of matrix metalloproteinases by peroxynitrite-induced protein S-glutathiolation via disulfide S-oxide formation. J Biol Chem. 2001;276(31):29596-602.

84. Okamoto T, Akuta T, Tamura F, van Der Vliet A, Akaike T. Molecular mechanism for activation and regulation of matrix metalloproteinases during bacterial infections and respiratory inflammation. Biol Chem. 2004;385(11):997-1006.

85. Moreno JJ, Pryor WA. Inactivation of alpha 1-proteinase inhibitor by peroxynitrite. Chem Res Toxicol. 1992;5(3):425-31.

86. Frears ER, Zhang Z, Blake DR, O'Connell JP, Winyard PG. Inactivation of tissue inhibitor of metalloproteinase-1 by peroxynitrite. FEBS Lett. 1996;381(1-2):21-4.

87. Landino LM, Crews BC, Timmons MD, Morrow JD, Marnett LJ. Pero-xynitrite, the coupling product of nitric oxide and superoxide, activates prostaglandin biosynthesis. Proc Natl Acad Sci U S A. 1996;93(26):15069-74.

88. Hortelano S, Alvarez AM, Bosca L. Nitric oxide induces tyrosine nitration and release of cytochrome c preceding an increase of mitochondrial transmembrane potential in macrophages. FASEB J. 1999;13(15):2311-7.

89. Drapier JC, Wietzerbin J, Hibbs JB, Jr. Interferon-gamma and tumor necrosis factor induce the L-arginine-dependent cytotoxic effector mechanism in murine macrophages. Eur J Immunol. 1988;18(10):1587-92.

90. Xie QW, Whisnant R, Nathan C. Promoter of the mouse gene encoding calcium-independent nitric oxide synthase confers inducibility by interferon gamma and bacterial lipopolysaccharide. J Exp Med. 1993;177(6):1779-84.

91. Karupiah G, Chen JH, Mahalingam S, Nathan CF, MacMicking JD. Rapid interferon gamma-dependent clearance of influenza A virus and protection from consolidating pneumonitis in nitric oxide synthase 2-deficient mice. J Exp Med. 1998;188(8):1541-6.

92. Bender BS, Croghan T, Zhang L, Small PA, Jr. Transgenic mice lacking class I major histocompatibility complex-restricted T cells have delayed viral clearance and increased mortality after influenza virus challenge. J Exp Med. 1992;175(4):1143-5.

93. Mozdzanowska K, Furchner M, Maiese K, Gerhard W. CD4+ T cells are ineffective in clearing a pulmonary infection with influenza type A virus in the absence of B cells. Virology. 1997;239(1):217-25.

94. Stein-Streilein J, Guffee J. In vivo treatment of mice and hamsters with antibodies to asialo GM1 increases morbidity and mortality to pulmonary influenza infection. J Immunol. 1986;136(4):1435-41.

95. Aldridge JR, Jr., Moseley CE, Boltz DA, Negovetich NJ, Reynolds C, Franks J, et al. TNF/iNOS-producing dendritic cells are the necessary evil of lethal influenza virus infection. Proc Natl Acad Sci U S A. 2009;106(13):5306-11.

96. Nin N, Sanchez-Rodriguez C, Ver LS, Cardinal P, Ferruelo A, Soto L, et al. Lung histopathological findings in fatal pandemic influenza A (H1N1). Med Intensiva. 2012;36(1):24-31.

97. Capelozzi VL, Parra ER, Ximenes M, Bammann RH, Barbas CS, Duarte MI. Pathological and ultrastructural analysis of surgical lung biopsies in patients with swine-origin influenza type A/H1N1 and acute respiratory failure. Clinics (Sao Paulo). 2010;65(12):1229-37.

98. Al-Nimer MS, Mahmood MM, Khazaal SS. Nitrostative stress status during seasonal and pdmH1N1 infection in Iraq. J Infect Dev Ctries. 2011;5(12):863-7.

99. van Riel D, Munster VJ, de Wit E, Rimmelzwaan GF, Fouchier RA, Osterhaus AD, et al. Human and avian influenza viruses target different cells in the lower respiratory tract of humans and other mammals. Am J Pathol. 2007;171(4):1215-23.

100. van Riel D, den Bakker MA, Leijten LM, Chutinimitkul S, Munster VJ, de Wit E, et al. Seasonal and pandemic human influenza viruses attach better to human upper respiratory tract epithelium than avian influenza viruses. Am J Pathol. 2010;176(4):1614-8.

101. Guarner J, Falcon-Escobedo R. Comparison of the pathology caused by H1N1, H5N1, and H3N2 influenza viruses. Arch Med Res. 2009;40(8):655-61.

102. Kuiken T, van den Brand J, van Riel D, Pantin-Jackwood M, Swayne DE. Comparative pathology of select agent influenza a virus infections. Vet Pathol. 2010;47(5):893-914.

103. Hers JF, Masurel N, Mulder J. Bacteriology and histopathology of the respiratory tract and lungs in fatal Asian influenza. Lancet. 1958;2(7057):1141-3.

104. Centers for Disease C, Prevention. Bacterial coinfections in lung tissue specimens from fatal cases of 2009 pandemic influenza A (H1N1) - United States, May-August 2009. MMWR Morb Mortal Wkly Rep. 2009;58(38):1071-4.

105. Beasley MB. The pathologist's approach to acute lung injury. Arch Pathol Lab Med. 2010;134(5):719-27.

106. Harms PW, Schmidt LA, Smith LB, Newton DW, Pletneva MA, Walters LL, et al. Autopsy findings in eight patients with fatal H1N1 influenza. Am J Clin Pathol. 2010;134(1):27-35.

107. Shieh WJ, Blau DM, Denison AM, Deleon-Carnes M, Adem P, Bhatnagar J, et al. 2009 pandemic influenza A (H1N1): pathology and pathogenesis of 100 fatal cases in the United States. Am J Pathol. 2010;177(1):166-75.

108. Mauad T, Hajjar LA, Callegari GD, da Silva LF, Schout D, Galas FR, et al. Lung pathology in fatal novel human influenza A (H1N1) infection. Am J Respir Crit Care Med. 2010;181(1):72-9.

109. Nakajima N, Van Tin N, Sato Y, Thach HN, Katano H, Diep PH, et al. Pathological study of archival lung tissues from five fatal cases of avian H5N1 influenza in Vietnam. Mod Pathol. 2013;26(3):357-69.

110. Thangavel RR, Bouvier NM. Animal models for influenza virus pathogenesis, transmission, and immunology. J Immunol Methods. 2014;410:60-79.

111. Bouvier NM, Lowen AC. Animal Models for Influenza Virus Pathogenesis and Transmission. Viruses. 2010;2(8):1530-63.

112. Fukushi M, Ito T, Oka T, Kitazawa T, Miyoshi-Akiyama T, Kirikae T, et al. Serial histopathological examination of the lungs of mice infected with influenza A virus PR8 strain. PLoS One. 2011;6(6):e21207.

113. Perrone LA, Plowden JK, Garcia-Sastre A, Katz JM, Tumpey TM. H5N1 and 1918 pandemic influenza virus infection results in early and excessive infiltration of macrophages and neutrophils in the lungs of mice. PLoS Pathog. 2008;4(8):e1000115.

114. Memoli MJ, Tumpey TM, Jagger BW, Dugan VG, Sheng ZM, Qi L, et al. An early 'classical' swine H1N1 influenza virus shows similar pathogenicity to the 1918 pandemic virus in ferrets and mice. Virology. 2009;393(2):338-45.

115. Watanabe T, Tisoncik-Go J, Tchitchek N, Watanabe S, Benecke AG, Katze MG, et al. 1918 Influenza virus hemagglutinin (HA) and the viral RNA polymerase complex enhance viral pathogenicity, but only HA induces aberrant host responses in mice. J Virol. 2013;87(9):5239-54.

116. Tumpey TM, Basler CF, Aguilar PV, Zeng H, Solorzano A, Swayne DE, et al. Characterization of the reconstructed 1918 Spanish influenza pandemic virus. Science. 2005;310(5745):77-80.

117. Itoh Y, Shinya K, Kiso M, Watanabe T, Sakoda Y, Hatta M, et al. In vitro and in vivo characterization of new swine-origin H1N1 influenza viruses. Nature. 2009;460(7258):1021-5.

118. Dybing JK, Schultz-Cherry S, Swayne DE, Suarez DL, Perdue ML. Distinct pathogenesis of hong kong-origin H5N1 viruses in mice compared to that of other highly pathogenic H5 avian influenza viruses. J Virol. 2000;74(3):1443-50.

119. Nishimura H, Itamura S, Iwasaki T, Kurata T, Tashiro M. Characterization of human influenza A (H5N1) virus infection in mice: neuro-, pneumo- and adipotropic infection. J Gen Virol. 2000;81(Pt 10):2503-10.

120. Garigliany MM, Habyarimana A, Lambrecht B, Van de Paar E, Cornet A, van den Berg T, et al. Influenza A strain-dependent pathogenesis in fatal H1N1 and H5N1 subtype infections of mice. Emerg Infect Dis. 2010;16(4):595-603.

121. McKimm-Breschkin JL, Rootes C, Mohr PG, Barrett S, Streltsov VA. In vitro passaging of a pandemic H1N1/09 virus selects for viruses with neuraminidase mutations conferring high-level resistance to oseltamivir and peramivir, but not to zanamivir. J Antimicrob Chemother. 2012;67(8):1874-83.

122. von Itzstein M, Wu WY, Kok GB, Pegg MS, Dyason JC, Jin B, et al. Rational design of potent sialidase-based inhibitors of influenza virus replication. Nature. 1993;363(6428):418-23.

123. Kim CU, Lew W, Williams MA, Liu H, Zhang L, Swaminathan S, et al. Influenza neuraminidase inhibitors possessing a novel hydrophobic interaction in the enzyme active site: design, synthesis, and structural analysis of carbocyclic sialic acid analogues with potent anti-influenza activity. J Am Chem Soc. 1997;119(4):681-90.

124. Varghese JN, McKimm-Breschkin JL, Caldwell JB, Kortt AA, Colman PM. The structure of the complex between influenza virus neuraminidase and sialic acid, the viral receptor. Proteins. 1992;14(3):327-32.

125. Ryan DM, Ticehurst J, Dempsey MH, Penn CR. Inhibition of influenza virus replication in mice by GG167 (4-guanidino-2,4-dideoxy-2,3-dehydro-N-acetylneuraminic acid) is consistent with extracellular activity of viral neuraminidase (sialidase). Antimicrob Agents Chemother. 1994;38(10):2270-5.

126. Sidwell RW, Smee DF. In vitro and in vivo assay systems for study of influenza virus inhibitors. Antiviral Res. 2000;48(1):1-16.

127. Tarbet EB, Hamilton S, Vollmer AH, Luttick A, Ng WC, Pryor M, et al. A zanamivir dimer with prophylactic and enhanced therapeutic activity against influenza viruses. J Antimicrob Chemother. 2014;69(8):2164-74.

128. Samson M, Pizzorno A, Abed Y, Boivin G. Influenza virus resistance to neuraminidase inhibitors. Antiviral Res. 2013;98(2):174-85.

129. Thorlund K, Awad T, Boivin G, Thabane L. Systematic review of influenza resistance to the neuraminidase inhibitors. BMC Infect Dis. 2011;11:134.

130. Storms AD, Gubareva LV, Su S, Wheeling JT, Okomo-Adhiambo M, Pan CY, et al. Oseltamivir-resistant pandemic (H1N1) 2009 virus infections, United States, 2010-11. Emerg Infect Dis. 2012;18(2):308-11.

131. U.S. Food and Drug Administration. FDA approves new drug to treat influenza. 2018.

132. Hayden FG, Sugaya N, Hirotsu N, Lee N, de Jong MD, Hurt AC, et al. Baloxavir Marboxil for Uncomplicated Influenza in Adults and Adolescents. N Engl J Med. 2018;379(10):913-23.

133. Centers for Disease Control and Prevention. Influenza (flu) 2016 (Available from: http://www.cdc.gov/flu/ (accessed Nov 16, 2016).

134. Jefferson T, Jones M, Doshi P, Del Mar C. Neuraminidase inhibitors for preventing and treating influenza in healthy adults: systematic review and meta-analysis. BMJ. 2009;339:b5106.

135. Jefferson T, Jones MA, Doshi P, Del Mar CB, Hama R, Thompson MJ, et al. Neuraminidase inhibitors for preventing and treating influenza in healthy adults and children. Cochrane Database Syst Rev. 2014(4):CD008965.

136. Santesso N, Hsu J, Mustafa R, Brozek J, Chen YL, Hopkins JP, et al. Antivirals for influenza: a summary of a systematic review and meta-analysis of observational studies. Influenza Other Respir Viruses. 2013;7 Suppl 2:76-81.

137. Moscona A. Neuraminidase inhibitors for influenza. N Engl J Med. 2005;353(13):1363-73.

138. Popescu FD, Popescu F. A review of antisense therapeutic interventions for molecular biological targets in asthma. Biologics. 2007;1(3):271-83.

139. Liao W, Dong J, Peh HY, Tan LH, Lim KS, Li L, et al. Oligonucleotide Therapy for Obstructive and Restrictive Respiratory Diseases. Molecules. 2017;22(1).

140. Stephenson ML, Zamecnik PC. Inhibition of Rous sarcoma viral RNA translation by a specific oligodeoxyribonucleotide. Proc Natl Acad Sci U S A. 1978;75(1):285-8.

141. Khvorova A, Watts JK. The chemical evolution of oligonucleotide therapies of clinical utility. Nat Biotechnol. 2017;35(3):238-48.

142. Godfrey C, Desviat LR, Smedsrod B, Pietri-Rouxel F, Denti MA, Disterer P, et al. Delivery is key: lessons learnt from developing splice-switching antisense therapies. EMBO Mol Med. 2017;9(5):545-57.

143. Aartsma-Rus A. New Momentum for the Field of Oligonucleotide Therapeutics. Mol Ther. 2016;24(2):193-4.

144. Eckstein F. Phosphorothioate oligodeoxynucleotides: what is their origin and what is unique about them? Antisense Nucleic Acid Drug Dev. 2000;10(2):117-21.

145. Bennett CF, Swayze EE. RNA targeting therapeutics: molecular mechanisms of antisense oligonucleotides as a therapeutic platform. Annu Rev Pharmacol Toxicol. 2010;50:259-93.

146. Altmann KH, Fabbro D, Dean NM, Geiger T, Monia BP, Muller M, et al. Second-generation antisense oligonucleotides: structure-activity relationships and the design of improved signal-transduction inhibitors. Biochem Soc Trans. 1996;24(3):630-7.

147. McKay RA, Miraglia LJ, Cummins LL, Owens SR, Sasmor H, Dean NM. Characterization of a potent and specific class of antisense oligonucleotide inhibitor of human protein kinase C-alpha expression. J Biol Chem. 1999;274(3):1715-22.

148. Kurreck J. Antisense technologies. Improvement through novel chemical modifications. Eur J Biochem. 2003;270(8):1628-44.

149. Cerritelli SM, Crouch RJ. Ribonuclease H: the enzymes in eukaryotes. FEBS J. 2009;276(6):1494-505.

150. Wu H, Lima WF, Zhang H, Fan A, Sun H, Crooke ST. Determination of the role of the human RNase H1 in the pharmacology of DNA-like antisense drugs. J Biol Chem. 2004;279(17):17181-9.

151. Chan JH, Lim S, Wong WS. Antisense oligonucleotides: from design to therapeutic application. Clin Exp Pharmacol Physiol. 2006;33(5-6):533-40.

152. Kjems J, Howard KA. Oligonucleotide delivery to the lung: waiting to inhale. Mol Ther Nucleic Acids. 2012;1:e1.

153. Zhang X, Shan P, Jiang D, Noble PW, Abraham NG, Kappas A, et al. Small interfering RNA targeting heme oxygenase-1 enhances ischemia-reperfusion-induced lung apoptosis. J Biol Chem. 2004;279(11):10677-84.

154. Griesenbach U, Kitson C, Escudero Garcia S, Farley R, Singh C, Somerton L, et al. Inefficient cationic lipid-mediated siRNA and antisense oligonucleotide transfer to airway epithelial cells in vivo. Respir Res. 2006;7:26.

155. Tanaka M, Nyce JW. Respirable antisense oligonucleotides: a new drug class for respiratory disease. Respir Res. 2001;2(1):5-9.

156. Juliano RL. The delivery of therapeutic oligonucleotides. Nucleic Acids Res. 2016;44(14):6518-48.

157. Seguin RM, Ferrari N. Emerging oligonucleotide therapies for asthma and chronic obstructive pulmonary disease. Expert Opin Investig Drugs. 2009;18(10):1505-17.

158. Popescu FD. Antisense- and RNA interference-based therapeutic strategies in allergy. J Cell Mol Med. 2005;9(4):840-53.

159. Wong JP, Christopher ME, Salazar AM, Sun LQ, Viswanathan S, Wang M, et al. Broad-spectrum and virus-specific nucleic acid-based antivirals against influenza. Front Biosci (Schol Ed). 2010;2:791-800.

160. Hatta T, Takai K, Nakada S, Yokota T, Takaku H. Specific inhibition of influenza virus RNA polymerase and nucleoprotein genes expression by liposomally endocapsulated antisense phosphorothioate oligonucleotides: penetration and localization of oligonucleotides in clone 76 cells. Biochem Biophys Res Commun. 1997;232(2):545-9.

161. Wu Y, Zhang G, Li Y, Jin Y, Dale R, Sun LQ, et al. Inhibition of highly pathogenic avian H5N1 influenza virus replication by RNA oligonucleotides targeting NS1 gene. Biochem Biophys Res Commun. 2008;365(2):369-74.

162. Zhang T, Wang TC, Zhao PS, Liang M, Gao YW, Yang ST, et al. Antisense oligonucleotides targeting the RNA binding region of the NP gene inhibit replication of highly pathogenic avian influenza virus H5N1. Int Immunopharmacol. 2011;11(12):2057-61.

163. Wong JP, Christopher ME, Salazar AM, Dale RM, Sun LQ, Wang M. Nucleic acid-based antiviral drugs against seasonal and avian influenza viruses. Vaccine. 2007;25(16):3175-8.

164. Ge Q, Pastey M, Kobasa D, Puthavathana P, Lupfer C, Bestwick RK, et al. Inhibition of multiple subtypes of influenza A virus in cell cultures with morpholino oligomers. Antimicrob Agents Chemother. 2006;50(11):3724-33.

165. Gabriel G, Nordmann A, Stein DA, Iversen PL, Klenk HD. Morpholino oligomers targeting the PB1 and NP genes enhance the survival of mice infected with highly pathogenic influenza A H7N7 virus. J Gen Virol. 2008;89(Pt 4):939-48.

166. Lupfer C, Stein DA, Mourich DV, Tepper SE, Iversen PL, Pastey M. Inhibition of influenza A H3N8 virus infections in mice by morpholino oligomers. Arch Virol. 2008;153(5):929-37.

167. Iversen P, Schnell F, Crumley S, Mourich D, Voss T. Post exposure efficacy of AVI-7100 against influenza A in mouse and ferret infection models. Thesis on 22nd European Congress of Clinical Microbiology and Infectious Diseases2012.

168. Beigel JH, Voell J, Munoz P, Kumar P, Brooks KM, Zhang J, et al. Safety, tolerability, and pharmacokinetics of radavirsen (AVI-7100), an antisense oligonucleotide targeting influenza a M1/M2 translation. Br J Clin Pharmacol. 2018;84(1):25-34.

169. Kaufmann SHE, Dorhoi A, Hotchkiss RS, Bartenschlager R. Host-directed therapies for bacterial and viral infections. Nat Rev Drug Discov. 2018;17(1):35-56.

170. Thulasi Raman SN, Zhou Y. Networks of Host Factors that Interact with NS1 Protein of Influenza A Virus. Front Microbiol. 2016;7:654.

171. Belser JA, Lu X, Szretter KJ, Jin X, Aschenbrenner LM, Lee A, et al. DAS181, a novel sialidase fusion protein, protects mice from lethal avian influenza H5N1 virus infection. J Infect Dis. 2007;196(10):1493-9.

172. Droebner K, Pleschka S, Ludwig S, Planz O. Antiviral activity of the MEK-inhibitor U0126 against pandemic H1N1v and highly pathogenic avian influenza virus in vitro and in vivo. Antiviral Res. 2011;92(2):195-203.

173. Lee SM, Cheung CY, Nicholls JM, Hui KP, Leung CY, Uiprasertkul M, et al. Hyperinduction of cyclooxygenase-2-mediated proinflammatory cascade: a mechanism for the pathogenesis of avian influenza H5N1 infection. J Infect Dis. 2008;198(4):525-35.

174. Lee SM, Gai WW, Cheung TK, Peiris JS. Antiviral effect of a selective COX-2 inhibitor on H5N1 infection in vitro. Antiviral Res. 2011;91(3):330-4.

175. Marsolais D, Hahm B, Edelmann KH, Walsh KB, Guerrero M, Hatta Y, et al. Local not systemic modulation of dendritic cell S1P receptors in lung blunts virus-specific immune responses to influenza. Mol Pharmacol. 2008;74(3):896-903.

176. Bottcher-Friebertshauser E, Stein DA, Klenk HD, Garten W. Inhibition of influenza virus infection in human airway cell cultures by an antisense peptide-conjugated morpholino oligomer targeting the hemagglutinin-activating protease TMPRSS2. J Virol. 2011;85(4):1554-62.

177. Li K, Zhou Z, Wang YO, Liu J, Zhao HB, Yang J, et al. Pretreatment of mice with oligonucleotide prop5 protects them from influenza virus infections. Viruses. 2014;6(2):573-81.

178. von der Leyen HE, Dzau VJ. Therapeutic potential of nitric oxide synthase gene manipulation. Circulation. 2001;103(22):2760-5.

179. Ding M, Zhang M, Wong JL, Rogers NE, Ignarro LJ, Voskuhl RR. Antisense knockdown of inducible nitric oxide synthase inhibits induction of experimental autoimmune encephalomyelitis in SJL/J mice. J Immunol. 1998;160(6):2560-4.

180. Hoque AM, Papapetropoulos A, Venema RC, Catravas JD, Fuchs LC. Effects of antisense oligonucleotide to iNOS on hemodynamic and vascular changes induced by LPS. Am J Physiol. 1998;275(3 Pt 2):H1078-83.

181. Parmentier-Batteur S, Bohme GA, Lerouet D, Zhou-Ding L, Beray V, Margaill I, et al. Antisense oligodeoxynucleotide to inducible nitric oxide synthase protects against transient focal cerebral ischemia-induced brain injury. J Cereb Blood Flow Metab. 2001;21(1):15-21.

182. Noiri E, Peresleni T, Miller F, Goligorsky MS. In vivo targeting of inducible NO synthase with oligodeoxynucleotides protects rat kidney against ischemia. J Clin Invest. 1996;97(10):2377-83.

183. de Vries EF, Vroegh J, Dijkstra G, Moshage H, Elsinga PH, Jansen PL, et al. Synthesis and evaluation of a fluorine-18 labeled antisense oligonucleotide as a potential PET tracer for iNOS mRNA expression. Nucl Med Biol. 2004;31(5):605-12.

184. Lennette DA. General principles for laboratory diagnosis of viral, rikettsial, and chlamydial infections. In: Lennette E, Lennette D, Lennette E, editors. General principles for laboratory diagnosis of viral, rikettsial, and chlamydial infections. Washington DC: American Public Health Association; 1995. p. 3-25.

185. Templin MV, Levin AA, Graham MJ, Aberg PM, Axelsson BI, Butler M, et al. Pharmacokinetic and toxicity profile of a phosphorothioate oligonucleotide following inhalation delivery to lung in mice. Antisense Nucleic Acid Drug Dev. 2000;10(5):359-68.

186. Livak KJ, Schmittgen TD. Analysis of relative gene expression data using real-time quantitative PCR and the 2(-Delta Delta C(T)) Method. Methods. 2001;25(4):402-8.

187. D'Alessio FR, Tsushima K, Aggarwal NR, Mock JR, Eto Y, Garibaldi BT, et al. Resolution of experimental lung injury by monocyte-derived inducible nitric oxide synthase. J Immunol. 2012;189(5):2234-45.

188. Nathan C. Inducible nitric oxide synthase: what difference does it make? J Clin Invest. 1997;100(10):2417-23.

189. Burggraaf S, Bingham J, Payne J, Kimpton WG, Lowenthal JW, Bean AG. Increased inducible nitric oxide synthase expression in organs is associated with a higher severity of H5N1 influenza virus infection. PLoS One. 2011;6(1):e14561.

190. Vom Steeg LG, Klein SL. Sex and sex steroids impact influenza pathogenesis across the life course. Semin Immunopathol. 2018.

191. Smee DF, von Itzstein M, Bhatt B, Tarbet EB. Exacerbation of influenza virus infections in mice by intranasal treatments and implications for evaluation of antiviral drugs. Antimicrob Agents Chemother. 2012;56(12):6328-33.

192. Margine I, Krammer F. Animal models for influenza viruses: implications for universal vaccine development. Pathogens. 2014;3(4):845-74.

193. Heneghan CJ, Onakpoya I, Thompson M, Spencer EA, Jones M, Jefferson T. Zanamivir for influenza in adults and children: systematic review of clinical study reports and summary of regulatory comments. BMJ. 2014;348:g2547.

194. Zheng BJ, Chan KW, Lin YP, Zhao GY, Chan C, Zhang HJ, et al. Delayed antiviral plus immunomodulator treatment still reduces mortality in mice infected by high inoculum of influenza A/H5N1 virus. Proc Natl Acad Sci U S A. 2008;105(23):8091-6.

195. Smee DF, Dagley A, Tarbet EB. Combinations of L-N(G)-monomethyl-arginine and oseltamivir against pandemic influenza A virus infections in mice. Antivir Chem Chemother. 2017;25(1):11-7.

196. Ali S, Leonard SA, Kukoly CA, Metzger WJ, Wooles WR, McGinty JF, et al. Absorption, distribution, metabolism, and excretion of a respirable antisense oligonucleotide for asthma. Am J Respir Crit Care Med. 2001;163(4):989-93.

197. Finotto S, De Sanctis GT, Lehr HA, Herz U, Buerke M, Schipp M, et al. Treatment of allergic airway inflammation and hyperresponsiveness by antisense-induced local blockade of GATA-3 expression. J Exp Med. 2001;193(11):1247-60.

198. Hussell T, Pennycook A, Openshaw PJ. Inhibition of tumor necrosis factor reduces the severity of virus-specific lung immunopathology. Eur J Immunol. 2001;31(9):2566-73.

199. Peper RL, Van Campen H. Tumor necrosis factor as a mediator of inflammation in influenza A viral pneumonia. Microb Pathog. 1995;19(3):175-83.

200. Damjanovic D, Divangahi M, Kugathasan K, Small CL, Zganiacz A, Brown EG, et al. Negative regulation of lung inflammation and immunopathology by TNF-alpha during acute influenza infection. Am J Pathol. 2011;179(6):2963-76.

201. Dunning J, Baillie JK, Cao B, Hayden FG, International Severe Acute R, Emerging Infection C. Antiviral combinations for severe influenza. Lancet Infect Dis. 2014;14(12):1259-70.

APPENDIX

EVMS
Eastern Virginia Medical School

William Wasilenko, Ph.D.
Senior Associate Dean for Research
Eastern Virginia Medical School
Office of Research, Suite 169 Andrews Hall
721 Fairfax Ave., Norfolk, VA 23507

July 20, 2017

Vilnius University Faculty of Medicine,
M. K. Čiurlionio str. 21, LT-03101 Vilnius, Lithuania
Tel. (8 5) 239 8700, Fax. (8 5) 239 8705
e-mail: mf@mf.vu.lt

A LETTER OF CONFIRMATION

This letter is to confirm that on 14 February 2007 the Institutional Animal Care and Use Committee at Eastern Virginia Medical School, Norfolk, Virginia, USA, approved the following protocol:

> EVMS IACUC #07-003 "*Prevention of Pulmonary Pathology from Influenza Virus Infection with Neuraminidase Inhibitors (Zanamivir; Oseltamivir Carboxylate; Permavir) and Anti-sense iNOS Treatment*"

Additional details about #07-003:
- The personnel approved to work on protocol #07-003 were: Stefan Gravenstein, Paul Aravich, Dean Howard, Tomas Kacergius and Norine Kuhn.
- The protocol was approved for the use of up to 262 BALB/c mice, but was not approved for Multiple Survival Surgery.
- Protocol #07-003 was closed on 17 February 2008.

Please accept this as official confirmation of formal review and prior approval.

William Wasilenko, Ph.D.
Senior Associate Dean for Research
Eastern Virginia Medical School

Frank Lattanzio, Ph.D., Chair,
Institutional Animal Care and Use Committee
Eastern Virginia Medical School

Office of Research

721 FAIRFAX AVENUE, SUITE 169
NORFOLK, VA 23507
TEL 757.446.8480
FAX 757.446.6019
www.evms.edu

Community focus. World impact.

LIST OF PUBLICATIONS

List of original papers:

1) **Zablockienė B**, Ambrozaitis A, Kačergius T. Gripo gydymo galimybės ir ateities perspektyvos. Vaikų pulmonologija ir alergologija 2017 (11); 1: 6208–6227.

2) **Zablockienė B**, Ambrozaitis A, Kačergius T, Žurauskas E, Bratchikov M, Gravenstein S. Gripo viruso sukelta azoto oksido gamyba pelių plaučiuose ir jos slopinimo metodas. Vaikų pulmonologija ir alergologija 2017 (20); 2: 6306–6313.

3) **Zablockienė B**, Kačergius T, Ambrozaitis A, Žurauskas E, Bratchikov M, Jurgauskienė L, Zablockis R, Gravenstein S. Zanamivir Diminishes Lung Damage in Influenza A Virus-infected Mice by Inhibiting Nitric Oxide Production. In Vivo 2018; 32: 473–478.

Presentations:

1) Ambrozaitis A, **Zablockiene B**, Kacergius T, Zurauskas E, Gravenstein S. Prevention of influenza-virus induced pulmonary histopathology in mice using antivirals and antisense oligonucleotides to indicible nitric oxide synthase. Abstract and poster in 11th Annual Conference of the Baltic Network Against Life-Threatening Viral Infections. April 24-27, 2014, Vilnius, Lithuania.

2) **Zablockiene B**, Kacergius T, Ambrozaitis A, Zurauskas E, Bratchikov M, Gravenstein S. Treatment with zanamivir and antisense oligonucleotides to inducible nitric oxide synthase decreases infuenza A virus-induced lung inflamation. Abstract and poster in Nordic Society of Clinical Microbiology and Infectious Diseases 2016. September 15-18, 2016, Rovaniemi, Finland.

3) **Zablockienė B**. Oral presentation "Gripo gydymas: naujos galimybės" in a conference "Apsinuodijimų ir infekcinių susirgimų sąlyčio taškai". 2017-02-09, Vilnius, Lithuania.

4) **Zablockienė B**. Oral presentation "New perspectives in the therapy of influenza", in "Baltic Young Infectologists Conference 2017", March 24-25, 2017, Riga, Latvia.

5) **Zablockienė B**. Oral presentation "Gripo virusai ir jų sukeliamos visuomenės sveikatos problemos" in a conference "Individualus požiūris į visuomenės sveikatą šaltuoju metų sezonu". 2017-10-07, Kaunas, Lithuania.

6) **Zablockienė B**, Kačergius T, Ambrozaitis A, Žurauskas E, Bratchikov M, Gravenstein S. Zanamivir Reduces Lung Pathology by Inhibiting Nitric Oxide Production in Influenza A Virus-Infected Mice. Poster in a conference "Life Science Baltics 2018", 2018-09-26/27, Vilnius, Lithuania.